Faculty of Science

Department of Applied Chemistry

Controlling Precipitation of Value Added Zirconia

Geoffrey A Carter

This thesis is presented for the Degree of

Doctor of Philosophy

of

Curtin University of Technology

June 2009

Declaration

"To the best of my knowledge and belief this thesis contains no material previously published by any other person except where due acknowledgment has been made. This thesis contains no material which has been accepted for the award of any other degree or diploma in any university".

Geoffrey A Carter

Signature:

Date: 30 of April 2009

Abstract

Advanced zirconia-based materials have many important applications in electronics
and medical applications, and of most interest to this research, solid oxide fuel cells
(SOFC) which is a key technology for alternative and hydrogen-based energy
generation. The SOFC in its most basic form is a device for converting hydrogen and
oxygen into water with a resulting generation of power. Most SOFC
manufacturers/developers are using zirconia doped with yttria as the electrolyte with
variations on the amount of yttria. The SOFC places high demands on the ceramic
components, placing significant demands on powder processing technology to enable
fabrication of reliable components. It has been shown that the process of co-
precipitation of three initially mixed chlorides, aluminium chloride, yttrium chloride
and zirconium oxychloride in aqueous solutions, can produce an oxide powder that
can be used in SOFC manufacture. Zirconia powders synthesised from aqueous
solution in this way have been found, however, to include hard agglomerates which
are detrimental to further processing and applications.

Industrial manufacture of zirconia and zirconia-yttria products can best be
summarised as four step operation; (1) hydrolyse of zirconyl chloride and mixing of
other solutions, (2) precipitation, (3) calcination (4) forward processing for particle
size, surface area and handle-ability characteristics . The use of aqueous solutions
allows for lower costs of production and reduced waste. However such production is
hampered by limited understanding of the fundamental chemistry particularly during
aqueous processing which limits the development of better powders for the
widespread use of SOFC's. The aim of this project was to develop an understanding
of these problems based on an industrial process that is in use within Western
Australia. The work has been broken up into five sections, with the first four dealing
with predominately non-stabilized zirconia and tracks the process from aqueous
chemistry through to final ceramic. The final section does the same for a 3 mole%
yttrium partially stabilised zirconia.

The influence of concentration and added chloride salts on the solution speciation of
zirconyl chloride solutions, and the precipitate formed upon addition of aqueous

ammonia, has been investigated using a combination of techniques, such as SAXS, DLS, ICP-OES, TEM and SEM.

To further investigate the precipitation process the effect of pH of precipitation, starting solution concentration, and agitation levels on the particle size of hydrous zirconia precipitates have been investigated. The pH of precipitation was also found to have a significant impact on the type of hydrous zirconia produced. TGA/DTA, micro combustion and TEM / EDS were used to investigate the difference in the powders produced at pH 3 and 12.

The two hydrous zirconium manufactured at pH 3 and 12 have been studied as further processing consistent with industrial procedures was undertaken, including how the differences in structure due to the pH of precipitation, may effect the calcination, in situ and ex situ x-ray diffraction was used for this.

With the knowledge developed thus far, two 3 mol% partially stabilised zirconia (P-SZ) samples suitable for the SOFC market were manufactured from solutions through to ceramics.

The combination of SAXS, DLS, in situ XRD, TEM, ICP, TGA/DTA, micro combustion, and standard ceramic testing was found to be excellent for providing comprehensive information on changes through an industrial process and will allow optimisation to produce powders suitable for SOFC applications.

Acknowledgments

For those who have helped, a heartfelt thankyou! For those who hindered, I forgive you. It's finished and that is acknowledgement enough. When work is undertaken, read and or contemplated I keep in mind a Confucian philosophy;

"The essence of knowledge is having it to apply" *Confucius 479 BC*

Each paper has acknowledgements pertaining to those who helped in the work. I have also endeavoured to be as inclusive of those who helped significantly in the naming of co-authors on the papers, this I think is the best way of acknowledging those who have helped with the science.

As always however the one person who helped above all others who isn't a co-author is my wife, this is yours as much as mine. Thanks bear!

Enjoy this work.

Geoff

Publications Included As Part of This Thesis

(Listed in order as found in this thesis)

Carter G. A., Ogden M. I., Buckley C. E., Maitland C., Paskevicius M., 2009, '*Ammonia-Induced Precipitation of Zirconyl Chloride and Zirconyl-Yttrium Chloride Solutions Under Industrially Relevant Conditions*', Journal of Powder Technology, vol. [188], pp 222-228.

Carter G., Hart R., Rowles M., Ogden M., Buckley C., 2009, '*The Effect of Processing Parameters on Particle Size in Ammonia-Induced Precipitation of Zirconyl Chloride Under Industrially Relevant Conditions*', Journal of Powder Technology, doi: 101016/j.powtec.200810.012.

Carter G., Rowles M., Hart R., Ogden M., Buckley C., 2008, '*From Zirconyl Chloride to Zirconia Ceramic, A Plant Operation Perspective*', Materials Forum, vol. [32], pp. 82-89.

Carter G., Hart R., Rowles M., Ogden M., Buckley C., 2009 '*Industrial Precipitation of Zirconyl Chloride: The Effect of pH and Solution Concentration on Calcination of Zirconia*', Materials Chemistry and Physics Doi: 10.1016/j.matchemphys.2009.05.014

Carter G., Hart R., Rowles M., Ogden M., Buckley C., 2009 '*Industrial Precipitation of Yttria Partially Stabilised Zirconia*', Journal of Alloys and Compounds, DOI:10.1016/j.jallcom.2009.02.005.

Statement of Contribution of Others

Geoff Carter's input into this project and the associated papers included the execution of all the experimental work, and a dominant contribution to the intellectual input involved in the project. As is almost always the case in the physical sciences, other scientists made contributions to the work that were significant enough to warrant co-authorship on the resulting journal articles. These are specified below.
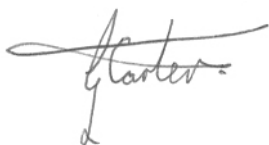
Ogden M. I., Buckley C. E., provided manuscript editing and project supervision.

Maitland C., provided specific technical knowledge on the operation and use of the SAXS instrument as well as sample preparation for SAXS investigation.

Paskevicius M., provided specific technical knowledge on the data interpretation software for SAXS analysis.

Hart R., provided specific technical assistance on the operation of the TEM and associated data analysis techniques.

Rowles M., provided specific technical assistance on the operation of the XRD and associated data analysis techniques.

_____   _____

Geoff Carter   Prof. Mark Ogden (Supervisor)

Copyright Declaration

"I warrant that I have obtained, where necessary, permission from the copyright owners to use any third-party copyright material reproduced in the thesis, or to use any of my own work in which copyright is held by another party".

Geoffrey A Carter

Signature:

Date: 30 of April 2009

List of Additional Publications By Geoffrey A Carter Relevant to Thesis But Not Forming Part of It.

Journal Articles

Carter G. A., van Riessen A., 2007, '*Neutron Diffraction of Zirconia-Dispersed Alumina With Increasing Stress and Temperature*', Journal of the American Ceramic Society, vol. [91], no. [2], pp. 559-560, DOI: 10.1111/j.1551-2916.2007.02161.x. ERA Journal Ranking = A*.

Carter, G. A., van Riessen, A. & Hart, R. D., 2006, '*Wear of Zirconia Dispersed Alumina at Ambient, 140 ºC and 250 ºC*', Journal of the European Ceramic Society, vol.[26], pp. 3547-3555. ERA Journal Ranking = A.

Conference Papers (Presented)

G. Carter, A., van Riessen, R. Hart, '*Wear Characteristics of Zirconia Dispersed Alumina*', Oral presentation, 2008 32nd International Conference & Exposition on Advanced Ceramics & Composites, Daytona Beach, Florida USA.

G. Carter, M. Rowles, M. I. Ogden, C. E. Buckley, '*Aqueous Processing of Zirconyl Chloride with Yttrium Chloride from Solutions to Ceramics*', Oral presentation, 2008 32nd International Conference & Exposition on Advanced Ceramics & Composites, Daytona Beach, Florida USA.

G. Carter, '*Control of Precipitation of Value Added Zirconia*', Oral presentation, 2006 Student-Industry-CRC Symposium, Gladstone Qld.

G. Carter, '*Yttria-Zirconia for Solid Oxide Fuel Cells: A Study into the Aqueous Chemistry*', Oral presentation, 2006 Parker Centre Research Seminar, Perth WA.

Carter G., Buckley C., Ogden M., '*Solid Oxide Fuel Cells: A SAXS Study of the Effects of Solution Concentration on Particle Size*', Oral presentation, 2006 Australian Institute of Physics 17th National Congress, Brisbane Qld.

Carter G., Buckley C., Ogden M., '*Solid Oxide Fuel Cells: A SAXS Study of the Effects of Solution Concentration on Particle Size*', Oral presentation, 2006 5th AINSE/ANBUG Neutron Scattering Symposium (AANSS 2006), Sydney NSW.

Conference Poster Presentations

Alistair G Mawson, **Geoffrey A. Carter**, Robert D. Hart, Nigel M. Kirby, Amanda C. Nachmann, '*Mechanical Properties of 8 mole % Yttria-Stabilised Zirconia for Solid Oxide Fuel Cells*' MaTe 2005, Fremantle, Western Australia.

Table of Contents

1. Introduction & Overview

1.1. Introduction

1.1.1.   Introduction to Project

Doral Specialty Chemical (DSC) is based in the Kwinana industrial area located in Western Australia. The manufacturing plant was initially constructed by ICI chemicals in the 1980's. ICI sold the establishment to Hanwa Advanced ceramics in the early 1990's who ran the plant until it was sold to Millennium Inorganic Chemicals in 2000. Millennium sold the plant to Doral Specialty Chemicals in 2004.

The plant has manufactured zirconia and zirconium chemicals since its construction. ICI chemicals developed a method for direct extraction of the zirconia from zircon sands which was colloquially termed the "double salt method", covered under patent no. AU-B-53972/86. This method of manufacture proved commercially non-competitive and was not pursued by Hanwa who introduced the manufacture of zirconium chemicals from imported zirconium oxy-chloride crystals. This is the processing route that is used currently and the methods developed are a mixture of the old ICI methods and the new method of manufacture using a different raw material.

Zircon is the mineral ($ZrSiO_4$) from which all zirconia materials are derived. It is separated from other mineral sand ores by a wet-gravity technique followed by dry-separation magnetic and electrostatic processes. World production of zircon was 900,000 tonnes in 1998; of which 300,000 tonnes was supplied by Western Australia. Industrial zirconia is principally used as an opacifier in ceramic glazes and refractories. High quality zirconia is used for the electronics market, mostly for multilayer ceramic capacitors and piezoelectric applications, and potentially as solid oxide fuel cells in both hydrogen and natural gas powered systems. The value of zircon exported as zircon sand is $1500 per tonne. The value of zircon as yttria stabilized zirconia is $300,000 per tonne (Internal Millennium Inorganic Chemicals Document 2002).

The market for zirconia has increasingly become more competitive and DSC and its previous owners have developed new products to take to the market place. One such product is yttria doped zirconia for use in the Solid Oxide Fuel Cell (SOFC) market. The ceramic of most interest is cubic zirconia (ZrO_2), in its fully stabilised cubic form using 10 mole % yttria (Y_2O_3). Yttria stabilised zirconia SOFC has the advantage of being able to use both hydrogen and lower grade fuels such as natural gas, and will therefore serve as the transitional technology through which the infrastructure of the hydrogen economy can mature.

Hydrogen can be used instead of, or in combination with, conventional fuels. In advanced technologies such as fuel cells, hydrogen can be directly converted to electricity and thermal energy with greater than 80% efficiency. The Australian Government released the "National Hydrogen Study" in November 2003 (Commonwealth Department of Industry, Tourism & Resources, 2003), which clearly recognised the critical role of hydrogen as a future energy source and the importance of research and development in all facets of the hydrogen economy.

DSC has developed a method of homogenously chemically mixing alumina into the zirconia-yttria matrix. However the development of larger scale manufacturing techniques is currently significantly hampered by a lack of fundamental understanding of the chemical processes that exist within the manufacturing system. Much of this is due to poor knowledge of zirconia aqueous solution chemistry in mixing tanks etc.

1.1.2. Yttria Doped Zirconia for Fuel Cells

The SOFC in its most basic form is a device for converting hydrogen and oxygen into water with a resulting electrical generation of power. The obvious difference between a SOFC and other fuel cells is that the major component in the anodes, cathodes and electrolytes are all or partially made from an oxide ceramic.

The SOFC is an intricate multi-component device requiring fabrication technologies that are complex, with each material in the device having to perform not only in its

own right but in conjunction with other components (Badwal, Fogger 1997). SOFC place high demands on both the materials that they are manufactured from as well as the manufacturing method. In addition, the components themselves are required to have good ionic/electrical properties as well as be able to withstand high operating temperatures whilst maintaining the mechanical properties that are required. They also must be reliable with typical life times of 40,000 - 50,000 hours (Badwal, Fogger 1997). For these reasons and more, most SOFC manufactures/developers are using zirconia doped with yttria as the electrolyte with variations on the amount of yttria (Ciacchi, Crane, Badwal, 1994).

Bellon, Ratnaraj, Rodrigo (2002) outline some of the important physical characteristics that a precursor powder requires for the manufacture of a planer SOFC and how these requirements effect the manufacturing of the components. Carter *et. al.* (2003) showed that the process of co-precipitation of three initially mixed chlorides, alumina chloride, yttrium chloride and zirconium chloride, can produce an oxide powder that has a homogeneous distribution of all three constituents. This homogeneity in solid solution allows for control of the zirconia polymorphs and leads to better processing ability in the manufacture of the parts of the SOFC.

1.1.3.   Plant Design and Process

The plant built to manufacture the yttria doped zirconia at DSC evolved from the existing plant which was designed for the original ICI process and had evolved to manufacture monoclinic zirconia. The existing plant could thus be used for the manufacture of monoclinic zirconia with the new smaller plant used for the high purity, high value fuel cell market. The plant process can be broken down into 8 stages; hydrolysis, mixing, precipitation, washing/air drying, humidity drying, calcination, milling and spray drying.

During the development cycle for the yttria doped zirconia it became evident that the product was not meeting the success criteria as defined by the requirements of Ceramic Fuel Cells Ltd., who were an integral part of the development cycle. This was due wholly to the presence of hard particles that were unmilled and/or

significantly larger than the required powder size present in the final product (Figure 1). The presence of this large particle fraction was new to the experience of the manufacturing plant, however, numerous researchers have noted the presence of hard agglomerates found in zirconia powders synthesised by aqueous precipitation, with some suggesting ways of preventing development of the agglomerates, which whilst useful in laboratory situations are not practical on a large commercial scale (Kaliszewski, and Heuer 1990, Lauci 1997, Bannister and Garrett 1975, Rajendran 1993, Li, Gao and Guo 1998). Monoclinic powder produced by the same process did not and has never developed the hard agglomerates and as such their presence was not anticipated.
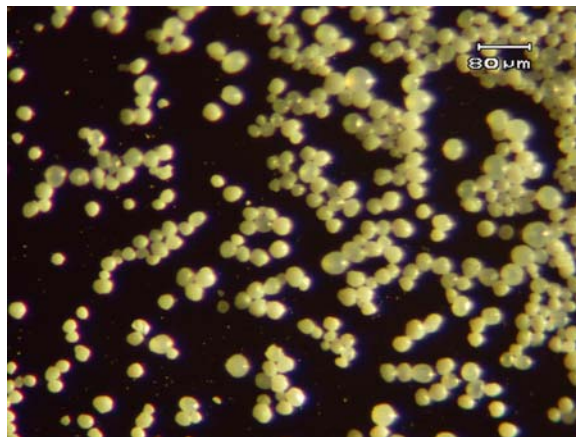
Figure 1. Optical micrograph of particles taken from ZY10A. Scale bar in top right hand corner.

A method for separating out the large agglomerates using sedimentation and ultrasonic de-agglomeration was developed by Carter and Titkov (2001) that allowed the agglomerates to be investigated using Scanning Electron Microscope (SEM) imaging and Energy Dispersive Spectroscopy (EDS). This work showed that the agglomerates had the same composition as that of the other powders. Since no major differences could be found in the composition, and the available literature suggested that the formation of the agglomerates was due to the precipitation process (Kaliszewski, and Heuer 1990, Lauci 1997, Bannister and Garrett 1975, Rajendran 1993, Li, Gao and Guo 1998), two plant trials were undertaken to develop a better understanding of the mechanisms at work. The two plant trials were both 2x2 full factorial Design of Experiment (DOE) trials and whilst not elucidating the actual

mechanisms at work demonstrated that the precipitation and changes in precipitation states influenced the presence of the problematic agglomerates (Carter 2002, Carter 2003).

1.1.4. This Research

Research was initiated to help improve the fundamental understanding of the precipitation-agglomeration process for the aqueous precipitation processes conducted at DSC with a focus on compositions used for the manufacture of SOFC.

The first step is to investigate the solution speciation of Zirconium Oxy Chloride (ZOC) and ZOC with yttrium chloride in aqueous solutions. This investigation was undertaken using Small Angle X-ray Scattering (SAXS) analysis. Zirconyl chloride was investigated using SAXS with differing concentrations in the solution (these solutions are distributed around commercially useful concentrations) as well as different trace element compositions in the starting solution as determined by ICP-OES. Further to this, zirconyl chloride doped with yttrium chloride solutions were made and investigated using SAXS. These solutions were mixed at the appropriate ratios for use in SOFC applications.

The second stage of the research was to develop an understanding of the precipitation process using a combination of SAXS and dynamic light scattering techniques. Crystallisation facilities were built and used to replicate the continuous precipitation process as used in DSC. A number of starting solution concentrations were tried along with time dependent investigations. In each case samples were taken from the precipitation process with a steric hindrance added and the flocculent size investigated using dynamic light scattering.

It is hoped that this improved understanding will allow DSC to optimise the manufacture of yttrium stabilised zirconia for SOFC applications and zirconia precipitation generally, and thus be more competitive in the market place.

1.1.5.   *Experimental Design*

The principle aim of this research is to further the understanding of the fundamental chemistry of precipitated zirconia-yttria ceramics, focusing on the solution chemistry and precipitation/co-precipitation methods used by industrial manufactures and in line with the requirements of the SOFC market. The key principles points of interest in undertaking this research were;

i)   Study of the solution phase structure of the zirconyl chloride system under industrially relevant conditions.

ii)   Study of the precipitation process, characterising the products formed as a function of the precipitation conditions.

iii)   Investigate links between the solution phase structure and the precipitated products through to sintered ceramics.

With this in mind it is relevant to discuss how such an investigation is to be undertaken and outline the experimental methods to be used.

It is clear from the above statement that this investigation is some what linear in its approach due to the cumulative knowledge affect. Thus it is important to develop an understanding of the solution dynamics prior to precipitating them. The constraining points are that the research has to be of industrial relevance so sample selection both in concentrations and compositions where predetermined.

1.2.   Doral Specialty Chemicals' Process

Doral Specialty Chemicals owns the Rockingham zirconium chemicals plant located at 1 Ward Rd Rockingham. This plant was initially owned and developed by ICI Chemicals.

The original plant process revolved around an ICI process known as the "Double Salt Method" (Australian Patent number AU-B-53972/86 and acceptance No 586467). The first part of the method is described in the patent documentation as:

" 1) A process for the preparation of Zirconium sulphate tetra hydrate comprising the steps of :

> (i)   *Leaching a zirconium source with sulphuric acid to produce an acid leach slurry;*
>
> (ii)   *Diluting the resulting acid leach slurry to produce zirconium sulphate tetra hydrate crystals in a diluted sulphuric acid slurry;*
>
> (iii)   *Separating said zirconium sulphate tetra hydrate crystals from the diluted acid;"*

The remaining process is described as being

"A process for the preparation of zirconium compositions which on calcinations form Zirconia, which process comprises:
Preparing an aqueous zirconium sulphate solution of pH not greater than zero; adding an ammonia source to said zirconium sulphate solution until the pH of said solution is in the range of from 0.1 to 2.5; and collecting the precipitated zirconium composition."

This plant and process was sold to Hanwa Advanced Ceramics in the early 1990's. Hanwa modified the process by commencing the process with imported zirconium oxy chloride crystals. The process was developed to run using existing plant equipment (developed to operate using the above double salt method with respect to the precipitation). The development of the new process was not documented (or the documents were not made available when the plant was purchased) and was rudimentary in its development. In the year 2000 Hanwa sold the Rockingham operation to Millennium Performance chemicals.

In the year 2001 Millennium Performance Chemicals started developing co-precipitated yttria zirconia powders. This was initiated using a newly built and commissioned small stream plant.

Doral Specialty Chemical purchased the Rockingham operations in the year 2004.

The basic process for both the production of zirconia-yttria based products and monoclinic zirconia products is shown in Figure 2.
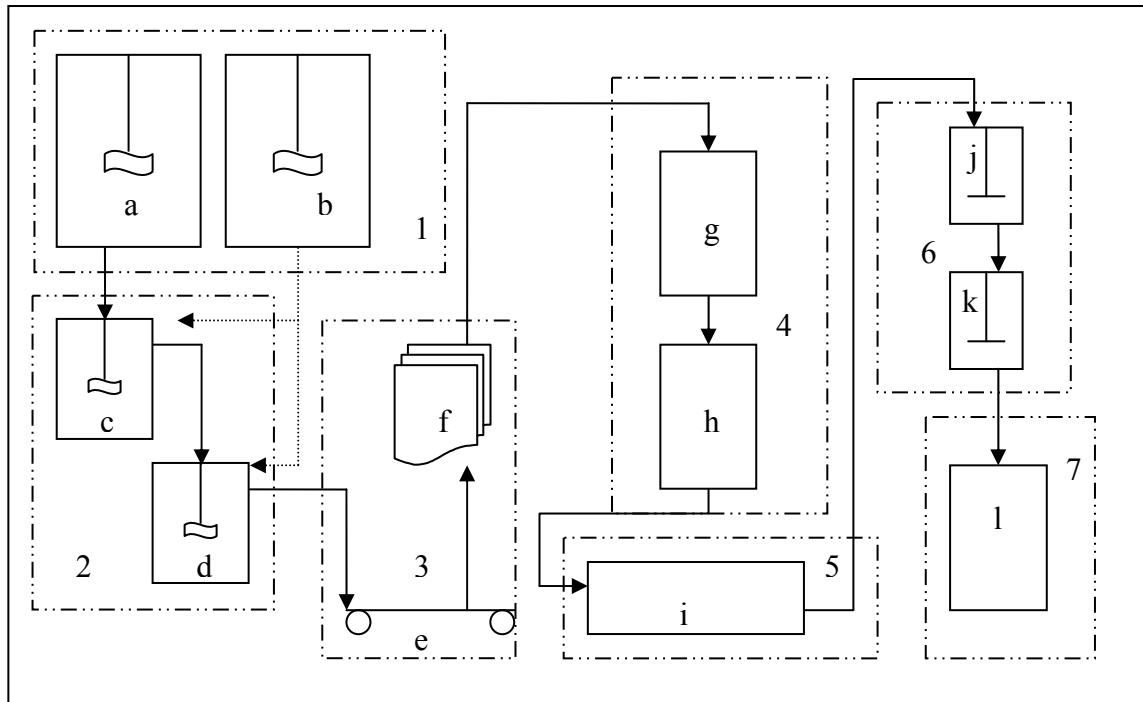
Figure 2. DSC diagrammatic description of process. 1) Mixing of acids and bases (a:- zirconyl chloride + water, b:- anhydrous ammonia + water), 2) Precipitation, (c:- zirconyl chloride solution + aqueous ammonia, d:- Flocculants from c + aqueous ammonia), 3) filtering/washing, (e:- belt filter flocculants + water + vacuum, f:- frame filter press cake from e + water + air), 4) Heat drying, 5) Calcinations, 6) Milling, 7) Spray drying.

The basic understanding of the chemical reactions at each stage is listed in the first instance for the production of monoclinic zirconia with yttria-zirconia solid solutions following:

1) Hydrolysis

$$4ZrOCl_2 \cdot 8H_2O \overset{water}{\Rightarrow} \left[Zr(OH)_2 \cdot 4H_2O\right]_4^{8+} + 8Cl^- + 12H_2O$$

2) Precipitation

$$ZrO^{2+} + 2Cl^- + 2NH_4OH \Leftrightarrow ZrO(OH)_2 + 2NH_4Cl$$

3) Drying

$$ZrO(OH)_2 \xrightarrow{\Delta H} ZrO - O + 2H$$

4) Calcination

$$ZrO - O \xrightarrow{\Delta H} ZrO_2$$
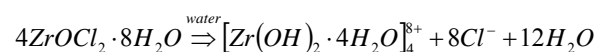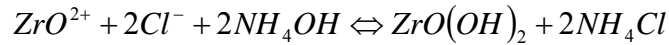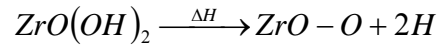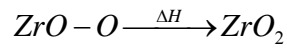
For yttria-zirconia solid solutions the hydrolysis of the zirconium is the same, with the general form of the precipitation equation being

$$(4-4x)Zr^{4+} + 4xY^{3+} + 8OH^- + 16H_2O \xrightarrow{aqueous} \{Zr_{(4-4x)}Y_{4x}(OH)_8(H_2O)_{16}\}^{(8-4x)+}$$
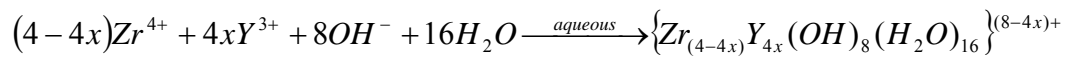
Where x is the mole fraction of yttria in the composition, i.e. for ZY3, $x = 0.03$.

Therefore substituting in

$$3.88Zr^{4+} + 0.12Y^{3+} + 8OH^- + 16H_2O \xrightarrow{aqueous} \{Zr_{3.88}Y_{0.12}(OH)_8(H_2O)_{16}\}^{7.88+}$$

After drying;

$$\{Zr_{3.88}Y_{0.12}(OH)_8(H_2O)_{16}\}^{7.88+} \xrightarrow{\Delta H} \{Zr_{3.88}Y_{0.12}(OH)_8\}^{7.88+} + 16H_2O$$

After calcination

$$\{Zr_{3.88}Y_{0.12}(OH)_8\}^{7.88+} \xrightarrow{\Delta H} Zr_{3.88}Y_{0.12}O_{7.94}$$
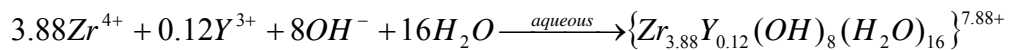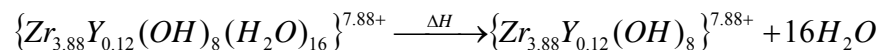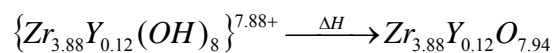
These equations are as supplied by the Millennium Research Centre in 2001, and will be discussed further in the appropriate section. A number of assumptions are made in formulating the equations, and there is some discussion on their validity in literature. An example of such is the exact species obtained after drying which may be the product $Zr(OH)_4$ or alternatively $ZrO(OH)_2$ as suggested by Huang, Tang and Zhang (2001).

1.3.   Solid Oxide Fuel Cells

1.3.1.   *Fundamentals of Solid Oxide Fuel Cells*

William Grove first demonstrated a fuel cell in principle in 1939 when he separated oxygen and hydrogen from water using an electric current, and then replaced the electrical power supply in the circuit with an ammeter which indicated a small current, thus showing that the electrolysis is reversible (Larminie and Dicks 2000 p.1). The basic chemical reaction is;

$$2H_2 + O_2 \rightarrow 2H_2O$$
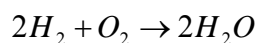
Fuel cells are a means of power generation, being different to conventional power generation technologies, in that electricity is produced electrochemically and not via a heat generation step (Foger and Badwal, 1997). The main driving force to develop fuel cells has been due to environmental concerns and the need to reduce carbon dioxide emissions, and their high energy conversion efficiency (Larminie and Dicks 2000 p. xi., Foger and Badwal 1997). Most fuel cells are limited in the fuels that they use, however the SOFC as well as the molten carbonate fuel cell can use both hydrogen and carbon monoxide as fuels (Larminie and Dicks 2000 p. 164).

The SOFC is a solid state device that uses an oxide ion-conducting ceramic material as the electrolyte. The SOFC allows negatively charged ion (O^{2-}) to be transferred from the cathode through the electrolyte to the anode (see Figure 3) (Larminie, Dicks 2000 p. 164).

Foger and Badwal (1997) discuss the general material requirements for fuel cell components at operating temperatures of 950 – 1000 ^{o}C and suggest that materials which fulfil such requirements are scarce. The first mentioned requirement is chemical stability and compatibility with other fuel cell components for which they are in direct contact with during the operation and fabrication. The stability must extend to the fuel cell operating environment, for example the air electrode must be stable in a highly oxidising atmosphere and the fuel electrode in a reducing environment, with the interconnects, manifolds, sealing and electrolyte material experiencing fuel environments on one side and oxidising conditions on the other (Foger and Badwal 1997).
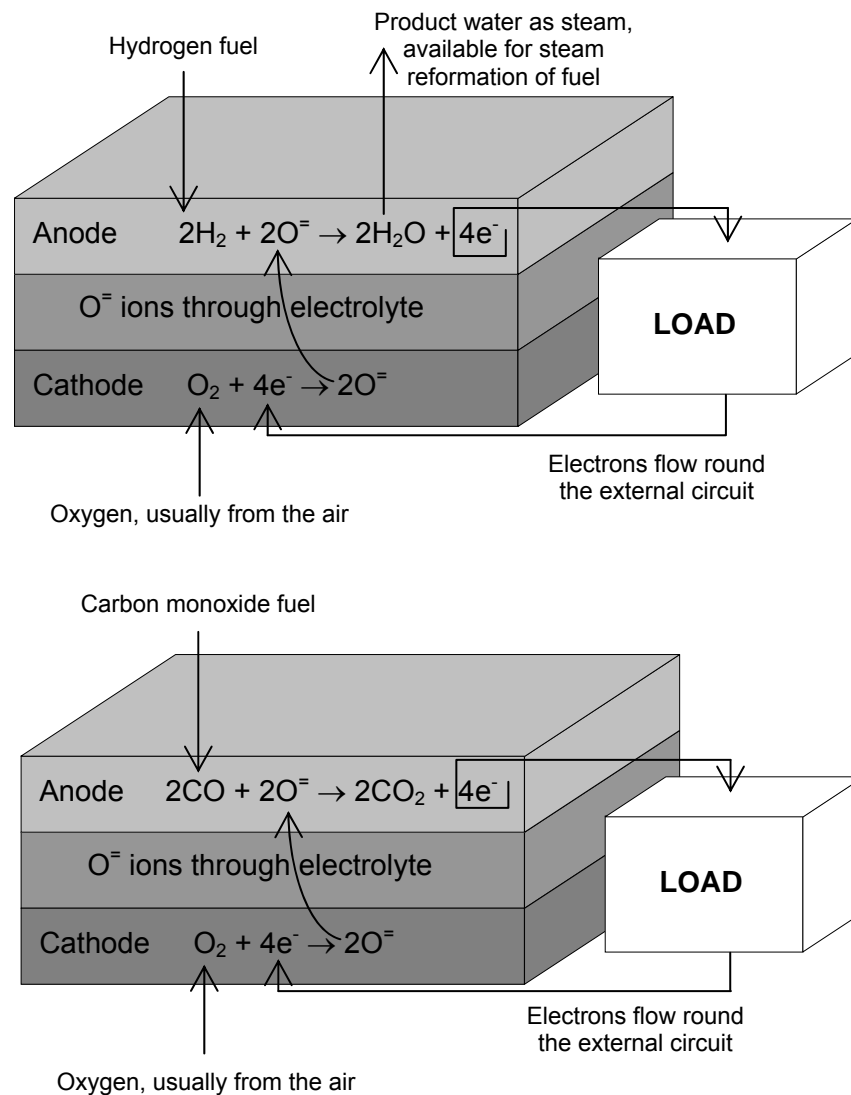
Figure 3.   Operation of SOFC (after Larminie and Dicks 2000 p164).

The second listed point by Foger and Badwal (1997) is for the right level of conductivity, and of the right type to be part of the materials characteristics. Both electrodes require high conductivity for electronic or a mixture of ionic and electronic conductivity. The electrolyte needs predominantly ionic conductivity with the interconnects being mainly electronic. The seals and manifolds in contrast need to be mainly insulators (Foger and Badwal 1997).

This is complicated if the cathode and anode materials have a mix of ionic and electronic conductivity (with high diffusion rates of O^{2-}), since then oxygen transfer can take place at the gas/electrode interface and this is not dependent on the existence of substantial three phase boundary between electrode, electrolyte and gas. This has the advantage of enhancing electrolyte/electrode contact area and reaction rates sites, thereby reducing over-potential losses (Foger and Badwal 1997).

Point three of Foger's and Badwal (1997) treatment on general materials requirements is that low vapor pressure will avoid loss of material which may lead to reaction or reactions with other components, or the formation of new phases with changes in its properties. This third point leads nicely into the fourth, being that the material needs to have structural phase stability from room temperature to the operating temperature of the fuel cell. This dovetails into microstructural stability requirements for the full range of temperatures experienced by the parts (Foger and Badwal 1997).

Structural support to the stack is provided by interconnects and electrolyte material in self supporting designs, as such the material needs to have the appropriate strength and toughness characteristics not only at room temperature (in terms of handling, processing of cell components), but also at the operating temperature that the parts are subjected to during operation of the SOFC. Additionally it is advantageous for these materials to have high thermal and mechanical shock resistance (Foger and Badwal 1997).

Fuel and air electrodes must have high catalytic activity to fuel oxidation and oxygen reduction reactions respectively with porous, but stable microstructure during the operating life of the cell. The fuel electrode should not promote carbon deposition as

this would adversely affect the performance of the cell and one of the advantages of SOFC's is that carbonaceous fuels can be used (Foger and Badwal 1997).

The final point made by Foger and Badwal (1997) is that the materials and fabrication methods must be economical and as easy as possible.

McEvoy (2001) states that the ideal solid electrolyte was identified by Nernst as zirconium oxide with a mixture of di- or trivalent substitutes in solid solution, with the material of preference being that of 8% yttria-zirconia. There have been investigations into a number of formulations used by SOFC manufactures and not all have used yttria with a number of authors investigating a number of novel formulations (Badwal et. Al. 1998. Badwal and Ciacchi 2000. Hassan et. al. 2002. Ciacchi, Crane, Badwal 1994. Badwal Ciacchi and Milosovic 2000. Bannister, Garrett, 1975. Bellon, Ratnaraj, Rodrigo 2002. Ahmed, Love, Ratnaraj, 2001. Ralph, Schoeler, Krumplet 2001.). It is however not practical to cover the full range of these and as such further discussion will be limited to yttria-zirconia based powders.

Stevens has a useful summary of zirconia as an electrolyte (1986 pp. 38-39). Zirconia as an oxygen ion conducting electrolyte has a cubic fluorite structure similar to other oxide electrolytes, and in particular it has a defect structure with a finite concentration of octahedral interstitial voids (Stevens 1986 p. 38). These interstitial voids have been calculated to be larger for the O^{2-} anions than for the Zr^{4+} as was found in practice, therefore it was assumed that the O^{2-} ions were the rate controlling species in the diffusion process. As the structure is fluorite in nature a complication arises since the zirconia needs to be stabilised with other oxides such as CaO, MgO and Y_2O_3 in solid solutions and is limited to specific compositions and also these ranges have a temperature dependence (Stevens 1986 p. 38). A further complication is added to this in that the solid solutions may undergo decomposition reactions (Stevens 1986 p. 38).

The basic/idealised electrochemical cell composition is based on the system

$$p_1O_2, Pt/zirconia\ electrolyte/Pt, p_{11}O_2$$
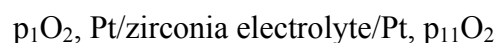
were p_1 and p_{11} are the pressure of the oxygen present.

As such an EMF (E) is generated across the electrolyte by the passage of oxygen ions. Thus the value obtained is related to the partial pressures of the oxygen at the electrodes which is given by:

$$E = \frac{RT}{4F} \int\limits_{p_1 O_2}^{p_{11} O_2} td(\ln pO_2) \qquad (1)$$

For ionic conductivity $t_{ion} \cong 1$, the EMF generated is

$$E = \frac{RT}{4F} \ln \frac{p_{11} O_2}{p_1 O_2} \qquad (2)$$

where F is the Faraday's constant, R is the gas constant and T is the temperature.

Such analysis is based on the assumption that thermodynamic equilibrium exists, and that the kinetics of the electrode interface reactions are sufficiently fast enough for representative voltages to be measured (Stevens 1986 p. 38). It can be seen from the equations that the EMF is also proportional to temperature.

Such analysis is stated for idealised systems, specifically for perfect single crystals. Commercially available zirconia electrolyte differs from this by having impurities present, in particular SiO_2 and or Al_2O_3. Incorporating these and other factors the real conduction process was first modelled by Bauerle (1969), with this work being used by Stevens (1986) to describe a network consisting of an electrode impedance, a grain boundary impedance and a bulk resistance of the zirconia. The diagrammatic representation is contained in Figure 4.
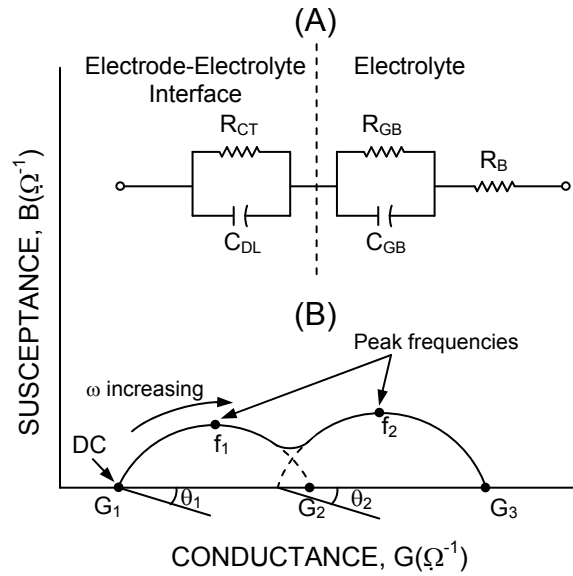
Figure 4. (A) The equivalent circuit for zirconia solid electrolyte with a porous platinum electrode. R_B = Bulk resistance, R_{GB} = grain boundary resistance, R_{CT} = charge transfer (boundary layer resistance), C_{GB} = grain boundary capacitance and C_{DL} = boundary or double layer capacitance. (B) Schematic of a complex admittance plot. (after Stevens 1986 p. 39).

1.3.2. Manufacture of Solid Oxide Fuel Cells

The manufacture of a typical self supporting planar SOFC in four steps is described below.

Step 1:- Powder and binder addition

In a batch materials fabrication process, the key ingredient is the metallic, ceramic or composite powder, this is self evident when one considers that once the binder is removed, the consolidated product is the only thing left (Mistler and Twiname 2000 p. 7). Therefore binders, plasticisers, solvents and surfactants are used simply to facilitate the fabrication process. Essentially the tape casting process is used to obtain and hold the powder particles in the desired configuration so that after sintering the final part has the desired size, shape and properties (Mistler and Twiname 2000 p. 7).

Tape casting is unique as a process in that the densification of the green ceramic comes from the forces generated wholly by the drying of the tape (slip casting whilst being a drying process has the added advantage of the capillary force generated by the plaster mould) (Mistler and Twiname 2000 p. 7). Particle size, size distribution and shape all play an important role in the densification of ceramics (Reed 1988 pp. 185-251). The surface area, or the specific surface area to be more precise, is of most importance in the tape casting process as it is the surface area that interacts with the organic additives (Mistler and Twiname 2000 p. 7).

It is common to group all of the organic groups into the generic term of "binders"; these are in reality a grouping of different products where the most common are solvents, homogenisers, surfactants and binders. The solvent allows the powder to flow as a fluid, with the homogeniser being an agent that works to make a system uniform, with the surfactant modifying the surface of the powder to impart the desired characteristics and the binders supplying the network that holds the entire chemical system together for further processing (Mistler and Twiname 2000 pp. 7-62).

The first stage is thus mixing the binder package with the powder to achieve the required rheological properties. Chapter 4 in Mistler and Twiname (2000 p. 83-185) outlines a number of ways to achieve this mixing, however the process can be seen as basically the same as mixing paint.

Step 2:- Tape Casting

Tape casting is a forming technique for producing flat ceramics. The tape thickness that can be achieved is generally in the range of 25 μm up to 1 mm, however it is possible to produce tapes down to 5 μm (Svenska Keraminstitutet 2003).
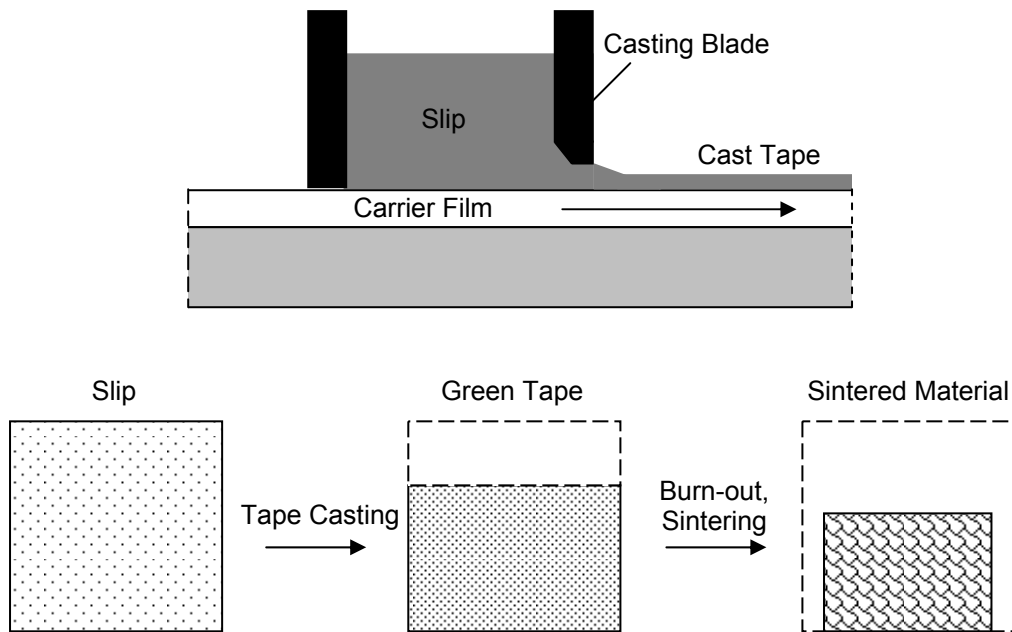
Figure 5.   Tape Casting process (After Svenska Keraminstitutet 2003).

The basic process can be seen in Figure 5. In essence it is a moving casting membrane that travels under a doctor blade. The slip is contained behind the doctor blade, which has a gap between itself and the casting membrane. The height of the gap can be seen as one of the main controlling points of the height of the green cast.

Step 3:- Shaping

Once the slip has been cast and dried the required shape is cut. As new technology becomes available, new and improved methods are introduced, however the most common in use today is blanking which is a punching process that uses a tool to cut the edges of the part (Mistler and Twiname 2000 p. 199). After blanking, the next step is the hole generation (some times refered to as Via generation), which can be achieved by hole punches and/or laser (Mistler and Twiname 2000 pp. 199-203).

It is obvious to the competent materials scientist that the above process is difficult in that the parts must be formed so that they are the right size and shape taking into account any shrinkage as well as not leading to any adverse changes in the material, such as cracking, or phase changes.

Step 4:- Sintering

Rahaman (2003) has an excellent treatment of sintering and a detailed discussion is not warranted here. It is pertinent to say that sintering needs to be controlled to give the required materials properties such as phase and grain size, but these are also material intrinsic properties and the combination of the right sintering cycle to material is of the utmost importance.

1.4. Zirconium Chemistry

1.4.1. Hydrolysis of Zirconium Oxy Chloride

The first stage of the manufacturing process of DSC is to hydrolyse crystals of Zirconium Oxy Chloride (ZOC) (This is also known as Zirconyl Chloride or Zirconyl Chloride Octahydrate). This is achieved by mixing ZOC in an agitated tank with water that has been treated to remove impurities. This step makes it difficult to directly relate the DSC process to much of the literature on zirconium chemistry as many researchers have avoided using aqueous solutions of zirconium due to its complex nature (Bradly et al 1952. Nabivanets, 1961. Zaitsev, Bochkarev 1962. Nabivanets, 1962. Yuranova, Komissarova, Plyushchev 1962. Zaitsev, Bochkarev, 1962. Marov, Ryabchikov, 1962. Milonjic, Ilic, Kopecni 1983). The research conducted on zirconium in aqueous solutions is often confusing. Elinson and Petrov (1969 p. 16) who conducted research in zirconium state *"The numerous published data on the chemistry of zirconium in aqueous solutions is often of a contradictory nature,"*. Their useful summary outlines numerous authors' work and the contradictions that have been experienced. For the reasons outlined above the following discussion is a useful introduction in terms of the current research being undertaken.

1.4.2. Zirconium Oxy Chloride

The starting material used by DSC is ZOC which is imported from China. The manufacturing process for the ZOC is usefully outlined by Choi (1965) and can be summarised as fritting zircon sand with caustic soda, the frit is thus a mixture of

sodium zirconate and sodium silicate. Water is then used to remove the soluble sodium silicate, this also hydrolyses the zirconate to an impure hydrous zirconium oxide, which is readily soluble in dilute acids. The washed frit may still contain 5% insoluble silica (Beyer et. al. 1954). For production of ZOC the frit is dissolved in hot concentrated hydrochloric acid in reaction vessels which yield the ZOC crystals when cooled.

The presence of silica in the product reduces its attractiveness as a commodity and a number of methods have been used to try and economically remove it including mechanochemical treatment (Puclin, Kaczmarek, Ninham, 1994).

The manufacturing process used in China is convoluted with numerous modifications and repeated steps so as to reduce the overall level of impurities in the ZOC. The process used by one manufacturer is detailed in point form below to highlight the difficulty of manufacturing ZOC.

Step 1 Process of Fusion

- Add 50% NaOH and maintain at temperature of $500^{o}C$ to evaporate any water, then add Zircon sand.
- Raise temperature to $600^{o}C$. Leave at temperature for 5 hours

Step 2 Cooling

- Cool for three hours.
- Remove powder from reaction kettle

Step 3 Water Leaching

- Slurry using de-mineralised water in agitated tank reaction takes 3 hours at $60^{o}C$
- Decant and filter
- Repeat three times

Step 4 transformation and filtration

- The filtrate is added to glass lined reaction vessel. pH is adjusted to three using 6% HCl at room temperature
- Temperature is increased to 60°C and left to stand for 30 minutes.
- Temperature is again raised to 105°C for 3 hours
- Product is then filtered
- Water wash then removes NaCl

Step 5 Acidify
- Mix filtrate with 33% HCl
- Heat to 110°C and maintain at temperature for three hours
- Steam is injected to maintain temperature
- Process is continued until a final concentration of ZrO$_2$ of 200 g/L is reached

Step 6 Cooling and Crystallisation
- Cooling can be through natural or forced cooling
- Once crystals have formed a centrifuge is used to filter product

Step 7 Hydrolysis
- Add flocculent and crystals to water
- Increase temperature to 80°C
- Filter using a centrifuge

Step 8 Concentration and cooling
- Transfer solution to glass lined concentrator
- Temperature is increased to 110°C using steam for approximately 5 hours
- The composition of the solution is then 200g/L ZrO$_2$ and HCl at 6.8 M.
- The solution is then aspirated and passed through a vertical condenser
- Once through the condenser the product is cooled for 72 hours were it crystallises out.

Step 9 Filtration
- The product is passed through a centrifuge

- The solid is then washed with HCl two or more times using 6.0 mol HCl followed by 4.5 mol HCl, with further washes being with concentrations above 15% of HCl. The number of washes is dependent on the trace element level of impurities required.

An area neglected in many studies of zirconium chemistry is that the manufacture of ZOC as outlined starts with a raw material that is mined and as with most geological products the composition of ore body can vary resulting in variations of types and levels of impurities being carried through to the final product. In the case of ZOC this is important as the concentration of hafnium in the product, whilst considered the same as zirconium by most manufacturers, is variable. This variability is related to the variation of concentration in the original ore body. The effect of such differences is not clear and has not been well researched.

From the previously described process the ZOC is in fact $ZrOCl_2.8H_2O$. Clearfield summarises the structure of the ZOC as having a metal coordination number of 8 with a square-antiprism coordination geometry. The structural features listed are $Zr_4(OH))_8.16H_2O^{8+} + 16Cl^-$ and the bond distance for the Zr-O bonds is given as 2.09 - 2.37 Å (Clearfield, Vaughan, 1956). This work was confirmed by infrared absorption spectra that confirmed the absence of a Zr-O double bond (Elinson, Petrov, 1969, p.18).

X-Ray diffraction studies of zirconyl halides (zirconium tetrachloride, bromide and iodide react with water to form salts which are commonly referred to as zirconyl halides) provided direct proof of the existence of polymeric species (Clearfield 1964). The stable phase that crystallizes from aqueous media is comprised of $ZrOX_2 \cdot 8H_2O$ where X is Cl, Br or I, and the zirconyl 'ion' is in reality a tetramer of the form $[Zr(OH)_2 \cdot 4H_2O]_4^{8+}$. The four zirconium atoms are located at the corners of a square that is slightly distorted and these are linked together by –ol bridges above and below the plane of the square (Clearfield 1964). The metal ion coordination is completed by four water molecules bonded to each metal centre with the eight oxygen atoms surrounding each zirconium as shown in Figure 6 . The halide ions are not bonded to the zirconium atoms but are held in the structure by electrostatic forces

and weak hydrogen bonds with the remainder of the water molecules along with the halide ions forming a matrix that holds the zirconyl complexes together (Clearfield 1964).
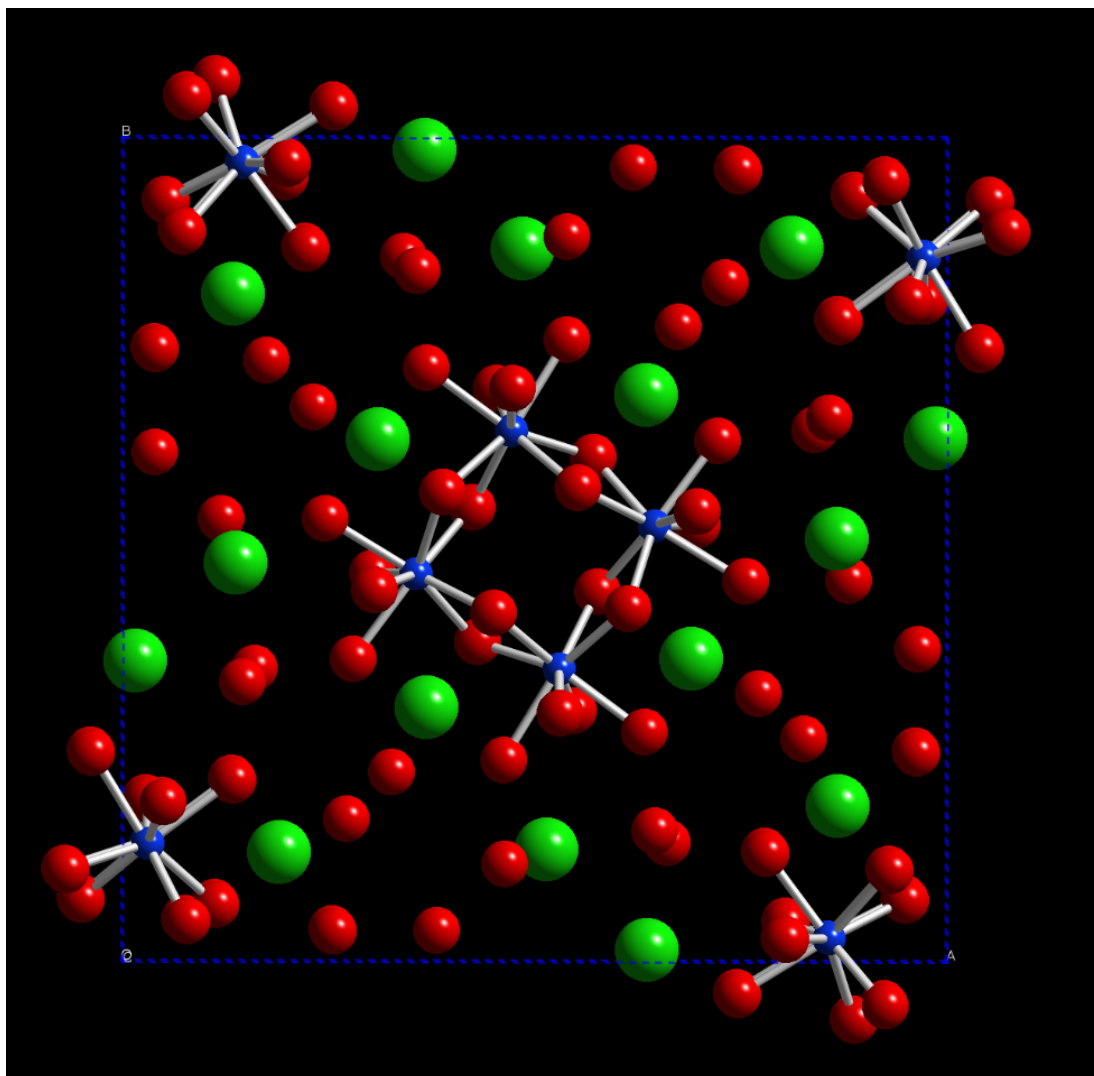
Figure 6.   Projection of one unit cell of $ZrOCl_2 \cdot H_2O$ on (001). The unit cell dimensions are $a = b = 17.08$, $c = 7.689$ Å. The z parameters in fractions of the c axis are $Zr = 0.001$, $Cl_1 = 0.364$, $Cl_2 = 0.488$, $O_8 = -0.184$, $O_2 = -0.281$, $O_3 = -0.007$, $O_4 = +0.007$, $O_9 = +0.282$ (after Clearfield 1964).

1.4.3.   Aqueous Chemistry of Zirconium

When the ZOC is added to water the pH of the resulting solution is approximately equal to that of HCl solutions of the same molarity (Blumenthal 1962). A variety of physicochemical methods have been applied to the study of aqueous solutions of

zirconium to elucidate the ion species. These studies are complicated by the sensitivity of the species to their environments and the slowness with which the systems attain equilibrium. When comparing the work of different authors it is particularly important to be cognizant of the exact conditions under which the experiments were conducted (Clearfield 1964). With this in mind Clearfield (1964) describes x-ray diffraction curves obtained from concentrated solutions of zirconyl and hafnyl halides indicated complexes, $[M_4(OH)_8(H_2O)_{16}]X_8$, where M = Zr or Hf and X = Cl or Br. In this work the halide ions were found to occupy specific sites which are marked as Cl_2 in Figure 6. There are eight such halide occupied sites in an isolated zirconyl ion; four are above the plane of the zirconium atoms and four below the plane. In contrast the crystal contains only four such sites, determined by symmetry and spatial considerations, thus in the crystal the remaining halogens occupy a second position (Figure 6) (Clearfield 1964). The exact number of halide ions associated with the tetramer was not determined with certainty but for the chloride ion it appeared to be eight.

Table 1. Ionic strength of solution and reaction equilibrium constant after Solovkin and Tsvetkova (1962).

	Reaction equilibrium constant
$Zr^{4+}_{aq} + H_2O \Leftrightarrow Zr(OH)^{3+}_{aq} + H^+_{aq}$	$K_1 = 0.60 \pm 0.05$
$Zr(OH)^{3+}_{aq} + H_2O \Leftrightarrow Zr(OH)_2{}^{2+}_{aq} + H^+_{aq}$	$K_2 = 0.24 \pm 0.01$
$Zr(OH)_2{}^{2+}_{aq} + H_2O \Leftrightarrow Zr(OH)_3{}^+_{aq} + H^+_{aq}$	$K_1 = 0.60 \pm 0.05$
$Zr(OH)_3{}^+_{aq} + H_2O \Leftrightarrow Zr(OH)_4{}^+_{aq} + H^+_{aq}$	$K_1 = 0.60 \pm 0.05$

The x-ray studies carried out using high solution concentrations yielded different results to other testing completed at lower concentrations. Slovokin and Tsvetkova (1962) built on the work of Connick and McVey (1949) and Connick and Reas (1951) in using chelating agents to determine the species of zirconium in aqueous solutions and perchloric acid solutions with Slovokin and Tsvetkova calculating the equilibrium constants for the four species that exist when Zr^{4+} is hydrolysed (Table 1). Elinson and Petrov (1969 p. 21) show that the hydrolysis of zirconium salts follow general rules with the hydrolysis of zirconium halides increasing with time and higher temperatures. The degree of hydrolysis of zirconium is affected by the

nature of the acid, for instance in perchloric acid solutions of zirconium salts it is less than in hydrochloric and nitric acid solutions (Elinson and Petrov 1969, p. 21).

The work of Connick and Reas (1951) showed that in solutions of 1 - 2 M perchloric acid and concentration of less than 10^{-4} M/L the system is monomeric. As the concentration is increased polymerisation starts, with only low molecular weight species being present (Clearfield 1964). Johnson and Kraus (1956), Kraus and Johnson (1953) studied ultracentrifugation of zirconium and hafnium in both chloride and perchlorate media and determined the polymerisation of zirconium and hafnium as a function of acidity (using HCl) (Figure 7). They found that zirconium was mono-dispersed in the range of 0.5 - 2 M HCl, while hafnium was mono-dispersed in the range 0.2 - 2M HCl. Clearfield (1964) found that the degree of polymerisation was between three and four and the charge per metal atom was about one.
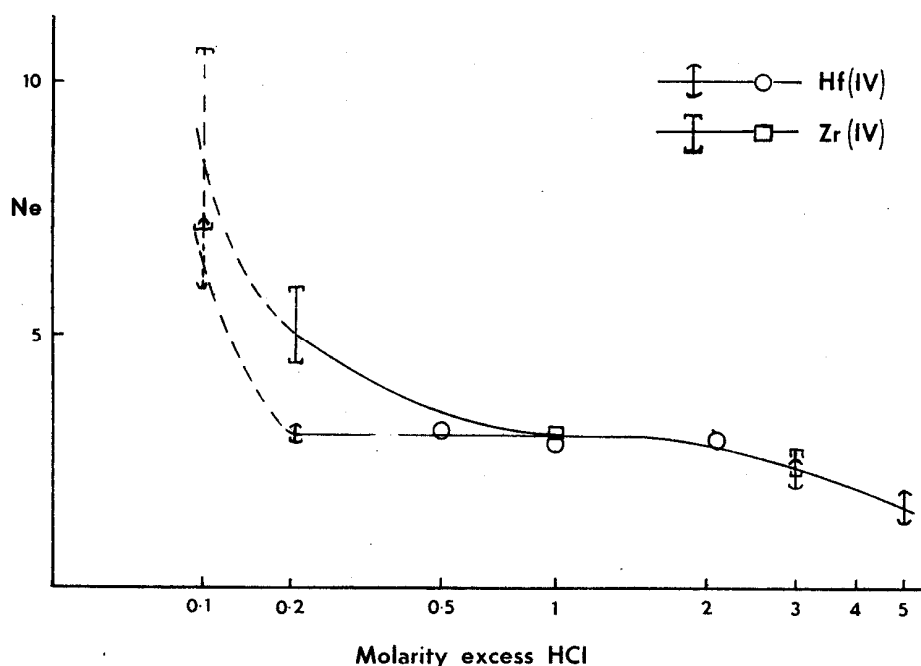

Figure 7. Average degree of polymerisation, Ne, of Hf(IV) and Zr(IV) solutions as a function of acidity (after Johnson and Kraus 1956) Copyright 1956 American Chemical Society.

Angstadt and Tyree (1962) conducted light scattering experiments on zirconyl chloride and concluded that in 2.8 M HCl the principle species is a trimer with a

charge of plus three ($[Zr_3(OH)_6Cl_3]^{3+}$) but in 0.75 M HCl the predominant species is a hexamer with a charge between plus five and plus six. A degree of polymerisation of close to four was calculated from the diffusion coefficients of the zirconium species in 1.5 M HCl.

In solutions of strong acids, for example greater than two molar $HClO_4$ or HCl the zirconium may only exist predominantly as water-solvated Zr^{4+}. This is dependent on the concentration of the zirconium and the presence of the complexing ions (Elinson and Petrov 1969, p.20). Solovkin and Tsevtkova (1962) showed that the actual extent of the hydrolysis depends on the acidity of the solution, the nature of the acid, the temperature, concentration of zirconium and other salts, types of anions in solution and the time. For example hydrolysis is greater in hydrochloric and nitric acid, than in perchloric acid. For the case of hydrochloric acid the initial hydrolysis is rapid, however equilibrium may not be reached for up to 10 days for solutions of 0.0022 - 0.125 M zirconyl chloride. Elinson and Petrov (1969, p. 27) cite the work of Starik *et. al.*, who studied the pH of solutions in relation to the state of microquantates of radioactive zirconium (Zr^{95}) in solutions. They show that in aqueous solutions, zirconium exists as simple or complex positively charged ions in concentrations of 10^{-9} to 10^{-11} M (pH 0-1.5), and as pH is increased negatively charged, highly dispersed colloids form (pH 1.5 - 5). This is summarised in Table 2 for Zr^{95} present in 10^{-9} M nitric acid solutions as various hydrolysed forms (Elinson and Petrov 1969, p. 27).

Table 2.   Forms of Zr in solution in the absence of ligands (after Elinson and Petrov 1969, p. 27).

pH	Ions and Molecules
0	Zr^{4+}, $Zr(OH)^{3+}$ (monomers)
0 - 1	Zr^{4+}, $Zr(OH)^{3+}$, $Zr(OH)_2^{2+}$, $Zr(OH)^{3+}$, $Zr(OH)_4^0$ (monomers)
1.0 - 1.5	$Zr(OH)^{3+,}$ $Zr(OH)_4^0$ (monomers)
1.5 - 4.0	$Zr(OH)_4^0$ (monomers), $[Zr(OH)_x^{4-x}]$ (polymers, pseudocolloids)
4.0 - 12	$[Zr(OH)_4]_n$ (true crystals)
> 12	Zirconates

Clearfield (1964) relates with the aid of Figure 7 that as acid concentrations increase beyond 2 M the system becomes polydispersed and depolymerisation occurs. Nabivanets (1961) and Lister and McDonald (1952), using electro-mitigation and ion exchange methods at high acidities, generally conclude that the proportion of cationic species decreases rapidly with increasing acid concentration up to $7 - 8$ M HCl and then increases slightly (Clearfield 1964). Cationic species were detected even in 15 M HCl , however appreciable amounts of anionic-zirconium species were not obtained until the HCl concentration exceeded 6 M. This then allows us to say that the zirconium cations must initially form neutral species with increasing chloride ion concentration (Clearfield 1964). This can be visualised using Figure 6 as occurring by the chloride ions occupying all eight of the sites, and depolymerisation is then thought to occur by displacement of hydroxyl by chloride ions with formation of Zr-Cl bonds (Clearfield 1964). Such depolymerisation can theoretically be repeated until monomeric, completely chlorinated species are obtained. However it was found that the species absorbed by an anion exchange resin in 15.3 M HCl had a Cl:Zr ratio of 4, thus even at high concentration hydroxo complexes are still present. This leads to the inference that it is not unlikely that the tetramer is present to some extent over the whole range of HCl concentrations and that it is possible to crystallise out zirconyl chloride from such solutions (Clearfield 1964). This can be neatly summarised in Figure 8.

Tetramer cation	$(H^+ + Cl^-)$ $\Leftrightarrow$	Neutral tetramer	$(H^+ + Cl^-)$ $\Leftrightarrow$	Lower mol wt cationic and neutral hydroxo, chloro species	Cl^- $\Leftrightarrow$	Anionic hydroxo, chloro species	Cl^- $\Leftrightarrow$	$ZrCl_6^{2-}$
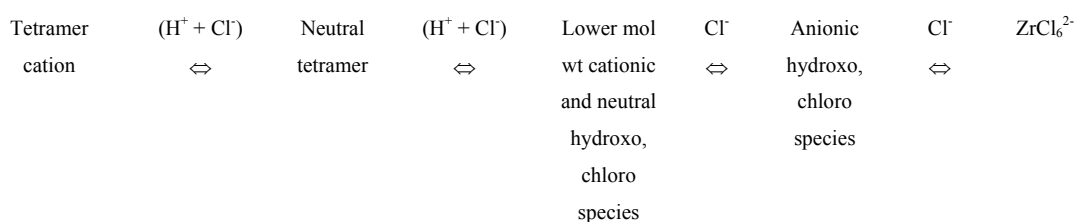
Figure 8.   Representation of depolymerisation sequence (after Clearfield 1964).

From Figure 7 it is obvious that as the acidity is reduced below approximately 0.5 M the system becomes polydispersed and the degree of polymerisation increases rapidly. Since the solution used did not reach equilibrium even after 10 days of centrifuging the curve is shown as dashed (Clearfield 1964).

Singhal et al (1996) conclude that speciation in the solution is inversely related to acidity i.e. that the species are larger as the acidity falls. These authors also offer

some modelled scattering curves for different chemical compositions. It is interesting that the Cl⁻ ions influence the modeling results with the conclusion that the scattering entity in 1.0M [H^+] added to a 0.2M zirconyl chloride solution is [$Zr_4(OH)_8(H_2O)_{16}Cl_x$]$^{(8-x)}$. This conclusion is drawn from the fact that R_g (radius of gyration) is 3.8 ± 0.2 Å.

Toth, Lin and Felker (1990) also used SAXS to investigate the R_g of zirconium in aqueous solutions however the starting material dissolved in water was $Zr(NO_3)_4$. They determined Rg for 0.035M, 0.3M and 1M Zr as 4.6, 4.5 and 4.7 Å respectively. Southon et. al. (2002) determined a similar R_g of 0.4 ± 0.04 nm for zirconyl nitrate solutions. It thus appears that there is a disparity between these authors (Toth, Lin and Felker 1990, Southon et. al. 2002, Singhal et. al 1996).

1.4.4.   Precipitation of Zirconium

The basic understanding of general precipitation is well documented and provides a basis to understand the precipitation of zirconium and zirconium-yttrium mixtures (Dirksen and Ring 1991, Nielsen 1964). Of particular significance here is the precipitation from aqueous solutions of zirconyl chloride as the pH is raised, the raising of the pH is typically achieved by the addition of NH_4OH although other bases can be used. Ammonia is the base of choice for zirconia manufacturers aiming for the advanced ceramic market as it produces zirconia with fewer trace element contaminants, such as Na as in the case of using NaOH as a replacement base. However it is recognised that ammonia is a more unfavourable waste product than caustic soda.

The precipitate that is formed from most solutions containing zirconium by the addition of a base is described as gelatinous white to seemingly clear amorphous product (Clearfield 1964, Mukherji 1970 pp.3-5, Solovkin and Tsevtkova 1962).

Again as listed previously the equation for the precipitation with aqueous ammonia as the medium for raising the pH is;

$$ZrO^{2+} + 2Cl^- + 2NH_4OH \Leftrightarrow ZrO(OH)_2 + 2NH_4Cl$$
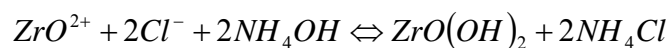
As previously mentioned this is the equation as supplied by Millennium Chemicals Research Centre Baltimore (USA). Whilst the form of the equation is reasonable a number of authors list an alternative product being $Zr(OH)_4$. The basis of several authors' work including Kovalenko and Bragdasarov (1961) revolves around assuming one structure over another, but as Kirby (2003) articulates, zirconium hydroxide is not of a definitive composition and is typically closer in structure to hydrated oxide, where the degree of hydration is dependent on many factors (Britton 1925; Singh and Banerjee 1961; Elinson and Petrov 1969, pp 7 − 8; Zaitsev and Bochkarev 1962a; Solovkin and tsevtkova 1962). Elinson and Petrov (1967 pp. 7-8) suggest that when solutions containing mostly Zr^{4+}, which is present in predominantly hot strong acids (> 1 N HCl), are precipitated the structure is of a composition closer to $Zr(OH)_4$. In comparison in weakly acidic solutions ($\cong$ 0.01 N), where the Zr is present in its hydrolysed polymeric form, the precipitate compositions are closer to $ZrO(OH)_2$.

As has been experienced with the zirconium in aqueous solutions, understanding the precipitates of zirconium is not simple and the literature can be of a contradictory nature. Thus it is prudent to start the discussion with Britton (1925) and move forward from this ground work. One of the key points from Britton's work, in which he carried out electrometric studies of the precipitation of hydroxides, was that the Cl^- to Zr ratio influenced the size of the precipitates. The inference within the work is that clear solutions mean smaller particles whilst the solutions that were opalescent have larger particles. The work, whilst not giving definitive answers, suggests that differences in the solution chemistry affect the precipitation process.

Larsen and Gammill (1950) conducted electrometric titration studies on zirconium and hafnium using zirconyl chloride as the base solution. In this work they produce tables and curves showing pH vs moles of OH^- added per mole of metal. On these curves (figure 1 p. 3615) are marked points at which precipitation and coagulation occur. These curves, apart from showing that both hafnium and zirconium behave in a very similar manner, show perchlorate, chloride and nitrate solutions behaving in

an almost identical fashion with respect to pH changes vs moles of OH⁻ added. Differences are observed however for the precipitation points. In the case of the zirconium species the chloride solution precipitated with almost 0.5 moles of OH⁻ added (this is equivalent to a pH of approximately 2) with the perchlorate and nitrate solutions precipitating at 1.0 mole added, an increase of 0.5 mole of OH⁻. The coagulation point is depicted above 1.5 moles of added OH⁻ (equivalent to approximately 6 pH points) with very little difference in the three solutions. Further points of interest on the curves are that the hafnium curve shows little difference in the precipitation points or coagulation points with the notable exception that both the chloride and perchlorate solutions precipitate at a point between 0.5 and 1.0 moles of added OH⁻ and the nitric solution's precipitation point is between 1.0 and 1.5 moles of added OH⁻.

The tables (in particular table 1 p. 3616) given by Larsen and Gammill (1950) summarise the concentration effects depicting the metal ion and salt concentration in moles per litre at the precipitation point. The other information given is the pH of precipitation and R, were R is the ratios of moles of hydroxyl ion added to the metal ion concentration. The R value is of importance in the context of the paper as the changes in this parameter are used as supporting evidence that in the case of the chloride solutions there is more than one species being precipitated out. Where an insoluble salt is precipitated out during a titration it could be expected that the R value would be a constant at all metal ion concentrations if the composition of the precipitate remains constant. The other proviso to this is that the cation-anion ratio was constant, with the exception of the salt effect on the solubility of the compound. This behaviour was found for the hafnium chloride solution, however for the zirconium nitrate and chloride solutions a pronounced decrease was observed. It was postulated that this was due to the formation of insoluble basic salts and that zirconium has a higher tendancy to form such basic salts than hafnium (Larsen and Gammill 1950).

To conclude the discussion on Larsen and Gammill's (1950) work it is appropriate to review their six conclusions. The first pointed out that in all cases in their work the pH of precipitation of hafnium was higher than that of zirconium. The second was that for perchlorate solutions the differences between hafnium and zirconium was

small, however the differences seen in the nitric and chloride solutions was marked and in the case of the zirconium chloride solution the zirconium precipitates at progressively lower ratios of hydroxyl ion added to the metal ion concentration as the metal ion concentration is reduced. Conclusion three was that in all cases increased anion concentration increases the pH of precipitation. The fourth relates that with sulphate solutions, the hafnium precipitates at lower pH's than the zirconium and that the precipitates are in all probability basic sulphates. The penultimate concluding point proposes a chemical formula for the precipitate from perchlorate solutions based around the slope of a straight line function of the logarithm of the hydroxyl ion concentration. The last point was that they had calculated the solubility products of the hydroxides for both hafnium and zirconium (Larsen and Gammill 1950).

The range of pH values for the precipitation points for differing concentrations of chloride ions was 1.88 to 2.29 (Larsen and Gammill 1950). These values are in line with the values postulated by Kovalenko and Bagdasaov (1961) who conducted dissolution studies on what they call solid $Zr(OH)_4$ where they found that dissolution in nitric acid occurs at a pH of 1.9 and increases up to a pH of 1.8. They thus detail that the precipitation must occur at these pH values as well. The solubility product was also calculated using a stoichiometric formula of $Zr(OH)_4$ in which they clarify the work by stating that the formula is assumed to be $Zr(OH)_4$. This suggests that they may not be confident in the validity of the formula.

Singh and Banerjee (1961), whilst conducting titration experiments on various solutions of zirconium, suggested that variations experienced whilst letting solutions of zirconyl chloride stand could be due to an equilibrium attained between the free acid and the salt and that this in turn affects how much base is needed to affect precipitation. This is one example of how it is thought that the solution chemistry influences the precipitation. Whilst they did not work on the speciation of the solution or the precipitate it does show a trend within the literature.

It is prudent to discuss the work of Huang et. al. (2001) who investigated the differences between zirconium hydroxide ($Zr(OH)_4 \cdot nH_2O$) and hydrous zirconia ($ZrO_2 \cdot nH_2O$). This structure is potentially different to the other structure described as $ZrO(OH)_2$ previously, but equally could be the same. No justification for its use over

the previously suggested structure (Britton 1925; Singh and Banerjee 1961; Elinson and Petrov 1969, pp 7 – 8; Zaitsev and Bochkarev 1962a; Solovkin and Tsevtkova 1962) is made in the paper by Huang et. al. (2001), but does show through the use of XPS and TGA that a difference does exist between hydrous zirconia and zirconium hydroxide and proposes a structure for the hydrous zirconia (see Figure 9). The binding energy found using XPS was 181.6 eV for zirconia (calcined at 500 C^o), 181.8 eV for hydrous zirconia and 183.6 eV for zirconium hydroxide. The method of manufacture for the hydrous zirconia used by Huang et. al. (2001) was detailed in earlier work by the same author (Huang et. al. 2000) in which they use agitated sodium hydroxide to which they add zirconium oxychloride. This is a semi solid state reaction in which the water contained within the zirconium oxy-chloride is used in the reaction. After the reaction is complete it is then washed using distilled water. The paper then goes on to state that after quickly precipitating, the product was filtered and washed. From this statement, one is left with many questions on the exact methods used and raises the following question. Is the reaction in fact a solid state reaction, or has the acid and base been dry-mixed then upon adding water the reaction occurs?

(A)   (B)
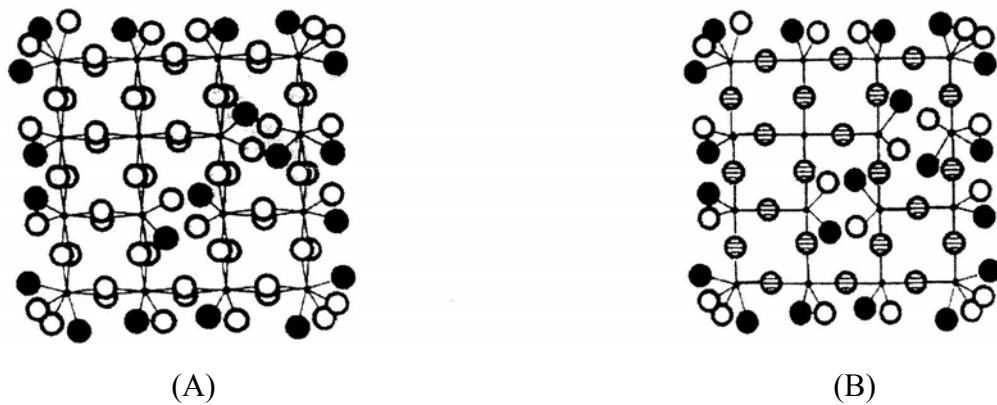
Figure 9.   (A) Schematic structure of $Zr(OH)_4$. (B) Schematic structure of Hydrous zirconia. (·) Zr; (⊜) oxide bond; (○) OH-; (●) H_2O. (After Huang et. al. 2001) Copyright 2001 American Ceramics Society.

The considerable work of Matsui et. al. (1995, 1997, 2000 and 2001) involves discussion of the formation of hydrous-zirconia using forced hydrolysis. Again the formula used is $ZrO_2 \cdot nH_2O$. The first paper in the series employs Raman

spectroscopy to investigate the formation process of hydrous zirconia. This work involved differing concentrations of zirconyl chloride solutions from 0.02 mol/l to 0.8 mol/l undergoing forced hydrolyses by heating, with the product undergoing Raman investigation. Figure 10 shows the spectra which has clear differences dependent on the concentration. For comparison Figure 11 is also supplied which is a Raman spectra of monoclinic zirconia. It is proposed in the work that the dependence of the Raman on the concentration is in fact a dependence on the H^+ and Cl^-. The chlorine content is summarised in Figure 12 which was used as justification for such claims. To investigate the Cl impact they added HCl and found that with 0.2 mol/l of HCl the peaks broaden which can be seen at the 180 cm^{-1} Raman band as the two peaks become one (see Figure 13). To separate out whether the effect was due to the Cl^- or the H^+ they used aqueous ammonia to change the H^+ concentration whilst keeping the Cl^- constant. They found that the line width of the Raman spectra of hydrous zirconia was affected by the H^+ ion concentration. A mechanism is then suggested as to how this occurs, when the $ZrOCl_2 \cdot 8H_2O$ is added to water, the tetramer complexes $[Zr(OH)_2 \cdot 4H_2O]_4^{8+}$ which are coordinated by water molecules are formed. Deprotonation then occurs to release H^+ from the coordinated water as described in the following;

$$\left[Zr(OH)_2 \cdot 4H_2O\right]_4^{8+} \Leftrightarrow \left[Zr(OH)_{2+x} \cdot (4-x)H_2O\right]_4^{(8-4x)+} + 4xH^+$$
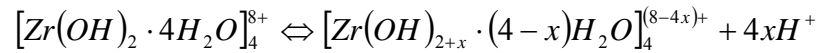
If the solution is heated the response is a shift towards the right and thus the concentrations of the H^+ ion and of $[Zr(OH)_{2+x} \cdot (4-x)H_2O]_4^{(8-4x)+}$ increase. As previously mentioned, Clearfield (1964) reported that crystalline hydrous zirconia is produced by the polymerisation of such a species. Kimura et. al (1991) found that crystalline zirconia has a positive ζ-potential at pH below 7.8, and Matsui et. al. (1995) used this information to propose that an electric double layer forms between the absorbed H^+ ions on the surface hydroxyl groups of the particle surface and Cl^- attracted from the solution. Therefore as the H^+ ions increases so does the Cl^-, and as the Cl^- ion interferes with the polymerisation between the crystal nucleus and the $[Zr(OH)_{2+x} \cdot (4-x)H_2O]_4^{(8-4x)+}$ growth of the zirconia particle is affected by the concentration of the attracted Cl^-.

Matsui et. al. (1995) used a combination of XRD, TEM and Raman spectroscopy to investigate the particle size produced with varying concentrations of zirconyl chloride and HCl. Unfortunately the figure they show relates only to a single concentration of zirconyl chloride (although this is not clear in the text) with varying levels of HCl. The particle size changes from approximately 70 Å at zero added HCl through to 30 Å with approximately 0.8 mol/l added HCl. The XRD and Raman work that was carried out additionally indicated that a structural change was taking place above a Cl/ZrO_2 ratio of ~0.5 wt% with the spectra of hydrous zirconia containing chlorine differing from the spectral patterns of monoclinic zirconia, with a weakened intensity of the Raman band. The TEM however indicated that the particle size was the same (Matsui et. al. 1995). With these experimental details and the work of Clearfield (1964) a proposed mechanism for the changes was put forward which can be summarised in the following. For solutions with high HCl concentrations the coordinated water molecules are substituted by Cl^-, with $[Zr(OH)_2Cl_m \cdot (4\text{-}m)H_2O]_4^{(8\text{-}4m)+}$ seeming to form as described by;

$$\left[Zr(OH)_2 \cdot 4H_2O\right]_4^{8+} + 4mCl^- \Leftrightarrow \left[Zr(OH)_2 Cl_m \cdot (4-m)H_2O\right]_4^{(8-4m)+} + 4mH_2O$$
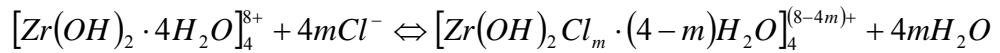
Thus hydrous zirconia containing chlorine is formed by the polymerisation of the tetramer complexes containing the Cl^- ions (Matsui et. al. 1995). This is not however a new explanation as Alison and Petrov (pp. 26 - 27) have an assumed structure for both coordinated water and the alternate Cl^- coordination. They also state that the bond between the Zr and OH are stronger than between the Zr and Cl ions, and relate the structure formation to acidity.
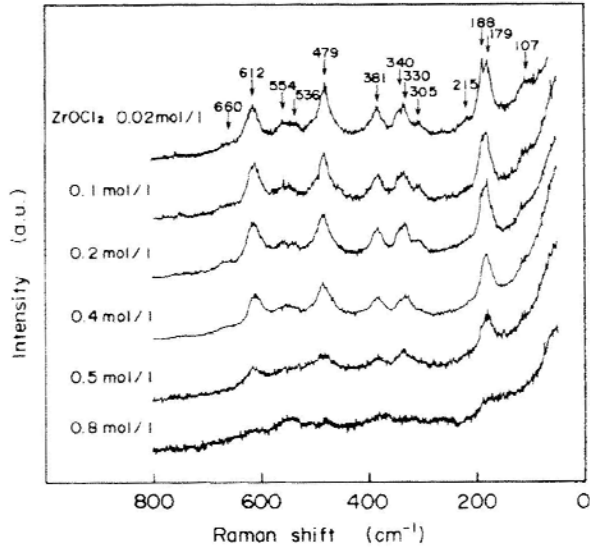
Figure 10. Raman spectra of hydrous-zirconia fine particles synthesized from aqueous solutions of various concentrations of $ZrOCl_2$. (After Matsui et. al. 1995) Copyright 1995 American Ceramics Society.
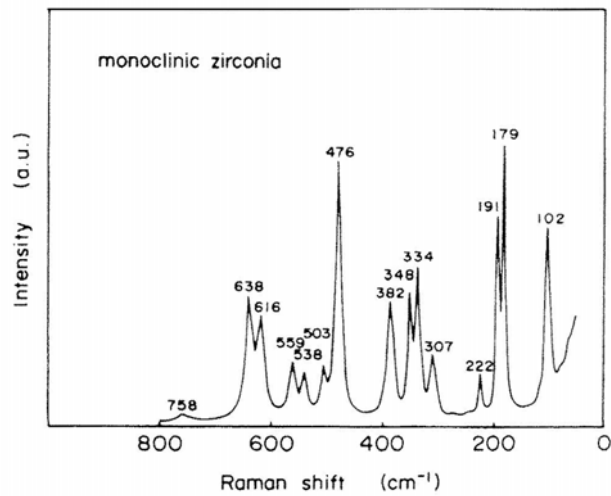
Figure 11. Raman spectra of monoclinic crystalline zirconia prepared by calcining hydrous zirconia synthesized from $ZrOCl_2$ concentrations of 0.4 mol/l. (After Matsui et. al. 1995) Copyright 1995 American Ceramics Society.
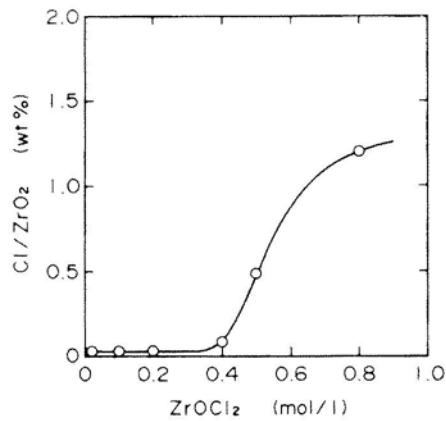
Figure 12. Chemical analysis of chlorine content in hydrous zirconia particles synthesized from aqueous solutions of various concentrations of $ZrOCl_2$. (After Matsui et. al. 1995) Copyright 1995 American Ceramics Society.
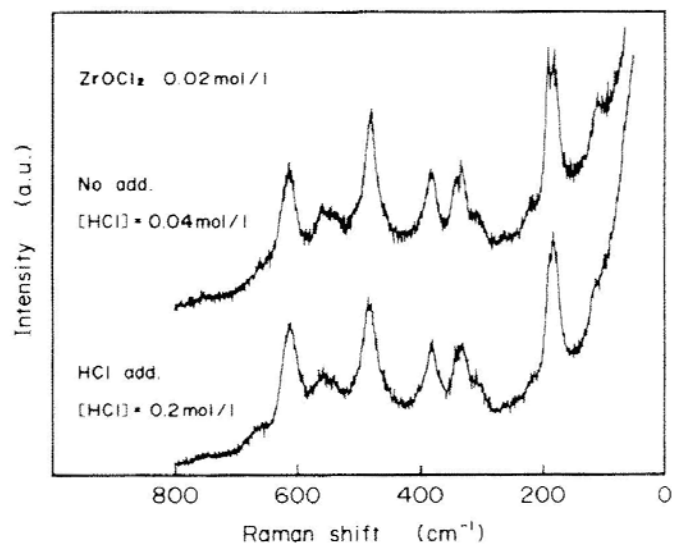
Figure 13. Raman spectra of hydrous zirconia synthesized from 0.02 mol/l $ZrOCl_2$ solutions with and without an addition of HCl (After Matsui et. al. 1995) Copyright 1995 American Ceramics Society.

1.5. Industrial Chemistry

1.5.1. General Industrial Precipitation

Batch or semi batch precipitation is the most commonly used precipitator in industry; generally there are two types, the single jet and the double jet (Myerson 2002

pp.158-159). With the double jet the two reactants are injected into an agitated vessel. It is common for the vessel to initially contain a certain amount of the solvent at preset conditions, and the reactant concentrations usually reflect the stoichiometry of the compound being precipitated as do the flow rates (Myerson 2002 pp.158 - 159). It is possible to control the feeds outside that required by stoichiometry however, so as to obtain one species above another, or to control the formation of a specific morphology of the precipitate (Myerson 2002 pp.158-159). This is the system that DSC's process is based around as they use a large agitated vessel into which the acid (zirconyl chloride) is injected, along with the base (aqueous ammonia), through separate injection lines. The control is achieved by monitoring the pH of the process as mentioned previously.

Within the general term "double jet" there are a number of variations. These centre about the point of injection of the two reactants in relation to each other and the impeller, as well as the height (in relation to distance from the base of the vessel) (Myerson 2002 pp.158 - 159). A specific example of how these factors may effect the precipitate is given by Myerson (2002 pp.158 - 159), where it is stated that a double jet system gives much larger precipitates and that the average size seems to be sensitive to the impeller stirring speed. Baldyga and Orciuch (2001) look at 3 aspects of the hydrodynamics of precipitation and give some good treatments of the effects of mixing on crystal size using computational fluid modelling by which they show that decreasing the diffusivity ratio D_{pt}/D_t increases the size of the precipitate; here the term D_{pt} is the particle turbulent diffusivity and has the units of m^2s^{-1} and D_t is the turbulent diffusivity with the same units. What this provides, in general terms, is a way at looking at the velocity field for a marked average fluid particle verses the average behaviour of an added solid particle. They present data for barium sulfate which shows such a dependence, and also use the standard method of the Reynolds number to describe the level of turbulence within the fluid system (Reynolds number is a standard concept within fluids studies and will not be treated here. It will however be briefly discussed in the experimental section with a calculation method used within this work being outlined). David (2001) also makes a differentiation between the two flow velocity fields and defines two terms. These are micro-mixing and macro-mixing, with micro-mixing being that which occurs around a reactant molecule, that is separate to the macro-mixing as experienced by the total fluid

stream. David's (2001) discussion is interesting not only in respect to such a differentiation, but also discusses the effects that different configurations of precipitators can have. In relation to the relevant flow fields however it is simple to summarise and to visualise, in that if a particle is agitated so that fluid around it is the same within the greater volume of the agitated vessel this will have an effect on the growth rate that differs to that of a particle that has a changing fluid volume surrounding it.

Roosen and Hausner (1988) discuss some ways in which agglomeration of precipitates can be influenced, they list nucleation rate, nucleation growth as being important to the strength of the agglomerates formed within the precipitation process. In this case the term agglomerates is used to describe; "a limited arrangement of primary particles, which forms a network of interconnective pores". The primary particles are held together by adhesion forces which are fully discussed in Pietsch (1991) particularly chapter 2, however the whole book is dedicated to the practical aspects of agglomeration and is useful reading. To summarize the adhesion forces, they are van der Waals forces, magnetic forces, electrostatic forces and liquid bridging (Pietsch 1991). Roosen and Hausner (1988) give a similar list but give additional, subdivisions being; electrostatic, van der Waals, liquid bridges, capillary forces, polymer bridges and solid bridges. They relate that the strength of the adhesion forces increases in the given sequence. The strength of such agglomerates can also be influenced by important precipitation parameters such as temperature, pH, concentration and type of reagents and solvents, sequence of mixing, reaction rate, method of mixing as well as the aging of the precipitates (Roosen and Hausner 1988, Myerson 2002 pp. 141 - 160).

Due to the high concentration and small particle sizes, the surface chemistry of precipitation systems as well as the colloidal stability is of importance (Myerson 2002 p. 143). The forces can be attractive or repulsive, the repulsive forces are due to the charged layer surrounding the particles and are thus electromagnetic, which is often termed the electrical double layer. The surface of the particles have a charged layer formed as a result of selective adsorption of ions. This part of the double layer is immobile and consists of tightly adsorbed ions in direct contact with the particle surface (Myerson 2002 p. 143). The solution adjacent to the particle comprises a

second layer in which the ions are more diffusely distributed, which penetrates into the liquid (termed the diffusion layer). The electrolyte concentration controls the extent of the diffusion layer. Increasing the electrolyte concentration causes this diffuse double layer to shrink closer to the particle, so that the electrostatic potential falls (Myerson 2002 p. 143).

In this work these parameters are not explored in detail but some aspects such as stirring rate will be considered while the precipitation process will be carefully controlled to ensure reproducibility.

1.6. References Cited in Introduction and Overview

Ahmed K., Love J., Ratnaraj R., 'High Performance Cell Development at CFCL' Electrochemical Society Proceedings Vol. 2001-16, 904-913 2001

Angstadt R. L., Tyree S. Y., 'The Nature of Zirconyl Chloride in Strong Hydrochloric Acid : Light Scattering', Journal of Inorganic Nuclear Chemistry Vol. 24, 913-917, 1962.

Australian Government, 'National Hydrogen Study' Commonwealth Department of Industry, Tourism & Resources, November 2003.

Australian Patent number AU-B-53972/86 and acceptance No 586467

Badwal S. P. S., Ciacchi F. T. Milosevic D., 'Oxygen-Ion Conducting Electrolyte Materials for Solid Oxide Fuel Cells' Ionics Vol. 6, 2000

Badwal S. P. S., Ciacchi F. T., Milosevic D., 'Scandia-Zirconia Electrolytes for Intermediate Temperature Solid Oxide Fuel Cell Operation' Solid State Ionics Vol. 136-137, 91-99 2000

Badwal S. P. S., Ciacchi F. T., Rajendran S., Drennan J., 'An Investigation of Conductivity, microstructure and Stability of Electrolyte Compositions in the system 9 mol% $(Sc_2O_3-Y_2O_3)-ZrO_2(Al_2O_3)$' Solid State Ionics Vol. 109, !67-186 1998

Baldyga J., Orciuch W., 'Some hydrodynamic aspects of precipitation' Powder Technology Vol. 121, 9-19 2001

Bannister M. J., Garrett W. G., 'Production of Stabilized Zirconia for use as a Solid-State Electrolyte' Ceramurgia International Vol. 1 N. 3, 127-133, 1975

Bauerle J. E. 'Study of solid electrolyte polarisation by a complex admittance technique', J. Phys. Chem. Solids 30 2657, 1969

Bellon, O. Ratnaraj, R. & Rodrigo, D 2002, 10YSZ based electrolyte materials for electrolyte supported SOFCs, *5th European SOFC Forum, Proceedings,* vol. 1, pp.184-190.

Beyer G. H., Spink D. R., West J. B., Wilhelm H. A., 'Castic Treatment of Zircon Sand' Neclear Engineering C.E.P. Symposium Series Vol. 50. No. 12, 67-72 1954

Bradly D. C., Abd-El Halim F. M., Sadek E. A., Wardlaw W., 'The preparation of Zirconium Alkoxides' Birkbeck College London, W.C.1. 2032-2035 1952

Britton, H., 'Electrometric studies of the precipitation of hydroxides. Part II. The precipitation of the hydroxides of zinc, chromium, beryllium, aluminium, bivalent tin and zirconium by use of the hydrogen electrode, and their alleged amphoteric nature', Journal Chemical Society Transaction., 127, 2120-2141, 1925.

Bluenthal W. B., 'Zirconium Chemistry in Industry' Journal of Chemical Education Vol. 39, No. 12, 605-610 1962

Carter, G. A., Titkov A., 'Technical Report MPC 10 Method for separation of coarse material' Internal Millennium Inorganic Chemicals Document 2001

Carter, G. A., 'Technical Report MPC 10 DOE plant trial MPD 041' Internal Millennium Inorganic Chemicals Document 2002

Carter, G. A., 'Technical Report MPC 14 DOE plant trial MPD 044' Internal Millennium Inorganic Chemicals Document 2003

Carter G. A., Hart R. D., Kirby N. M., Milosevic D., Titkov A. N. 2003, 'Chemically-Mixed Powders For Solid Oxide Fuel Cells', *Journal of the Australasian Ceramic Society* Vol. 39, No. 2 149-153.

Clearfield A. 'Structural Aspects of Zirconium Chemistry' Review Pure and Applied Chemistry 14, 91 91-108 1964

Clearfield A., Vaughan P. A., 'The crystal structure of Zirconyl chloride Octahydrate and zirconyl Bromide Octahydrate' Acta Cryst. 9 555-559 1956

Ciacchi F. T., Crane K. M., Badwal S. P. S., 'Evaluation of Commercial Zirconia Powders for Solid Oxide Fuel Cells' Solid State Ionics Vol. 73, 49-61 1994

Connick R. E., Reas H. W., 'The hydrolysis and polymerisation of Zirconium in Perchloric Acid Solution' Journal of the American Chemical Society Vol. 73, 1173-1176 1951

Connick R. E., McVey W. H., 'The aqueous Chemistry of Zirconium' Journal of the American Chemical Society Vol. 71, 3182-3191 1949

Choi M. S., 'Preparation of Pure Zirconyl Compounds From Zircon Caustic Frit' The Canadian Mining and Metallurgical Bulletin Feb. 1965

David R., 'General rules for prediction of the intensity of micromixing effects on precipitations' Powder Technology Vol. 121, 2-8 2001

Dirksen J. A., Ring T. A., 'Fundamentals of Crystallization: Kinetic Effects on Particle Size Distribution and Morphology' Chemical Engineering Science, Vol. 46, No. 10, 2389-2427 1991

Elinson S. V., Petrov K. I., 'Analytical Chemistry of Zirconium and Hafnium' Ann Arbor-Humphrey Science Publishers, London 1969

Foger K., Badwal S. P. S., 'Materials For Solid Oxide Fuel Cells' Materials Forum Vol. 21, 187-224 1997

Huang C., Tang Z., Zhang Z., 'Differences between Zirconium Hydroxide ($Zr(OH)_4 \cdot nH_2O$) and Hydrous Zirconia ($ZrO_2 \cdot nH_2O$)' Journal of American Ceramic Society vol. 84, No. 7, 1637-1638 2001

Hassan A. A. E., Menzler N. H., Blass G., Ali M., Buchkremer H. P., Stover D., 'Influence of alumina dopant on the properties of yttria-stabilized zirconia of SOFC applications' Journal of Materials Science Vol. 37, 2002

Johnson, J.S., Kraus K. S., 'Hydrolytic Behavior of Metal Ions VI. Ultracentrifugation of Zirconium (IV)and Hafnium (IV) Effect of Acidity on the Degree of Polymerization', Journal of the American Ceramic Society, 78, 3937-3943, 1956.

Kovalenko P. N., Bagdasarov K. N., Russian Journal of Inorganic Chemistry Vol. 6 No. 3, 272-275 1961

Kaliszewski M. S., Heuer A. H., 'Alcohol Interaction with zirconia Powders' Journal of American Ceramic Society vol. 73, No. 6, 1504-1509 1990

Kirby, N.M., PhD, Barium zirconate ceramics for melt processing of barium cuprate superconductors, 2003, Curtin University of Technology, Perth, Western Australia.

Kraus K. A., Johnson J. S., 'Hydrolytic Polymerisation of Zirconium (IV)' Journal of the American Chemical Society Vol. 75, 5769 1953

Li W., Gao L., Guo K. J., ' Synthesis of Yttria-Sabilized Zirconia Nanoparticles by Heating of Alcohol-Aqueous Salt Solutions' NanoStructured Materials Vol. 10, No. 6, 1043-1049 1998

Lauci M., 'Powders Agglomeration Grade in the ZrO_2-Y_2O_3 Coprecipitation Process' Key Engineering Materials Vols. 132-136, 89-92 1997

Larminie J., Dicks A., 'Fuel Cell Systems Explained' John Wiley and Sons, West Sussex, 2000

Larsen E. M. and Gammill M., 'Electrometric Titrations of Zirconium and Hafnium Solutions', American Chemical Society, Vol. 72, 3615-3619, 1950.

Lister B. J. A., McDonald L. A., 'Some aspects of the solution chemistry of zirconium', Journal of the Chemical Society, 4315-4330, 1952.

Marov I. N., Ryabchikov D. I. 'Complex Formation of Zr (iv) and Hf (iv) with chloride, nitrate and oxalate ions' Russian Journal of Inorganic Chemistry Vol 7 No5 533-539 1962

Mistler R. E., Twiname E. R., 'Tape Casting Theory and Practice' The American Ceramic Society, 735 Ceramic Place Westerville OH 43081 2000

Milonjic S. K., Ilic Z. E., Kopecni M. M., 'Sorption of Alkali Cations at the zirconium Oxide/Aqueous Electrolyte Interface' Colloids and Surfaces, 6, 167-174 1983

McEvoy A. J., 'Materials for High-Temperature Oxygen Reduction in Solid Oxide Fuel cells' Journal of Materials Science Vol. 36, 1087-1091, 2001

Myerson A. S., 'Handbook of Industrial Crystallization Second edition', Butterworth Heinemann, Boston225 Wildwood Ave Woburn MA 01801-2041, 2002

Matsui K., Michiharu O., 'Formation Mechanism of Hydrous-Zirconia Particles Produced by Hydrolysis of $ZrOCl_2$ Solutions' Journal of American Ceramic Society vol. 80, No. 8, 1949-56 1997

Matsui K., Michiharu O., 'Formation Mechanism of Hydrous-Zirconia Particles Produced by Hydrolysis of $ZrOCl_2$ Solutions: II, Powders' Journal of American Ceramic Society vol. 83, No. 6, 1386-92 2000

Matsui K., Michiharu O., 'Formation Mechanism of Hydrous-Zirconia Particles Produced by Hydrolysis of $ZrOCl_2$ Solutions: III, Kinetics Study for the Nucleation and Crystal-Growth Processes of Primary particles' Journal of American Ceramic Society vol. 84, No. 10, 2303-12 2001

Matsui K., Suzuki H., Michiharu O., 'Raman Spectroscopic Studies on the Formation Mechanism of Hydrous-Zirconia Fine Particles' Journal of American Ceramic Society vol. 78, No. 1, 146-52 1995

Mukherji A. K., 'Analytical Chemistry of zirconium and hafnium', Pergamon Press, Oxford, 1970.

Nabivanets B. I., 'Study of The State of Zirconium in Solution by Absorption on Ion-exchange Resins' Russian Journal of Inorganic Chemistry Vol. 7 No. 5, 609-611 1962

Nabivanets B. I., 'Electromigration of Zirconium Ions in Perchloric, Hydrochloric, and Nitric Acids' Russian Journal of Inorganic Chemistry Vol. 6 No. 5 586-590 1961

Nielson A. E., 'Kenetics of Preciitation', Pergamon, Oxford, 1964

Pietsch W., 'Size Enlargement by Agglomeration' John Wiley and Son Baffins Lane Chichester Sussex England, 1991

Puclin T., Kaczmarek W. A., Ninham B. W., 'Dissolution of $ZrSiO_4$ after mechanical milling with Al_2O_3', Materials Chemistry and Physics, 40, 75-81, 1994

Rajendran S., 'Production of Nano-Crystalline Zirconia Powders and Fabrication of High Strength Ultra-Fine-Grained Ceramics' Materials Forum Vol. 17, 333-350 1993

Rahaman M.N., 'Ceramic Processing and Sintering Second Edition', Marcel Dekker, New York, 2003.

Ralph J. M., Schoeler A. C., Krumpelt M., 'Materials for Lower Temperature Solid Oxide Fuel Cells' Journal of Materials Science Vol. 36, 1161-1172 2001

Reed J. S. 'Introduction to the principles of Ceramic Processing' John Wiley and Sons, New York, 1988

Roosen A., Hausner H., 'Techniques for Agglomeration Control During Wet-Chemical Powder Synthesis' Advanced Ceramic Materials Vol. 3, No. 2, 131-37 1988

Svenska Keraminstitutet (Swedish Ceramic Institute) 'Tape Casting' Box 5403, SE-402 29 Goteborg, Sweden Http://www.sci.se

Stevens R., 'Zirconia and Zirconia Ceramics' Magnesium Elektron Publication No. 113, Magnesium Elektron ltd, Manchester England, 1986

Singh R. P., Banerjee N. R., 'Electrometeric Studies on the precipitation of hydrous oxides of some Quadravalent Cations. Part 1. Precipitation of Zirconium Hydroxide from solutions of zirconium salts' Journal Indian Chemical Society Vol. 38. No. 11, 865-870 1961

Singh R., Gill C., Lawson S., Dransfield G. P., 'Sintering, microstructure and mechanical properties of commercial Y-TZPs', Journal of Materials Science, 31, 22, 6055-6062, 1996.

Solovkin A. S., Tsvetkova S. V., 'The Chemistry of Aqueous Solutions of Zirconium salts (Does The Zirconyl Ion Exist?)' Russian Chemical Reviews Vol. 31, No. 11, 655-669 1962

Southon P.D., Bartlett J. R., Woolfrey J. L., Ben-Nissan B., 'Formation and characterization of an aqueous zirconium hydroxide colloid'. Chemistry Materials, 14(10), 4313-4319, 2002.

Toth, L.M., Lin J. S., Felker L. K., 'Small-Angle X-ray Scattering from Zirconium(IV) Hydrous Tetramers'. Journal of Physics Chemistry, 95(8), 3106-3108, 1990.

Yuranova L. I., Komissarova L. N., Plyushchev V. E., 'Solubility and Thermal Stability of Zirconium and Hafnium Oxide nitrate Hexahydrates' Russian Journal of Inorganic Chemistry Vol. 7 No. 5, 546-548 1962

Zaitsev L. M., Bochkarev G. S., 'Preparation of Some Oxalato-Compounds of Zirconyl' Russian Journal of Inorganic Chemistry Vol. 7 No. 7, 802-806 1962

Zaitsev L. M., Bochkarev G. S., 'Peculiarities in the behaviour of zirconyl in solutions' Russian Journal of Inorganic Chemistry Vol. 7 No.4 411-414 1962

Declaration

2. Ammonia-Induced Precipitation of Zirconyl Chloride and Zirconyl-Yttrium Chloride Solutions Under Industrially Relevant Conditions

Carter G. A., Ogden M. I., Buckley C. E., Maitland C., Paskevicius M., 2009, '*Ammonia-Induced Precipitation of Zirconyl Chloride and Zirconyl-Yttrium Chloride Solutions Under Industrially Relevant Conditions*', Journal of Powder Technology, vol. [188], pp 222-228.

Ammonia-induced precipitation of zirconyl chloride and zirconyl–yttrium chloride solutions under industrially relevant conditions

Geoffrey A. Carter [a,b], Mark I. Ogden [a,*], Craig E. Buckley [b], Clinton Maitland [b], Mark Paskevicius [b]

[a] AJ Parker Centre for Integrated Hydrometallurgy Solutions, Nanochemistry Research Institute, Curtin University of Technology, PO Box U1987, Perth, Western Australia, 6845, Australia
[b] Centre for Materials Research, Curtin University of Technology, PO Box U1987, Perth, Western Australia, 6845, Australia

ARTICLE INFO

ABSTRACT

The influence of concentration and added chloride salts on the solution speciation of zirconyl chloride solutions, and the precipitate formed upon addition of aqueous ammonia, has been investigated. Crystalline zirconium oxychloride octahydrate samples available on an industrial scale were investigated using ICP-OES, XRD and SEM. The samples had a remarkably consistent level of the trace elements and LOI and contained approximately 2 wt.% hafnium. Zirconyl chloride solutions at industrially relevant concentrations of 0.81 and 1.62 M were studied by small angle X-ray scattering, and the particle radii were found to be unchanged within experimental error. Yttrium–zirconium mixed solutions relevant to the Solid Oxide Fuel Cell market (containing 3, 5, 8 and 10 mol% yttrium) were also investigated, and it was found that the added yttrium did not significantly change the particle radii or particle-particle distances.

Solutions at the same concentrations were then precipitated using a continuous double jet precipitation apparatus with aqueous ammonia as the base. Using DLS it was found that the zirconyl chloride solution at higher concentration yielded a larger precipitated particle size (1.0 ± 0.1 μm, 4.2 ± 0.1 μm). The yttrium–zirconium mixed solutions were found to give a consistent increase in particle size with increasing yttrium levels (2.0 ± 0.1 μm, 3.7 ± 0.2 μm, 4.5 ± 0.1 μm and 4.9 ± 0.2 μm). To investigate if the growth effect was most influenced by the cations or the increasing chloride concentrations, sample solutions containing mixtures of caesium chloride/zirconyl chloride and calcium chloride/zirconyl chloride with the same concentration of added chloride anions as that of the 8 mol% yttrium–zirconium sample were precipitated. The increased particle size was found to be most dependent on the type of cation and did not appear to be as significantly dependent on the concentration of chloride ions.

© 2008 Elsevier B.V. All rights reserved.

1. Introduction

Interest has been growing in zirconium and its behaviour, generated by the increased interest in Solid Oxide Fuel Cells (SOFC). The SOFC in its most basic form is a device for converting hydrogen and oxygen into water with a resulting electrical generation of power. The materials requirements of zirconia for the highly demanding Solid Oxide Fuel Cell (SOFC) market have been outlined in the literature [1,2]. The current technology for SOFC applications is based around zirconia doped with varying amounts of yttria to give the required crystallographic and mechanical properties required for the respective SOFC design and manufacturing processes [3]. Industrial manufacture of zirconia and zirconia–yttria products can be summarised as a three step operation; (a) hydrolysis of zirconyl chloride and mixing of other solutions, (b) precipitation, (c) calcination [4]. The use of aqueous solutions allows for lower costs of production and reduced waste thus being an industrially attractive way of manufacturing sub-micrometer zirconia and zirconia–yttria composites [5]. A problem with this

method is the production of hard agglomerates within the final powder [6–12]. The limited understanding of the fundamental chemistry, particularly during aqueous processing, has complicated attempts to overcome these difficulties. While some control can be achieved through the use of additives such as alcohols and other dispersants [13–15], or controlled hydrolysis using urea [14,16], for example, these methods are not readily applied to large scale industrial processing. The aim of our work is to improve understanding of the fundamental solution chemistry of the industrial process, and how this relates to the subsequent precipitation processes, and ultimately the properties of the final ceramic product.

The solution structure of zirconyl chloride is dominated by the cyclic tetramer $[Zr_4(OH)_8(OH_2)_{16}]^{8+}$, as determined using techniques such as small-angle X-ray scattering (SAXS), and extended X-ray absorption fine structure (EXAFS) spectroscopy [17,18]. It has been proposed that these tetramers can condense to form oligomers and eventually colloidal particles of "Zr(OH)₄", where the cyclic tetramers are connected by double hydroxy bridges [18]. It has been reported that a further increase in particle size involves aggregation of primary crystallites, based on dynamic light scattering (DLS) experiments in combination with transmission electron microscopy (TEM) [19]. Again condensation reactions

involving bridging hydroxyl or oxide species are believed to be involved. In support of this hypothesis, it has been shown that addition of methanol can inhibit further growth of precipitated particles, presumably by replacing non-bridging hydroxyl groups with methoxy groups, steric hindrance inhibiting further growth [5,8,9,11]. Ethanol has been reported to act in a similar manner to reduce agglomeration and inhibit growth [15]. This is useful when investigating growth of zirconium precipitation as treating the precipitates with alcohol quenches the growth at a given point in time, allowing comparison of the precipitates in relation to input variables.

The monoclinic polymorph is the most thermodynamically stable form of zirconia; a transformation to the tetragonal polymorph occurs at ~1400 K, and then to the cubic phase at ~2700 K [20]. Doping with cations of lower valency, such as yttrium(III), stabilises these high temperature forms, producing materials for use in solid oxide fuel cells as mentioned above [21]. It has been proposed, for an aqueous co-precipitation method, that the yttrium cation substitutes for a zirconium cation in the tetrameric structure, leading to the precipitation of an amorphous solid solution [22]. However, the tetramer structure is reported to be highly kinetically stable, at least under acidic conditions [17]. It is evident that unresolved issues remain and studies are further complicated by the changes in structure that are induced in the subsequent sintering stages [6].

The precipitate that is formed from most solutions containing zirconium by the addition of a base is described as a gelatinous white to clear amorphous product and is generally assumed to be $ZrO(OH)_2$, but may also be $Zr(OH)_4$ [23,24]. The equation for the precipitation upon increasing the pH with aqueous ammonia can be considered to be;

$$ZrO^{2+} + 2Cl^- + 2NH_4OH \Leftrightarrow ZrO(OH)_2 + 2NH_4Cl$$

Many authors assume a specific composition for the precipitate, but as Kirby [25] articulates, zirconium hydroxide is a poorly defined material and is typically closer in structure to hydrated oxide, where the degree of hydration is dependent on many factors [24,26–29]. Elison and Petrov [27] suggest that when solutions containing mostly Zr^{4+}, which is predominantly present in hot strong acids (>1 M HCl), are precipitated the resulting material is closer to $Zr(OH)_4$ in composition. In comparison, in weakly acidic solutions ($\cong$0.01 M), where the Zr is present in its hydrolysed polymeric form, the precipitate compositions are closer to $ZrO(OH)_2$.

These early studies also showed that solution composition influenced particle size of the precipitate. For example, Britton's electrometric studies of the precipitation of hydroxides found that the Cl to Zr ratio appeared to influence the size of the precipitates [26]. Here we report the influence of concentration and added chloride salts on the solution speciation of zirconyl chloride solutions, and the precipitate formed upon addition of aqueous ammonia.

2. Experimental procedure

2.1. Samples

Samples of $ZrOCl_2.8H_2O$ crystals from 20 one tonne bulk bags were supplied by Doral Specialty Chemicals (Rockingham, Western Australia). The supplied $ZrOCl_2.8H_2O$ was analysed for trace element levels using Inductive Coupled Plasma Optical Emission Spectroscopy (ICP-OES). The samples were also analysed for their Loss On Ignition (LOI) and ZrO_2 content.

Solutions of 100 g/L and 200 g/L of ZrO_2 (0.81 M and 1.62 M of $ZrOCl_2$) were made from zirconyl chloride crystals dissolved with milli-q water by allowing them to stand for 10 days. The samples used in the solutions came from sample bags 1, 2 and 16. These were chosen as samples representative of those with no trace elements evident (sample 16) and those with the main trace elements present. Sample 1 contained 10 ppm Al whilst sample 2 contained 20 ppm of Na and S.

Yttrium chloride was made by reacting HCl with yttria in a 1:3 stoichiometric ratio then diluting with milli-q water to a concentration of 100 g/l for the oxide. This solution was added to the zirconyl chloride solution to give 3, 5, 8 and 10 mol%.

Both the caesium chloride and calcium chloride solutions were made from solid chloride salts and milli-q water to match the concentration of the yttrium chloride solution. The solutions were added to the zirconyl chloride to give the same total Cl ion concentration as that of the 8 mol%, yttrium–zirconium mixture.

The ammonia solution was 28% AR grade.

2.2. Solution mixing

All solutions were aged for 10 days prior to use. Solutions were mixed to achieve the desired final compositions at least 24 h prior to use and left under agitation for that period using a standard laboratory magnetic stirrer and PTFE coated bar.

2.3. Small angle X-ray scattering

The small angle scattering technique was employed using the NanoSTAR SAXS instrument at Curtin University of Technology. Two sample detector distances of 65.0 and 22.8 cm were used in order to provide structural information over a wide q-range (where $q = 4\pi sin\theta/\lambda$ is the scattering vector, 2θ is the scattering angle, and $\lambda = 1.5418$ Å (Cu K_α) is the wavelength of incident radiation). The 2-dimensional detector system allowed for the detection of any anisotropy in the scattering pattern.

The SAXS sample solutions were contained within sealed glass capillaries with an external diameter of 0.5 mm and a wall thickness of 0.01 mm where the listed wall thickness variation was 0.01 mm. A long collection time of 18 h was used for each sample in order to increase the signal to noise ratio of the scattering pattern. A milli-q water sample (also in a 0.5 mm glass capillary) was used for the subtraction of the background scattering pattern. The raw 2-dimensional data files were background subtracted, and since they only displayed isotropic scattering were radially averaged over 360° in order to provide 1-dimensional data sets of the scattered intensity I and the scattering vector q. These data sets were then converted so that their scattered intensities were on an absolute scale. This was achieved using the method outlined by Buckley et al. [30], using a highly cross-linked polyethylene S-2907 standard (from Oak Ridge National Laboratories) with a collection time of 3 h.

The SAXS data was analysed using the Irena 2 SAS modelling macros [31] in the software package Igor Pro 5 (Wavemetrics, Oregon USA). The Irena macros contain a fitting package which utilises the UFM developed by Beaucage [32–34]. The UFM is especially useful for
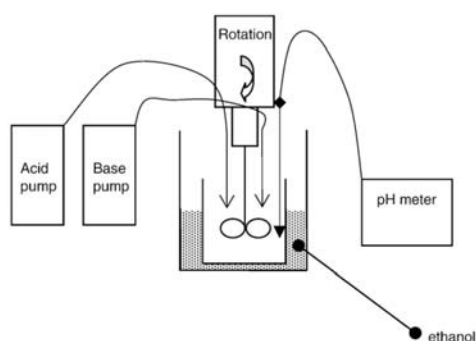

Fig. 1. Diagram of precipitation rig used in experimentation.

49

Table 1
Trace element levels by ICP-OES and LOI of 20 samples

	Trace element (ppm)										Gravimetric (wt.%) LOI
	Al	Ca	Cr	Fe	Na	Ni	P	S	Si	Ti	
Detection limit	10	20	10	10	20	10	20	20	20	5	
Sample number											
1	10	–	–	–	–	–	–	–	–	–	64.4(1)
2	–	–	–	–	20	–	–	20	–	–	64.8(1)
3	10	–	–	10	–	–	–	–	–	–	63.8(1)
4	–	–	–	10	20	–	–	–	–	–	64.6(1)
5	–	–	–	–	20	–	–	–	–	–	64.4(1)
6	–	–	–	–	20	–	–	–	–	–	61.4(1)
7	–	–	–	10	20	–	–	20	–	–	64.0(1)
8	10	–	–	–	20	–	–	–	–	–	65.4(1)
9	–	–	–	–	–	–	–	–	–	–	65.0(2)
10	–	–	–	–	20	–	–	–	–	–	65.6(1)
11	–	–	10	–	20	–	–	–	–	–	64.1(1)
12	10	–	10	–	20	–	–	–	–	–	64.6(1)
13	–	–	10	–	–	–	–	–	–	–	64.6(1)
14	–	–	–	–	–	–	20	–	–	–	67.2(1)
15	–	–	–	–	–	–	–	–	–	–	63.9(1)
16	–	–	–	–	–	–	–	–	–	–	64.5(1)
17	–	–	–	–	–	–	–	–	–	–	64.2(1)
18	–	–	–	–	–	–	–	–	–	–	64.5(1)
19	–	–	–	–	–	–	–	–	–	–	64.0(1)
20	–	–	–	–	–	–	–	–	–	–	66.3(1)

– denotes less than detectable limits.
Value in brackets denotes the uncertainty in the last decimal place.

modelling the present system because it is such a generalised scattering model. The scattering model can be customised to include the scattering from any number of structural levels which exist over various *q*-ranges in the scattering pattern. Each structural level consists of both a Guinier regime (which describes the size of the particular structure, i.e. the radius of gyration R_g of the particle) and a power-law regime (which describes how that structure is organised, i.e. whether it has smooth surfaces or is disordered). The Irena macros also incorporate a hard sphere structure factor that allows for the scattering from particle-particle correlations to be modelled (assuming they are spherical), and the HPMSA structure factor which accounts for the structure of a dispersion of charged colloidal particles (also spherical) of moderate to high densities interacting through a screened coulomb potential [35,36].

2.4. Precipitation

The system used was developed to approximate a continuous double jet precipitator, a typical industrial system (Fig. 1). The injection pumps for both the acid and base feeds were Gilson Minipulse 3 peristaltic pumps. The injection lines were positioned directly above the outer edge of the agitation impeller set 180° from each other. The pH meter was positioned 90° from both the acid inlet and base inlet with the base of the probe in the same plane horizontally as the centre of the impeller. The mixing vessel overflows into a second which contained ethanol to quench the precipitation process.

The feed rate was controlled to give a constant pH of 6 with a variation of 0.5 of a pH point. The value of 6 was used as it was found through experimentation that this point was the easiest point to control the system and it is well above the reported precipitation point of pH 1.86 to 2.79 dependent on the free HCl in the solution [26], as well as being low enough as to be economical in relation to the amount of base required. The flow rate chosen was sufficient to give approximately 1 h residence time in the first vessel, this varied minimally as the acid addition was controlled to be the same rate for all precipitations, however small variations in the amount of base used to obtain a pH of 6 resulted in some small changes in residence times. The agitator and impeller used were constant throughout the trials, as was the size of the vessels. The speed of agitation was adopted to give a Reynolds number that places the fluid volume well within the turbulent regime.

The pH of the solutions was measured using an ORION model 720A Bench-top pH meter with a Hanna 0406A glass pH electrode. Prior to measurement the instrument was calibrated using pH 7 and 4 buffer solutions it was also checked against a pH 1 buffer solution.

The reaction was commenced using a 50/50 mix by volume of milli-q water and ethanol, in the overflow vessel. The reaction vessel was initially charged with milli-q water that was agitated. The system was allowed to run to equilibrium over a period equal to 4 residence times to allow the system to come to process equilibrium. The overflow vessel was then emptied and replaced, and the system was run for a further 4 residence times. Samples for analysis were then collected from the overflow vessel. Ethanol was added at 10 min intervals to the overflow vessel so that a relatively constant 20% (by volume) alcohol to solution ratio was maintained.

2.5. Particle sizing

The particle sizing was determined using a Malvern Zetasizer nano series NANO-ZS instrument and associated proprietary software. Samples for particle sizing were sonicated in a Cole/Palmer 8891 sonic bath for 5 min, The refractive index used was that measured using a VEB Carl Zeiss Jena Abbe refractometer Model G, for a 20% alcohol/milli-q water mix.
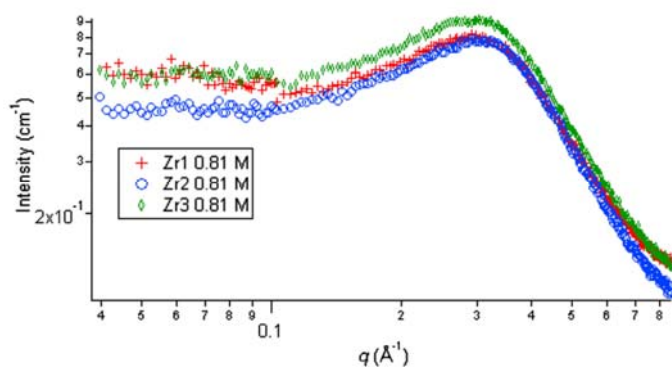

Fig. 2. SAXS data after correction for 0.81 M zirconyl chloride samples. The horizontal axis is the scattering vector q in Å^{-1} whilst the vertical axis is the absolute intensities in cm^{-1}.
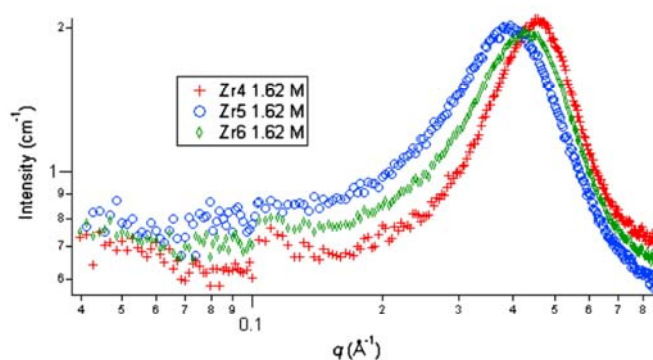
50

Fig. 3. SAXS data after correction for 1.62 M zirconyl chloride samples.

2.6. Microscopy

Images of particles were obtained using a Philips XL30 Scanning Electron Microscope (SEM). To allow for SEM investigation the solutions of precipitated hydrated zirconia were placed on stubs with carbon tape and allowed to dry under infrared light. Once dry they were carbon coated in a vacuum. Optical microscopy was conducted using a Nikon Eclipse Me600 microscope in reflected light with varying objective lenses.

3. Results

3.1. Sample analysis

The possibility that process variations were caused by trace impurities in the supplied zirconyl chloride was investigated by analysing a number of batches by Inductively Coupled Plasma Optical Emission Spectrometry (ICP-OES) (Table 1). The detectable contaminants were found to be Al, Cr, Fe, Na and S, although all were only present at the limit of detection.

The ICP results indicated that industrially available zirconyl chloride supplied is remarkably consistent and shows that only limited trace elements (in the order of the limits of detection) are present.

3.2. SAXS analysis of solutions

The impact of solution speciation upon subsequent precipitation processes of zirconyl chloride is not clear from existing literature. In particular, we aimed to determine if the introduction of yttrium resulted in any changes that might impact on the production of hard agglomerates. Johnson and Kraus conducted ultracentrifugation studies on zirconyl chloride and discussed the affects of ageing with the conclusion that ageing increases the degree of polymerization significantly [37], whilst Clearfield suggests that solutions may not have come into equilibrium even after 10 days [23]. As the literature reviewed was inconclusive on the ageing time, 10 days was chosen somewhat arbitrarily as the ageing time with the justification that the significant data collection times used in the SAXS work (18 h per sample) would be less than 10% of the ageing time. It was envisaged that this would limit the ageing effects during SAXS data collection. It was also assumed that few manufacturers would have solutions standing for greater than 10 days.

Fig. 2 shows the background-corrected, absolute scaled SAXS data for the 0.81 M zirconyl chloride solutions and Fig. 3 shows the results for the 1.62 M zirconyl chloride solutions. Fig. 4 is the data for the zirconyl chloride and yttrium chloride solutions; the concentration of the zirconyl chloride was 0.81 M. The data can be clearly grouped into two classes, based on the solution concentration (0.81 M. and 1.62 M.). The data displayed in Fig. 2 correspond well with that given by Toth et al. who reported a peak for a 0.6 M solution of Zr(IV) occurring just below 0.3 Å^{-1} with the peak for a sample of 1 M concentration occurring at approximately 0.35 Å^{-1} [38]. These results correlate with the solutions presented here, where a maximum peak occurs at 0.30 Å^{-1} for a 0.81 M solution and between 0.4 and 0.5 Å^{-1} for the 1.62 M solutions.

Generally the average Bragg like spacing between domains d_p is determined from $2\pi/q_{max}$, where q_{max} is the value of q for the
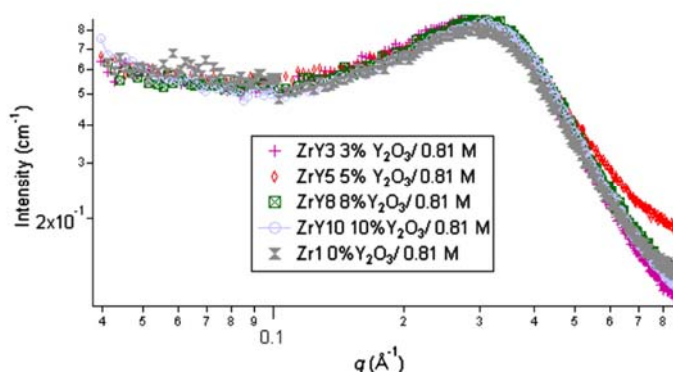

Fig. 4. SAXS data after correction for all yttrium–zirconium mixed samples, from 0 to 10 mol%.

51

Table 2
Results of SAXS and precipitate particle size analyses, including pH, concentration, radius of gyration R_g (Å), particle radius R (Å), packing factor k and particle to particle interaction distance d_p (Å), and precipitate particle size mean diameter p (μm)

Sample	Concentration (M)	Added cations	pH	$R_g\pm$ 0.3 Å	k	$R\pm$ 0.4 Å	d_p (Å)	p (μm)
Zr1	0.81		0.74	4.4	1.64	5.7	21	1.0(1)
Zr2	0.81		0.74	4.3	1.80	5.6	21	
Zr3	0.81		0.73	4.4	1.62	5.7	21	1.1(1)
Zr4	1.62		0.45	3.9	5.24	5.1	14	
Zr5	1.62		0.46	3.9	3.80	5.1	15	
Zr6	1.62		0.47	4.1	3.70	5.3	16	4.2(1)
ZrY3	0.81	YCl$_3$ (3 mol%)	0.77	4.3	1.60	5.6	22	2.0(1)
ZrY5	0.81	YCl$_3$ (5 mol%)	0.76	4.3	1.31	5.6	21	3.7(2)
ZrY8	0.81	YCl$_3$ (8 mol%)	0.77	4.3	1.70	5.6	22	4.5(1)
ZrY10	0.81	YCl$_3$ (10 mol%)	0.72	4.3	1.74	5.6	20	4.9(2)
ZrCa4	0.81	CaCl$_2$ (4.2 mol%)	0.76					2.6(1)
ZrCs13	0.81	CsCl (12.7 mol%)	0.76					1.8(1)

maximum peak intensity and thus this is the distance between particles [32]. Since several of the peak shapes in our work are a convolution of the Guinier particle size and the correlation between particles, the average radial distance between particles η is determined either from the UFM [32] or the HPMSA (see Supplementary Information for details on the data analysis). The average radial distance between particles η is similar to the Bragg like spacing but relates a circle of radius η that separates each particle. Table 2 contains the relevant structural and chemical information for the solutions analysed by SAXS. A key point that can be extracted from these data is that the particle radius of the solution species is not changing significantly as solution concentration is increased, nor is it changing up on the addition of yttrium chloride. Toth et al. investigated solutions with concentrations from 0.035 to 1 M of Zr and concluded that the R_g of the lower concentrations was 4.5 Å±0.1 Å with the higher concentrations returning 4.6 Å±0.1 Å, consistent with the results reported here [38].

It appears that there is no significant change in the solution speciation of zirconyl chloride solutions, at least as reflected by the particle radius, with changes in concentration or addition of yttrium chloride. Our investigations thus moved on to the precipitation step of the process.

3.3. Particle size

The aim of this section of the work was to determine how solution composition might impact on the precipitation of the zirconyl
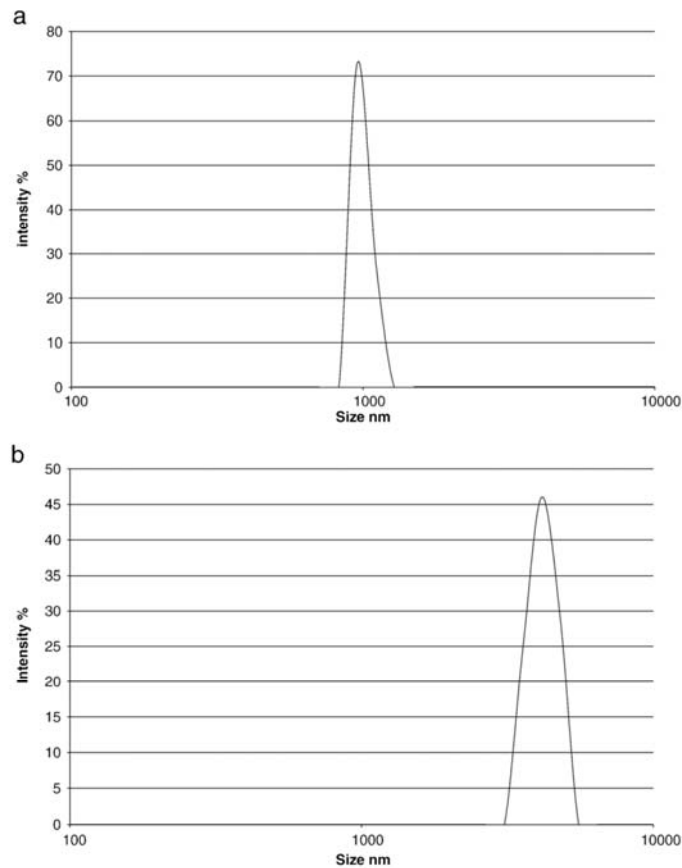

Fig. 5. (a) DLS results for 0.81 M precipitates (PS 990 nm), (b) DLS results for ZrY8 precipitates (PS 4480 nm).

oxyhydroxide upon addition of base. The experiments were designed to allow the precipitation to proceed for a certain residence time, after which the growth would be quenched by the introduction of ethanol. To assess and confirm the effect of ethanol in quenching the further growth of the particles, precipitation of a sample of 8 mole% yttrium doped zirconyl chloride was carried out with and without added ethanol in the overflow vessel. With the addition of ethanol the precipitate produced was well dispersed and appeared to be suitable for particle sizing even after standing for 24 h. In the absence of ethanol, a gelatinous cake resulted that was very dense and difficult to remove from the vessel. Only partial dispersion was possible, and optical microscopy showed many 20 to 30 μm spherical particles, in addition to a large number of smaller particles. The particles were soft and readily broken or deformed. These results indicated that the alcohol is acting as suggested in the literature and inhibiting growth and agglomeration [8,9,11,15].

The DLS particle sizing results are given in Table 2. Fig. 5(a) and (b) are examples of the results from the DLS; all results contained single well-defined peaks. The results listed in Table 2 were developed using at least 15 tests on the same sample. To confirm the reproducibility of the test regime five replicates were made of Zr1 and ZrY8, which were found to be consistent within the standard deviation of the analysis.

To support the DLS results optical and electron microscopy was performed to directly determine the size of the particles. Initially, the samples were washed with ethanol, and then resuspended in ethanol and deposited onto a slide for imaging. The samples were found to be hygroscopic, and this was ascribed to residual ammonium chloride, which has poor solubility in ethanol. The washing regime was thus altered to a mixture of 65% methanol, 20% milli-q water, and 15% reacted solution. The filtrate was then re-suspended in ethanol, and spin coated onto a glass slide. These particles were carbon coated and imaged using SEM. Imaging was complicated by the fact that the particles suffered from some transformation in the beam. The transformation is believed to be dehydration where the hydrated zirconium transforms to zirconia. A low beam current and accelerating voltage with large spot size and working distance was required, resulting in less than ideal images (Fig. S1). Nevertheless, it was possible to use the measurement facilities of the XL30 SEM software to determine the size of the particles. The particle sizes were found to be, on average, 20–30% smaller than those measured by DLS. This is not unexpected, since the particles may have dehydrated to some extent upon isolation, and the DLS measures the hydrodynamic radius of the particles.

In Table 2 it is evident that increasing the zirconyl chloride concentration has a dramatic effect, doubling of the concentration (0.81 M to 1.62 M) results in a four times increase in particle size (1.0±0.1 μm to 4.2±0.1 μm). An increase in particle size was expected since the effective supersaturation is higher in the more concentrated solution, leading to increase in growth rate over the residence time of the experiment.

A more remarkable result is the increase in particle size with increasing addition of yttrium chloride (Table 2). The SAXS results described above suggested that the zirconyl chloride solution species was unchanged with added yttrium chloride, so this increase in precipitated particle size is unlikely to be related to changes in solution speciation. Britton suggested that the Cl to Zr ratio influenced the precipitate size [26]. In addition, an increase in aggregate size with added yttrium chloride has been reported more recently, although without specific comment on the origin of the effect [14]. To investigate if the effect was due to the increased chloride concentration as suggested, a solution of caesium chloride was added to the zirconyl chloride solution and precipitation carried out. The caesium chloride was doped into the zirconyl chloride to give the same overall chloride concentration as that of the sample containing 8 mol% yttrium (ZrY8). The added caesium chloride did result in an increase in the precipitate particle size, however, the increase did not approach that found for the ZrY8 sample (Zr3≈1.0, ZrCs13≈1.8; ZrY8≈4.5 μm). To further investigate these results, a solution with added calcium chloride was precipitated. This

solution was prepared again to match the chloride concentration of both the ZrCs13 and 8 mol% yttrium samples (ZrY8). The particle size was found to be larger than the ZrCs13 sample but smaller than yttrium sample (ZrCa4≈2.6 μm). From this it is possible to say that the growth seen in the yttrium doped samples is not entirely due to the change in chloride concentration. This suggests that the cations are taking part in the precipitation process to allow growth of the precipitates and that the charge of the cations influences the particle size. A possible explanation is that the cations are enhancing the coagulation of the initially formed particles, which would suggest that the precipitate surface carries a negative charge. The greater efficacy of the higher charge cations is consistent with this hypothesis, and further investigation is underway to characterise the surface charge of the precipitate.

4. Conclusions

Samples of industrially available crystalline zirconium oxychloride octahydrate were investigated. ICP-OES found that the major trace elements were only present at the limit of detection. SAXS investigation of solutions at two industrially relevant concentrations of zirconyl chloride (0.81 and 1.62 M) suggested that the zirconyl speciation was unchanged. Addition of yttrium chloride also had little effect on the SAXS measurement particle radii.

Precipitation was performed using aqueous ammonia as the base. The precipitate particle sizes were measured by DLS with the 1.62 M solution found to have a significantly larger particle size than the 0.81 M solution (4.2 μm, 1.0 μm). The particle sizes were confirmed by electron microscopy, and were found to be in reasonable agreement. The effect on particle size of adding yttrium chloride was also investigated. Samples of 3, 5, 8 and 10 mol% yttrium–zirconium were found to have increasing particle size with increasing yttrium concentration (2.0, 3.7, 4.5, and 4.9 μm respectively). Experiments were carried out to determine if the change in particle size was predominantly a result of the added cations, or anions. Precipitations were performed with added caesium chloride and calcium chloride, such that the chloride concentration matched that of the 8 mol% yttrium–zirconium solution in each case. The precipitate particles sizes increased with the cation charge (ZrCs13, 1.8 μm; ZrCa4 2.6 μm; ZrY8, 4.5 μm), all being larger than the system with no additives (1.0 μm), despite the fact that the chloride concentration is constant. Thus, it appears from these data that the particle size increase is dependent on the charge of the added cation, and less so on the chloride concentration.

From this work it is evident that the growth rate of precipitated particles for zirconyl chloride solutions is dependent on the concentration of the starting solution as well as the concentration of added cation and the type of cation present. Controlling these factors may enable optimisation of the precipitate particle size. The impact of added cations on properties such as particle surface charge, and on downstream processing of the zirconia is under investigation.

Appendix A. Supplementary data

Supplementary data associated with this article can be found, in the online version, at doi:10.1016/j.powtec.2008.04.087.

References

[1] O. Bellon, R. Ratnaraj, D. Rodrigo, 10YSZ based electrolyte materials for electrolyte supported SOFC's, 5th European SOFC Forum, 2002.

53

[2] K. Foger, S.P.S. Badwal, Materials for solid-oxide fuel cells, Mater. Forum 21 (1997) 187–224.
[3] F.T. Ciacchi, K.M. Crane, S.P.S. Badwal, Evaluation of commercial zicronia powders for solid oxide fuel-cells, Solid State Ionics 73 (1–2) (1994) 49–61.
[4] G. Carter, R.D. Hart, N.M. Kirby, D. Milosevic, A.N. Titkov, Chemically-mixed powders for solid oxide fuel cells, J. Australas. Ceram. Soc. 39 (2) (2003) 149–153.
[5] S.L. Jones, C.J. Norman, Dehydration of hydrous zirconia with methanol, J. Am. Ceram. Soc. 71 (4) (1988) C190–C191.
[6] M. Bannister, W. Garrett, Production of stabilized zirconia for use as a solid-state electrolyte, Ceramurg. Int. 1 (3) (1975) 127–133.
[7] A.G. Belous, K.V. Kravchyk, E.V. Pashkova, O. Bohnke, C. Galven, Influence of the chemical composition on structural properties and electrical conductivity of Y–Ce–ZrO₂, Chem. Mater. 19 (21) (2007) 5179–5184.
[8] M.S. Kaliszewski, A.H. Heuer, Alcohol interaction with zirconia powders, J. Am. Ceram. Soc. 73 (6) (1990) 1504–1509.
[9] M. Lauci, Powders agglomeration grade in the ZrO₂–Y₂O₃ coprecipitation process, Key Eng. Mater. 132–136 (1997) 89–92.
[10] W. Li, L. Gao, J.K. Guo, Synthesis of yttria-stabilized zirconia nanoparticles by heating of alcohol aqueous salt solutions, Nanostruct. Mater. 10 (6) (1998) 1043–1049.
[11] S. Rajendran, Production of nano-crystalline zirconia powders and fabrication of high strength ultra-fine-grained ceramics, Mater. Forum 17 (1993) 333–350.
[12] J.S. Reed, Introduction to the Principles of Ceramic Processing, John Wiley and Sons, New York, 1988.
[13] M.Q. Li, Making spherical zirconia particles from inorganic zirconium aqueous sols, Powder Technol. 137 (1–2) (2003) 95–98.
[14] A.P. Oliveira, M.L. Torem, The influence of precipitation variables on zirconia powder synthesis, Powder Technol. 119 (2–3) (2001) 181–193.
[15] S.Y. Wang, X. Li, Y.C. Zhai, K.M. Wang, Preparation of homodispersed nano zirconia, Powder Technol. 168 (2) (2006) 53–58.
[16] Y.X. Huang, C.J. Guo, Synthesis of nanosized zirconia particles via urea hydrolysis, Powder Technol. 72 (1) (1992) 101–104.
[17] C. Hagfeldt, V. Kessler, I. Persson, Structure of the hydrated, hydrolysed and solvated zirconium(IV) and hafnium(IV) ions in water and aprotic oxygen donor solvents. A crystallographic, EXAFS spectroscopic and large angle X-ray scattering study, Dalton Trans. 14 (2004) 2142–2151.
[18] P.D. Southon, J.R. Bartlett, J.L. Woolfrey, B. Ben-Nissan, Formation and characterization of an aqueous zirconium hydroxide colloid, Chem. Mater. 14 (10) (2002) 4313–4319.
[19] M.Z.C. Hu, M.T. Harris, C.H. Byers, Nucleation and growth for synthesis of nanometric zirconia particles by forced hydrolysis, J. Colloid Interface Sci. 198 (1) (1998) 87–99.
[20] M. Fernandez-Garcia, A. Martinez-Arias, J.C. Hanson, J.A. Rodriguez, Nanostructured oxides in chemistry: characterization and properties, Chem. Rev. 104 (9) (2004) 4063–4104.

[21] R.M. Ormerod, Solid oxide fuel cells, Chem. Soc. Rev. 32 (1) (2003) 17–28.
[22] X. Bokhimi, A. Morales, A. Garcia-Ruiz, T.D. Xiao, H. Chen, P.R. Strutt, Transformation of yttrium-doped hydrated zirconium into tetragonal and cubic nanocrystalline zirconia, J. Solid State Chem. 142 (2) (1999) 409–418.
[23] A. Clearfield, Structural aspects of zirconium chemistry review, Pure Appl. Chem. 14 (1964) 91–108.
[24] A.S. Solovkin, S.V. Tsvetkova, The chemistry of aqueous solutions of zirconium salts (does the zirconyl ion exist?), Russ. Chem. Rev. 31 (11) (1962) 655–669.
[25] N.M. Kirby, Barium zirconate ceramics for melt processing of barium cuprate superconductors, Curtin University of Technology, Perth, Western Australia, 2003.
[26] H. Britton, Electrometric studies of the precipitation of hydroxides. Part II. The precipitation of the hydroxides of zinc, chromium, beryllium, aluminium, bivalent tin and zirconium by use of the hydrogen electrode, and their alleged amphoteric nature, J. Chem. Soc., Trans. 127 (1925) 2120–2141.
[27] S.V. Elinson, K.I. Petrov, Analytical Chemistry of Zirconium and Hafnium, Ann Arbor-Humphrey Science Publishers, London, 1969.
[28] R.P. Singh, N.R. Banerjee, Electrometric studies on the precipitation of hydrous oxides of some quadravalent cations. Part 1. Precipitation of zirconium hydroxide from solutions of zirconium salts, J. Indian Chem. Soc. 38 (11) (1961) 865–870.
[29] L.M. Zaitsev, G.S. Bochkarev, Peculiarities in the behaviour of zirconyl in solutions, Russ. J. Inorg. Chem. 7 (4) (1962) 411–414.
[30] C.E. Buckley, C. Maitland, D. Scott, G. Carter, J. Connolly, Comparison of specific surface area determined from small angle X-ray scattering (SAXS) and BET, J. Australas. Ceram. Soc. 40 (2) (2004) 7–12.
[31] J. Ilavsky, Irena 2 SAS modelling macros, Advanced Photon Source, Argonne National Laboratory, 2005.
[32] G. Beaucage, Approximations leading to a unified exponential power-law approach to small-angle scattering, J. Appl. Crystallogr. 28 (1995) 717–728.
[33] G. Beaucage, D.W. Schaefer, Structural studies of complex-systems using small-angle scattering — a unified Guinier power-law approach, J. Non-Cryst. Solids 172 (1994) 797–805.
[34] G. Beaucage, T.A. Ulibarri, E.P. Black, D.W. Schaefer, Multiple size scale structures in silica-siloxane composites studied by small-angle scattering, Hybrid Organic-Inorganic Composites, ACS Symposium Series, 1995, pp. 97–111.
[35] J.P. Hansen, J.B. Hayter, A rescaled MSA structure factor for dilute charged colloidal dispersions, Mol. Phys. 46 (3) (1982) 651–656.
[36] J.B. Hayter, J. Penfold, An analytic structure factor for Macroion solutions, Mol. Phys. 42 (1) (1981) 109–118.
[37] J.S. Johnson, K.S. Kraus, Hydrolytic behavior of metal ions VI. Ultracentrifugation of zirconium (IV) and hafnium (IV) effect of acidity on the degree of polymerization, J. Am. Chem. Soc. 78 (1956) 3937–3943.
[38] L.M. Toth, J.S. Lin, L.K. Felker, Small-angle X-ray scattering from zirconium(IV) hydrous tetramers, J. Phys. Chem. 95 (8) (1991) 3106–3108.

54

3. The Effect of Processing Parameters on Particle Size in Ammonia-Induced Precipitation of Zirconyl Chloride Under Industrially Relevant Conditions.

Carter G., Hart R., Rowles M., Ogden M., Buckley C., 2009, '*The Effect of Processing Parameters on Particle Size in Ammonia-Induced Precipitation of Zirconyl Chloride Under Industrially Relevant Conditions*', Journal of Powder Technology, doi: 101016/j.powtec.200810.012.

The effect of processing parameters on particle size in ammonia-induced precipitation of zirconyl chloride under industrially relevant conditions

G.A. Carter [a,b], R.D. Hart [b], M.R. Rowles [c], C.E. Buckley [b], M.I. Ogden [a,*]

[a] Nanochemistry Research Institute, Curtin University of Technology, PO Box U1987, Perth, Western Australia, 6845, Australia
[b] Centre for Materials Research, Curtin University of Technology, PO Box U1987, Perth, Western Australia, 6845, Australia
[c] Commonwealth Scientific Industrial Research Organisation (CSIRO) Minerals Clayton South, Victoria, Australia

ARTICLE INFO

ABSTRACT

The effect of pH of precipitation, starting solution concentration, and agitation levels on the particle size of hydrous zirconia precipitates have been investigated. It was found that all three variables affect the particle size of the hydrous zirconia. The smallest particle size is produced by a 0.81 M starting solution, precipitated at pH 12 with a high agitation level. The pH of precipitation was also found to have a significant impact on the type of hydrous zirconia produced. TGA/DTA, micro combustion and TEM/EDS were used to investigate the difference in the powders produced at pH 3 and 12. This work suggests that powders produced at pH 3 will have a structure similar to $Zr[OH]_4$ whilst those at pH 12 are more likely $ZrO[OH]_2$. XRD and micro-combustion suggest that the powders produced at pH 3 retained ammonium chloride whilst those produced at pH 12 did not. The filtration rates for the pH 3 product were significantly faster than that of the powders made at pH 12 which is significant in the industrial production of these materials.

© 2008 Elsevier B.V. All rights reserved.

1. Introduction

Recent studies of hydrous zirconia for the eventual preparation of yttria stabilised zirconia have investigated the formation of hard agglomerates produced during aqueous precipitation of hydrous zirconia precursor from zirconyl chloride solutions [1]. The formation of these hard agglomerates is industrially relevant as they are a significant impediment to the use of these materials in the large scale production of ceramic powders for purposes such as solid oxide fuel cells [2,3]. Whilst not the primary focus of the reported studies, literature suggests both zirconium species and precipitate particle size can be affected by the pH of precipitation, concentration and agitation rate [4,5]. These properties are crucial in the industrial processing of these powders as they impact on parameters such as filtration rates and rheology. These effects eventually result in processing and performance issues in the ceramics produced [1].

Larsen and Gammill [6] conducted electrometric titration studies on zirconium and hafnium using zirconyl and hafnyl chlorides as the base solutions. They produced tables and curves showing precipitation occurs for zirconium at pH of approximately 2 and coagulation occurred pH ~6. The hafnium curve shows little difference in the precipitation points or coagulation points from the zirconyl solution.

Later extensive work by Clearfield [4] suggested that the precipitation process was a hydrolytic polymerisation, and that precipitation occurred at a low pH and was completed before the end

point of neutralisation is reached. Clearfield explains that this is due to the retention of anions by the precipitate and that the amount of anion retention is dependent on pH, decreasing as the pH of precipitation increases. It was suggested that this behaviour indicates that the precipitates should be viewed as basic salts of variable composition [4]. Larsen and Gammill [6] also postulated the formation of basic salts by zirconium compounds and used this to explain differences found between the precipitation of hafnium and zirconium with respect to chloride ion content. The range of pH values for the precipitation points for differing concentrations of chloride ions was 1.88 to 2.29 [6]. These values agree with the results of Kovalenko and Bagdasaov [7] who conducted dissolution studies on what they call solid $Zr(OH)_4$ where they found that dissolution in nitric acid occurs at a pH of 1.9 and increases up to a pH of 1.8. They suggest that the precipitation must occur at these pH values as well. The solubility product was also calculated using a stoichiometric formula of $Zr(OH)_4$ although it is made clear in the paper that this formula is an assumption. Huang et al. [8] investigated the differences between zirconium hydroxide (Zr $(OH)_4 \cdot nH_2O$) and hydrous zirconia ($ZrO_2 \cdot nH_2O$) but did not investigate the previously suggested structure $ZrO(OH)_2$ [9–13].

The nature of zirconium hydroxide species precipitated under acidic conditions has also been investigated using thermal and X-ray techniques [14,15]. The suggested structure, which differs from the previous literature, is $Zr_4O_3(OH)_{10} \cdot 6H_2O$. The authors compare this structure with α-$Zr_4(OH)_{16}$, β-$Zr_4O_2(OH)_{12}$ and γ-$Zr_4O(OH)_8$ with the major difference being the coordinated water ([14] and references therein). The suggested structure for hydroxides produced at pH 4 and 3 is the same although no data are shown for the pH 3 sample [14].

* Corresponding author. Tel.: +61 8 9266 2483; fax: +61 8 9266 4699.
E-mail address: m.ogden@exchange.curtin.edu.au (M.I. Ogden).

56

Table 1
Particle size and filtration rates for varying pH, concentrations of zirconyl chloride and agitations

pH	Concentration of starting solutions	Agitation level	PSD (nm)	Filtration rate minutes
3	0.81	Low	1820	6.8
3	0.81	High	1130	7
3	1.62	Low	3390	4.3
3	1.62	High	2160	5.9
12	0.81	Low	309	>20
12	0.81	High	49	>60
12	1.62	Low	743	>15
12	1.62	high	73	>60

Clearfield [16] reviews a number of the papers discussed in [14] and points out that the majority of these authors have neglected the work he completed [4] in their assessments of the polymerisation process that zirconium undergoes. He reiterates that the differences seen in the polymorphs of zirconia after calcination can be related to the speed at which the zirconia is produced, with a slower process leading to a more ordered structure that thus forms the tetragonal polymorph and a faster reaction leading to monoclinic. Whilst not directly linked to the wet chemistry, the polymorphs produced have been reported to be associated with crystallite size, with a transition from tetragonal to monoclinic occurring when crystallites grow above 30 nm [17].

Roosen and Hauser discuss some ways in which agglomeration of precipitates can be influenced, listing nucleation rate and nucleation growth as being important to the strength of the agglomerates formed

within the precipitation process [18]. In this case the term agglomerates is used to describe; "a limited arrangement of primary particles, which forms a network of interconnective pores". The primary particles are held together by adhesion forces which are fully discussed in [19]. The strength of such agglomerates can also be influenced by important precipitation parameters such as temperature, pH, concentration and type of reagents and solvents, sequence of mixing, reaction rate, method of mixing as well as the aging of the precipitates [18,20].

The authors have reported previously the effects of acidity on the formation of zirconium species and the effect of concentration and counter cations on the particle size of the precipitates [1]. The current work examines in more detail the effects of pH, concentration and agitation upon the zirconium species, precipitate particle size, and various processing parameters, thus concentrating on the variables that are simplest to control from a continuous precipitation plant operational perspective.

2. Experimental

Detailed sample preparation method for all solutions is available in the literature [1,21]. Briefly, solutions were made from zirconyl chloride crystals (supplied by Doral Specialty Chemicals Western Australia) dissolved in milli-q water. Two concentrations, 0.81 and 1.62 M, of zirconyl chloride were used. The zirconyl chloride used had been tested for trace elements by ICP-OES and returned less than detectable results [1]. The sample solutions were aged for 10 days at ambient temperature prior to use, all samples were used within 24 h of the 10 day aging period.
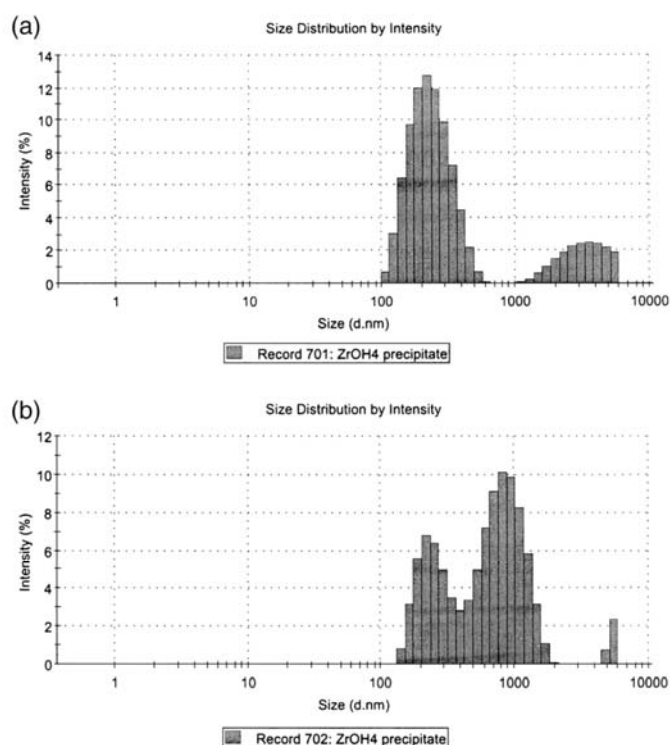

Fig. 1. Histogram from DLS (intensity vs. size) of re-suspended filter cake, (a) precipitated at pH 12. (b) Precipitated at pH 3.

The agitation rate was measured by determining the Reynolds number which was calculated using the standard formula for impellers [22]

$$R_N = \frac{\rho ND^2}{\mu} \qquad (1)$$

where

ρ	density
μ	viscosity
N	rotational speed
D	impeller diameter.

The target Reynolds number was 10,000, being above the turbulent transition zone, for what is defined below as high agitation and a Reynolds number of 5000 for the low agitation [22].

The precipitation method and particle sizing by Dynamic Light Scattering (DLS) are also detailed in [1]. In summary the zirconyl chloride solution and aqueous ammonia were injected into an agitated vessel in the same plane as the impeller rotation. The solution overflowed into a bath of ethanol, which quenches particle growth. The system was started using milli-q water run into equilibrium using four residence times at which point the bath of ethanol was changed. As discussed previously the ethanol is used as a steric hindrent to quench further particle growth [1].
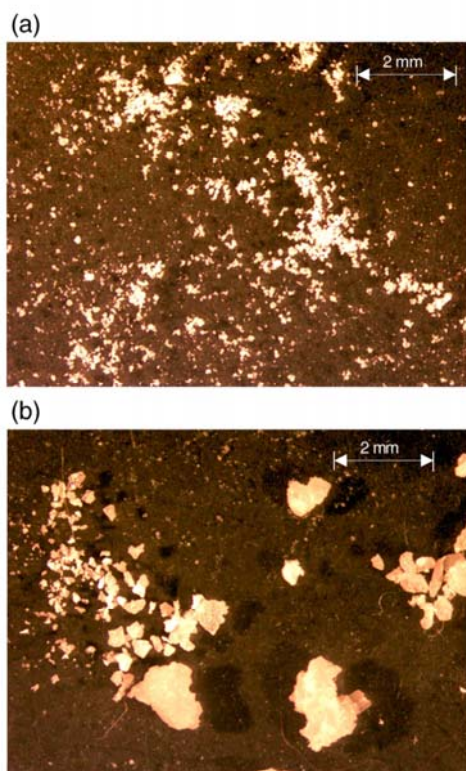
Fig. 2. Optical micrograph of 0.81 M dried precipitates (a) precipitated at pH 12. (b) Precipitated at pH 3.

The precipitate was isolated using a Whatmans 541 125 mm diameter filter paper in Büchner funnel and vacuum flask. 304.8 Torr of vacuum was supplied by a Dynavac ODI diaphragm vacuum pump. To determine filtration rates 250 mL of suspension was poured into the Büchner funnel and the filtration rate timed. Timing was started when vacuum was applied and was stopped once the fluid was not visible within the cake.

The effect that filtering may have on the particle size distribution was investigated. Samples from the filter cakes of the 0.81 M zirconyl chloride precipitated at both pH 3 and 12 were taken. The cake was re-suspended by adding 5 g of filter cake to 100 ml of ethanol and agitated using a sonic bath for 3 min. The suspension was then tested using DLS.

Diffraction data were obtained using an *in-situ* powder XRD system. Samples were placed on a platinum sample well measuring $20.0 \times 7.0 \times 0.4$ mm. Each sample was hand ground in a mortar and pestle with ethanol and was applied directly onto the Pt sample well as a thick slurry. The X-ray data were obtained using an X-ray diffractometer incorporating an Inel CPS-120 curved, position-sensitive detector. The angular range of the detector is 120° 2θ, facilitating rapid, simultaneous data accumulation. Data were collected in the reflection mode using Cu Kα radiation operated at 35 kV and 30 mA. Datasets of 60 s in duration were collected. The XRD patterns were interpreted with the aid of Jade 6.0.3 analytical software (MDI 2003).

DTA/TGA was conducted using a TA Instruments 2969 SDT V3.0F on filter cake that had been dried in a drying oven for 48 h at 55 °C.

Raman spectroscopy was similarly undertaken on filter cake that had been dried for 48 h at 55 °C.

Micro-combustion analysis was conducted by Dr Thomas Rodemann of the Vibrational Spectroscopy and Elemental Analysis Central Science Laboratory, University of Tasmania.

Optical microscopy was conducted using a Nikon SMZ 800 microscope with a SPOT insight Colour Model 3.2.0 digital camera with external light. Calibration of sizing was achieved using a Graticules LTD $200 \times 0.01 = 2$ mm graticule.

TEM imaging was carried out on well dispersed samples of precipitates on carbon film. Washed and dried precipitate from 0.81 M solutions at high agitation for both 3 and 12 pH along with calcined ZrO$_2$, were investigated using a JEOL 2011 transmission electron microscope operated at 200 kV. Energy dispersive spectra for well separated single crystals were collected at 500–1500 counts per second for 100 live seconds. Elemental compositions of these crystals using calculated k factors were determined using the thin film method [23,24].

3. Results

Table 1 shows the variation of particle size for three variables, pH (3 or 12), zirconyl chloride concentration (0.81 or 1.62 M) and agitation (high or low). All three variables were shown to significantly affect the particles size. Increased pH produced smaller particles, increased agitation produced smaller particles and increasing zirconyl chloride concentrations produced larger particles. The largest variation was due to changes of pH. The particle size of the precipitates of zirconium hydroxide produced at pH 12 is one or two orders of magnitude smaller than those produced at pH 3; e.g. using high agitation of 0.81 M solutions, at pH 12 particles were 49 nm compared to 1130 nm at pH 3 (Table 1).

Precipitates produced at pH 12 showed greater variability of particle sizes, e.g. for the 1.62 M solution the difference between the low and high Reynolds number agitation is approximately 10 times (73 vs 743 nm). In contrast for the pH 3 sample, the change with agitation for the 0.81 solution is only 1.5 times (1130 vs 1820 nm). This could indicate that the particles produced at a higher pH are more prone to mechanical degradation. To test if mechanical degradation was causing the particle size differences the filter cake was redispersed in ethanol using a sonic bath. DLS was used to investigate
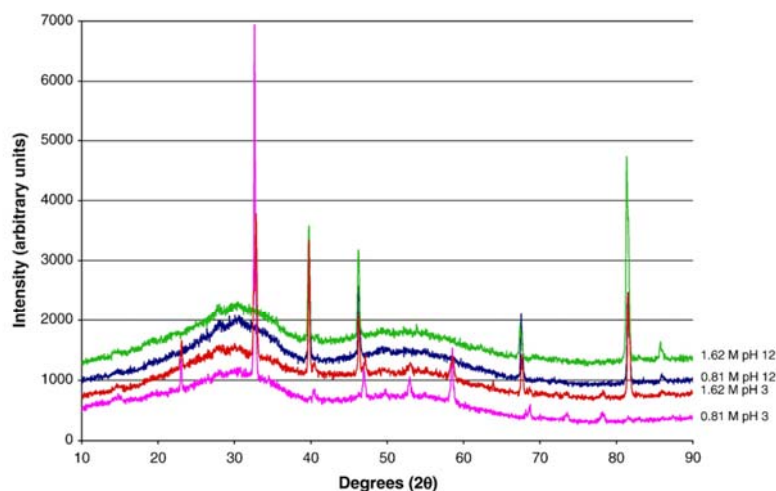
Fig. 3. XRD trace of 0.81 M, 1.62 M, pH3 and 12 precipitated, dried powder showing an amorphous hump (Cu K radiation operated at 35 kV and 30 mA).

the PSD of the re-suspended materials (Fig. 1). The results indicated the pH 12 sample was effected less by the filtration and re-suspension than the sample produced at pH 3, although both had a bimodal distribution. The resuspended pH 12 sample had the majority of the particles distributed in the region of the initial precipitate, although the distribution displayed is broader. This suggests that mechanical degradation is not the major mechanism that produces the smaller particle size for the pH 12 precipitates. We believe the higher availability of base allows a faster rate of precipitation which in turn leads to the production of smaller particles.

Increased agitation generally results in smaller particles, and the results described here are consistent with that expectation. The filtration rates showed a strong dependence on particle size, as expected. Precipitates produced at pH 12 would be unusable industrially as the time taken to filter was excessive.

Fig. 2 shows optical micrographs of the dried filter cakes obtained from 0.81 M high agitation solutions at pH 3 and 12. Solutions precipitated at pH 12 produced fine well divided powders whilst those

produced at pH 3 contained large aggregated particles that were difficult to break apart using a mortar and pestle.

The large differences demonstrated suggested the possibility of different zirconia phases being responsible for the varying products. The four high agitation dried precipitates were examined using powder X-Ray Diffraction (XRD) returning a mostly amorphous XRD pattern (Fig. 3). A noticeable difference is the peaks seen at 32 and 58°2 theta for both of the pH 3 samples which are absent in the pH 12 samples. This is due to residual salammoniac (NH$_4$Cl PDF# 07-007). The peaks observed at 39, 46, 67, 81, 86° 2θ are due to the platinum from the sample holder used (PDF# 04-0802).

The presence of ammonium chloride in the samples produced at pH 3, whilst making sense chemically, was counter intuitive in light of the ease with which the filtering and subsequent washing of the filter cake was achieved.

To further investigate the products Raman spectroscopy was carried out (Fig. 4) but the patterns returned did not show any changes between either of the starting solution concentrations or the
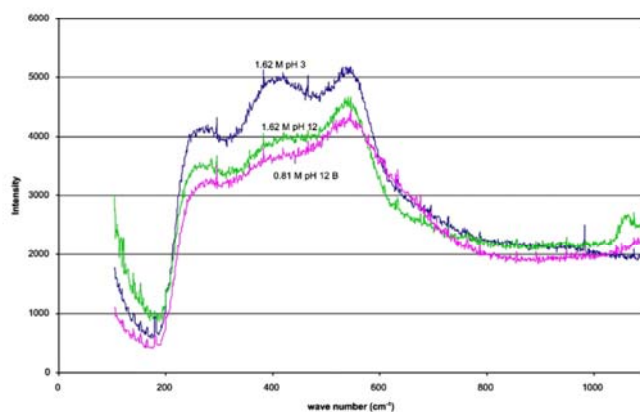

Fig. 4. Raman spectra 0.81 M, 1.62 M, pH 12 and a 1.62 M, pH 3 precipitated, dried powder. (developed using a Dilor Labtram 1B with excitation HeNe − 632.82 nm and a 600 lines/mm diffraction grating).
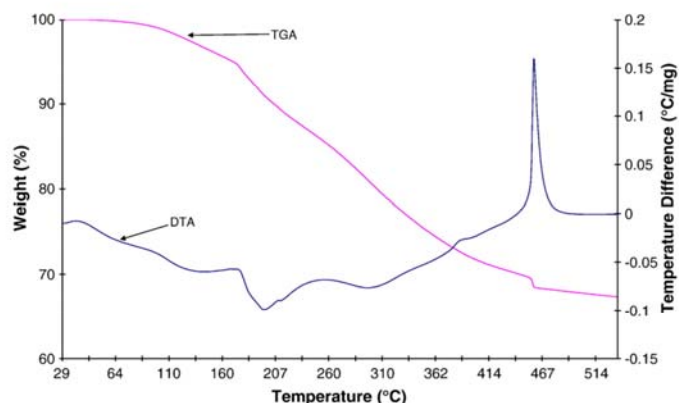
59

Fig. 5. TGA/DTA of 0.81 M solution precipitates pH 3.

pH's of precipitation. Raman spectroscopy of hydrous-zirconia which was produced by refluxing aqueous zirconyl chloride solutions of differing concentrations has been reported [25]. The data presented show a dependence on solution concentration to the amount of crystallinity determined. The higher concentrations used showed a decreasing tendency to match the spectra given for monoclinic zirconia and thus it was concluded that the material is hydrous zirconia. Huang et al. [8] discuss at length the differences between hydrous zirconia and zirconium hydroxide and use TGA and XRD to show the differences between the two species.

To investigate the differences in the powder produced by the two different pH values TGA/DTA was conducted (see Figs. 5 and 6). The mass lost for the pH 12 product was 21%, this is in close agreement to the theoretical value of 22.6% for transformation from $Zr[OH]_4$ to ZrO_2 suggesting that the structure present at a pH 12 may be $Zr[OH]_4$ (see Fig. 6). Rajendran [2] shows three DTA curves where two have smooth single endothermic events the same as seen in Fig. 6 whilst the third curve had two separate events similar to that found in Fig. 5. The literature explanation was that the two with the smooth endotherms were produced using ethanol and that the ethanol induces the removal of the physisorbed and chemically bound water. The two powders produced using ethanol also had two exotherms reminiscent

of the ones seen in Fig. 6 with the first occurring around 304 °C being a broad hump with the second being a sharp exotherm. It was suggested that the first broad hump is in all likelihood related to the decomposition of zirconium ethoxide, whilst the second is due to crystallisation [2]. Similar cases can be made in the case of this work however the mass loss from the transformation to ZrO_2 closely matched the expected value of 22.6% which allows the presence of little else but $Zr[OH]_4$. The pH 3 precipitated samples that were washed in the same manner as the pH 12 samples had ammonium chloride present as demonstrated by the XRD, as well as water incorporated within the structure along with ethanol if reasoning such as that reported previously was to be used [2].

The presence of these additional components was tested by TGA/DTA with a mass spectrometer attached. Whilst not allowing quantitative analysis, it was expected that distinct points of evolution of water, ethanol and CO_2 would be found. It was found that ethanol was evolved by both the pH 12 and pH 3 samples as was water and CO_2. The points of evolution vary greatly between the pH 12 and pH 3 samples. This then does not allow for the assumption of the structure for the pH 12 to be $Zr[OH]_4$ as no provision is made for the ethanol. However if the alternative $(ZrO[OH]_2)$ structures is assumed the theoretical change in mass from this to ZrO_2 is 12.8% and this would thus allow for 8.2%
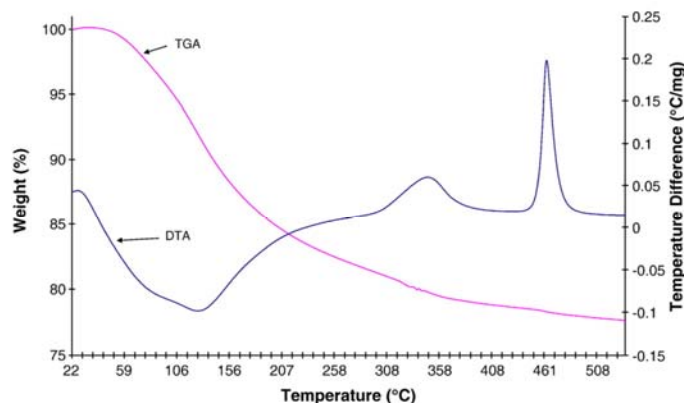

Fig. 6. TGA/DTA of 0.81 M solution precipitates pH 12.

of ethanol. The pH 3 sample had a 32.5% mass loss which allows the starting structure of $Zr[OH]_4$ then as a transformation to ZrO_2 would leave 9.9% of mass loss unaccounted for which is in reasonable agreement with the difference displayed by the pH 12 sample (Fig. 7).

To further quantify the products that were being evolved during heating, micro-combustion analysis was preformed on the powders produced at a high agitation with a concentration of 0.81 M precipitated at pH 3 and 12 (Table 2). The pH 3 and 12 powders produced had 9.9% and 8.2% mass loss unaccounted for and the values returned in the micro-combustion account well for these masses.

In the case of the powder produced at pH 3 the micro-combustion results agree well with the XRD results by showing a high nitrogen signature indicating the presence of ammonium chloride whilst the pH 12 show only limited nitrogen and higher C consistent with the presence of ethanol as proposed previously [2].

Elinson and Petrov [11] found that zirconium hydroxides produced from strong hot acidic solution (>1 N HCl) have the structure of $Zr[OH]_4$ whilst those produced in weakly acidic solutions were chiefly $ZrO[OH]_2$.

This is in agreement with the structures proposed above. Guo et al. [14] alternatively proposed that the structure of zirconium hydroxide produced in acid is $Zr_4O_3(OH)_{10}·6H_2O$. They show TGA/DTA curves for gels produced at pH 4 to justify this structure. These TGA/DTA curves are very different from those produced during this work with one possible explanation being experimental differences.

As the structures proposed to be produced at pH 3 ($Zr[OH]_4$) and 12 ($ZrO[OH]_2$) contain different oxygen to zirconium ratios, samples of each were investigated for the O wt.% using TEM EDS. The O wt.% returned by EDS for both the pH 3 and 12 precipitated powders as well as a sample of monoclinic zirconium powder (supplied by Millennium Specialty Chemical Rockingham 2003 Z0.5) are shown in Fig. 8.

Although EDS spectroscopy is not an ideal technique for quantitative determination of light elements the authors have successfully used this method to determine Al:O ratios in wear debris from alumina ceramics [26]. ZrO_2 has 26 wt.% O which is in close agreement with the monoclinic sample tested; this result validates the method used in relation to these samples. Twenty
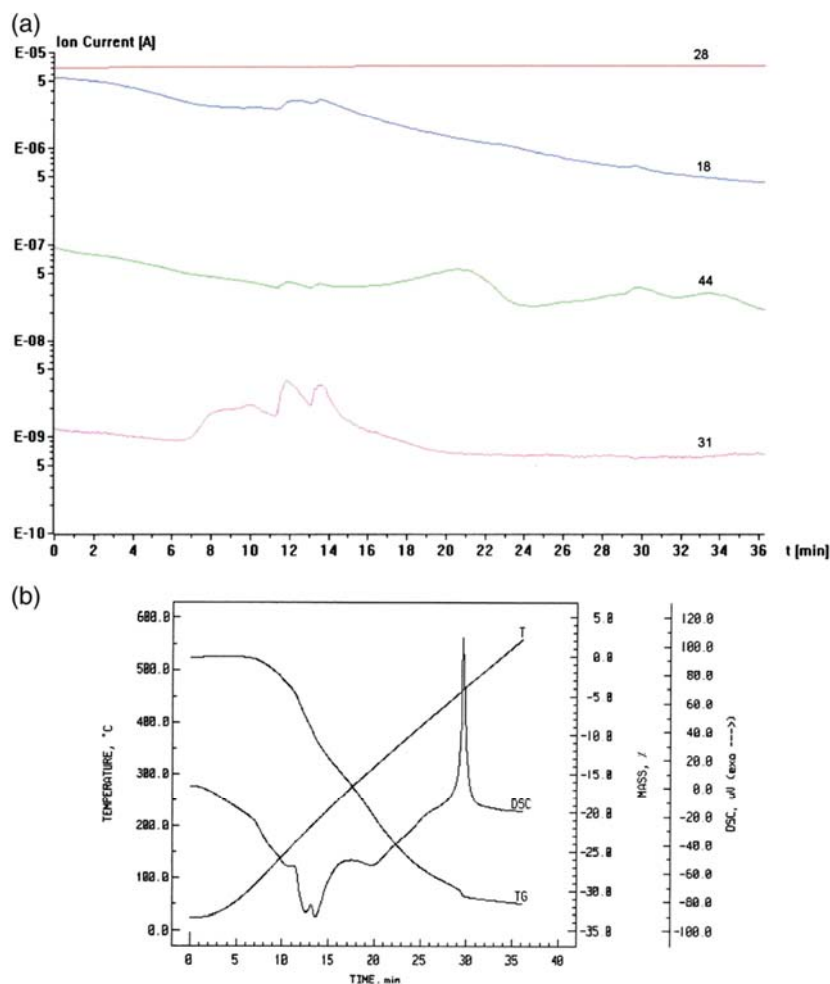

Fig. 7. TGA/DTA with mass spectrometry, (a) MS output for pH 3 sample (b) TGA/DTA output for pH 3 sample (c) MS output for pH 12 sample and (d) TGA/DTA output for pH 12.
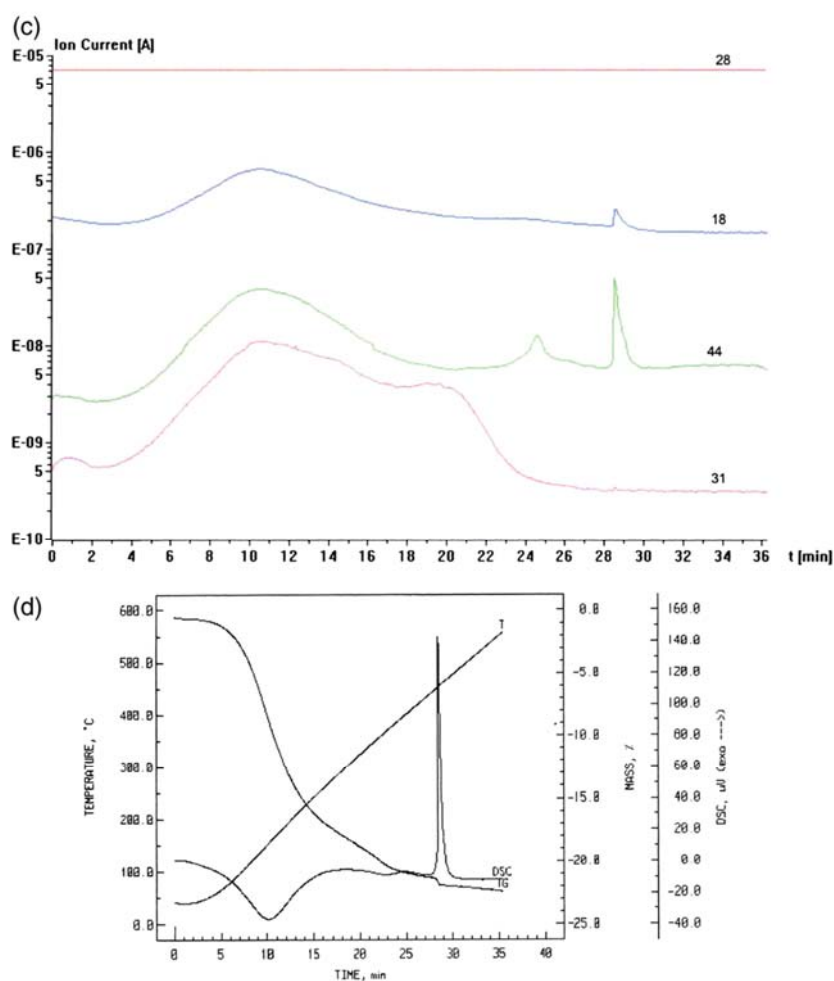
61

Fig. 7 (continued).

particles of each material were examined. Whilst within the limits of the experimentation it is difficult to distinguish the amount of oxygen present in the two precipitated samples due to the uncertainties, a trend was evident, with the pH 3 sample having a higher wt.% O than the pH 12 sample. This result supports the premises that the precipitation conducted at pH 3 results in the formation of $Zr[OH]_4$ whilst the pH 12 precipitation results in a structure most like $ZrO[OH]_2$ as suggested by TGA/DTA and micro-combustion work.

The use of the TEM was made particularly difficult by the samples undergoing transformation due to the high vacuum and beam current. This was particularly evident in the powder produced at pH 3, (see Fig. 9) all care was taken to exclude such samples from the statistical analysis used in the EDS. It was however possible to take 3 EDS results from the same pH 3 produced sample one after the other without shifting the beam and obtain decreasing values of wt.% O for each collection period with the last collection period resulting in a transformation of the sample. Typical values were 45 wt.% O on the

first collection 35 wt.% O on the second and 29 wt.% O on the last. This transformation added to the spread of the results and the subsequent increase in the uncertainty's, in addition these values are normalised for Zr and O and do not take into account any H.

Apart from supporting the structural differences suggested, the TEM work also showed the significant morphological difference in the powders as suggested by the PSD differences and the ability to re-suspend the filter cake. Fig. 10(a) shows a typical particle of the pH 3 powder that has little evidence of being a loose agglomeration; it is more reminiscent of a well compacted cake. In contrast Fig. 10(b) is typical of the pH 12 precipitated powder that has the appearance of a loose aggregation of fine sub particles.

4. Conclusions

Concentration of starting solutions, agitation levels and the pH that the precipitation is conducted at all affect the particle size distribution for the hydrous zirconium that is produced. The largest change is due

Table 2
Micro-combustion results

Element	pH 3 (%)	pH 12 (%)
N	4.52	0.2
C	0.29	3.34
H	2.81	2.40
Total % evolved	7.62	5.94

to pH with the smallest change occurring when comparing a pH 12 sample with low agitation and a starting concentration of 1.62 M (PS of 743 nm) with a pH 3 sample with the other processing parameters remaining the same (3390 nm); this is an increase by 4.5 times. The largest change occurred when comparing a pH 12 precipitation with high agitation and 1.62 M solution concentration (PS 73 nm) with the same processing parameters except for the precipitation being carried out at pH 3 (2160 nm) which is an increase of greater than 29 times. The effect of the pH of precipitation is most remarkable in that it overshadows all of the other processing parameters with the PS being smaller by 1 to 2 orders of magnitude for those samples precipitated at a pH 12 in comparison to those produced at pH 3. From an industrial processing perspective, the small PS of the precipitate at pH 12 (743 to 49 nm dependent on processing parameters) leads to significant difficulty in filtering which is an important issue.

An order of magnitude change in PS is not limited to pH changes however as within those precipitations tests carried out at pH 12 changes in the level of agitation also produced order of magnitude differences. The higher agitation in all cases produced smaller PS. As expected lower solutions concentrations were found to produce smaller PS.

The differences seen in the filtering and subsequent differences in morphology of the dried powders, were investigated initially using XRD which showed that those powders produced at pH 3 had retained greater amounts of ammonium chloride. To further investigate the composition of the precipitates TGA/DTA and TGA-MS along with micro-combustion analysis were used with the results suggesting that the pH of precipitation causes differences in the structure of the hydrated zirconium. The pH 3 powders are thought to have a structure most closely resembling $Zr[OH]_4$ whilst those produced at pH 12 are consistent with a formulation of $ZrO[OH]_2$.

TEM with EDS was used to investigate the zirconium to oxygen content of powders produced at both pH values as well as a zirconia sample. It was found that the pH 3 sample had almost 43 wt.% O whilst the pH 12 sample had approximately 32 wt.% O. The difficulty in using TEM EDS for light elements precludes detailed analysis but the results returned are in accordance with the different degrees of hydration suggested by the TGA/DTA, and micro-combustion work. The effect
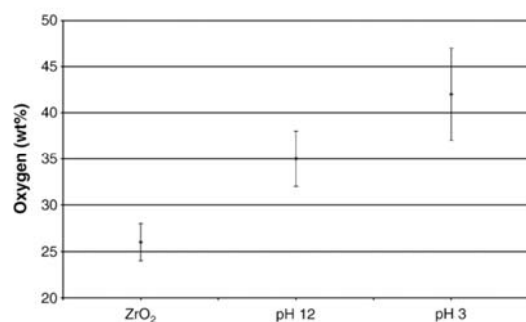

Fig. 9. TEM micrograph of pH 3 powder after transformation in TEM.

(a)

(b)

Fig. 8. Oxygen wt.% from TEM EDS for pH 3 and 12 produced powders as well as a monoclinic zirconia sample.

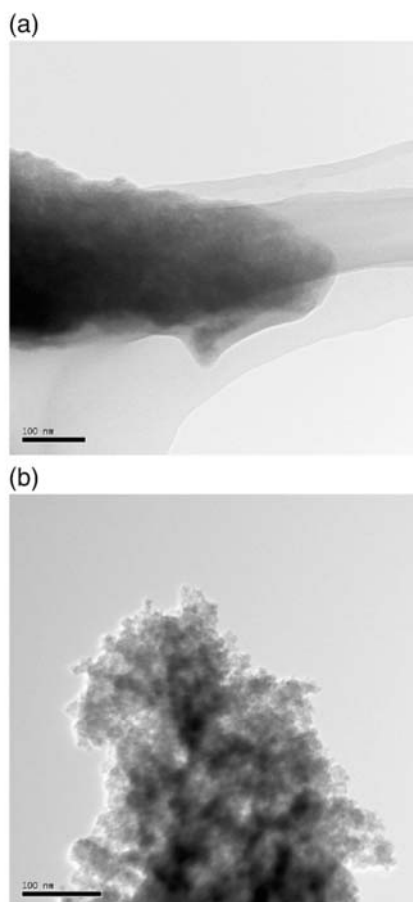**Fig. 10.** TEM micrograph of (a) pH 3 powder and (b) of pH 12 powder.

that the differing degrees of hydration has on the ceramic process further down stream in the manufacturing process is unclear.

It makes some sense, however, in operational situations to use lower pH precipitation as this will have the double benefit of allowing for lower base input with associated cost reduction and the PS that allows for the most economical filtering. The tuning of both solution concentration and agitation may allow for the targeting of specific PS. In all cases, however, the final ceramic properties must be considered. The structural differences and or other differences between the manufacture systems may impact on the final ceramics.

Acknowledgements

References

[1] G.A. Carter, et al., Ammonia-induced precipitation of zirconyl chloride and zirconyl-yttrium chloride solutions under industrially relevant conditions. Powder Technology. In Press, Corrected Proof, doi:10.1016/j.powtec.2008.04.087.
[2] S. Rajendran, Production of nano-crystalline zirconia powders and fabrication of high strength ultra-fine-grained ceramics, Materials Forum 17 (1993) 333–350.
[3] M. Lauci, Powders agglomeration grade in the ZrO2-Y2O3 coprecipitated process, Key Engineering Materials 132–136 (1997) 89–92.
[4] A. Clearfield, Structural aspects of zirconium chemistry review, Pure and Applied Chemistry 14 (1964) 91–108.
[5] S.V. Elinson, K.I. Petrov, Analytical Chemistry of Zirconium and Hafnium, London Ann Arbor-Humphrey Science Publishers, 1969.
[6] E.M. Larsen, M. Gammill, Electrometric titrations of zirconium and hafnium solutions', American Chemical Society 72 (1950) 3615–3619.
[7] Kovalenko, Bagdasaov, The solubility of zirconium hydroxide, Russian Journal of Inorganic Chemistry 6 (3) (1961) 272–275.
[8] C. Huang, Z. Tang, Z. Zhang, Differences between zirconium hydroxide (Zr(OH)4 × nH2O) and hydrous zirconia (ZrO2 × nH2O), Journal of American Ceramic Society 84 (7) (2001) 1637–1638.
[9] Britton, Electrometric studies of the precipitation of hydroxides. Part 2, Journal of the Chemical Society, Transactions 127 (2) (1925) 2120–2141.
[10] R.P. Singh, N.R. Banerjee, Electrometric studies on the precipitation of hydrous oxides of some quadravalent cations. Part 1. Precipitation of zirconium hydroxide from solutions of zirconium salts, Journal Indian Chemical Society 38 (11) (1961) 865–870.
[11] S.V. Elinson, K.I. Petrov, Analytical chemistry of zirconium and hafnium, Analytical Chemestry of Elements, London Ann Arbor-Humphrey Science Publishers, 1969.
[12] L.M. Zaitsev, G.S. Bochkarev, Peculiarities in the behaviour of zirconyl in solutions, Russian Journal of Inorganic Chemistry 7 (4) (1962) 411–414.
[13] A.S. Solovkin, S.V. Tsvetkova, The chemistry of aqueous solutions of zirconium salts (Does the zirconyl ion exist?), Russian Chemical Reviews 31 (11) (1962) 655–669.
[14] G.-Y. Guo, Y.-L. Chen, W.-J. Ying, Thermal, spectroscopic and X-ray diffractional analyses of zirconium hydroxides precipitated at low pH values, Materials Chemistry and Physics 84 (2–3) (2004) 308–314.
[15] G.-Y. Guo, Y.-L. Chen, A nearly pure monoclinic nanocrystalline zirconia, Journal of Solid State Chemistry 178 (5) (2005) 1675–1682.
[16] A. Clearfield, The mechanism of hydrolytic polymerization of zirconyl solutions, Journal Materials Research 5 (1) (1990) 161–162.
[17] R.C. Garvie, The occurrence of metastable tetragonal zirconia as a crystallite size effect, Journal of Physical Chemestry 69 (4) (1965) 6.
[18] A. Roosen, H. Hausner, Techniques for agglomeration control during wet-chemical powder synthesis, Advanced Ceramic Materials 3 (2) (1988) 131–137.
[19] W. Pietsch, Size Enlargement by Agglomeration, John Wiley and Son, Baffins Lane Chichester Sussex England, 1991.
[20] A. Myerson, Handbook of industrial crystallization second edition, Boston 225 Wildwood Ave Woburn MA 01801-2041, Butterworth Heinemann, 2002.
[21] G. Carter, et al., From zirconyl chloride to zirconia ceramic, a plant operation perspective, Materials Forum 32–2008 (2008) 82–89.
[22] R. Perry, D. Green, Perry's Chemical Engineers Handbook seventh edition, New York USA, McGraw-Hill, 1997.
[23] G.W. Lorimer, Quantitative X-ray microanalysis of thin specimens in the transmission electron microscope; a review, Mineralogical Magazine 51 (1987) 49–60.
[24] W.B. Jepson, J.B. Rowse, The composition of kaolinite—an electron microprobe study, Clays and Clay Minerals 23 (1975) 310–317.
[25] K. Matsui, et al., Raman spectroscopic studies on the formation mechanism of hydrous-zirconia fine particles, Journal of American Ceramic Society 78 (1) (1995) 146–152.
[26] G.A. Carter, A. van Riessen, R.D. Hart, Wear of zirconia dispersed alumina at Ambient, 140 °C and 250 °C, Journal of the European Ceramic Society 26 (2006) 3547–3555.

4. From Zirconyl Chloride to Zirconia Ceramic, A Plant Operation Perspective

Carter G., Rowles M., Hart R., Ogden M., Buckley C., 2008, '*From Zirconyl Chloride to Zirconia Ceramic, A Plant Operation Perspective*', Materials Forum, vol. [32], pp. 82-89.

FROM ZIRCONYL CHLORIDE TO ZIRCONIA CERAMICS, A PLANT OPERATION PERSPECTIVE

G. A. Carter[1], M. R. Rowles[2], R. D. Hart[3], M. I. Ogden[1] and C. E. Buckley[3]

[1] AJ Parker Centre for Integrated Hydrometallurgy Solutions, Nanochemistry Research Institute, Curtin University of Technology, PO Box U1987, Perth, Western Australia, 6845, Australia
[2] Commonwealth Scientific Industrial Research Organisation (CSIRO) Division of Minerals Clayton South, Victoria Australia
[3] Centre for Materials Research, Curtin University of Technology, PO Box U1987, Perth, Western Australia, 6845, Australia

ABSTRACT

The differences between two hydrous zirconium filter cakes manufactured at pH 3 and 12 were studied and further processing consistent with industrial procedures was undertaken. The loss on drying was found to be approximately 23% for both filter cakes, however for the loss on ignition the ph 3 sample was found to have a 12% higher loss at 33%. The specific surface area (SSA) was found to be 238 m^2/g for the pH 3 sample and 312 m^2/g for pH 12. The pH 12 sample showed a linear decrease of SSA with calcination temperature and both samples achieved the same SSA after 1000 °C. The pH 3 sample took 29 hours to attrition mill to a target D90 of less than 2 μm, the pH 12 sample achieved the same target in 26 hours. X-ray diffraction revealed that both samples had crystallite sizes in the order of 30 nm and greater than 90% monoclinic phase. Both samples achieved approximately 86% theoretical density when uniaxially pressed and sintered, corresponding with 20% linear shrinkage. The pH 3 sample had greater statistical variability in most results, indicating it would be harder to control. Differences in appearance when tape cast were also noted for the two powders.

KEYWORDS: Zirconia, Monoclinic, Industrial Processing, Tape Casting

1. INTRODUCTION

Stevens[1] shows that zirconia has widespread uses as an engineering ceramic, including as a dielectric in capacitors, transformation toughening agent in other ceramics such as alumina and oxygen ion sensors. Most of the literature available for zirconia focuses on the ceramic properties of the material.[2] Over recent years the Nanochemistry Research Institute (NRI) and Centre for Materials Research (CMR) at Curtin University of Technology in Western Australia have been studying the processing of zirconyl chloride to zirconia using an industrially relevant aqueous route. The route is similar to that used by a local company that is of a proprietary nature.

In previous work using Small angle X-ray Scattering, Dynamic light scattering, micro-combustion and thermogravimetric techniques the authors have found that changes in solution concentrations, added cations, agitation levels within reaction vessel and the pH of precipitation all affect the particle size of the precipitate.[3] It was shown that the pH at which the zirconium hydroxide powder precipitates influences the level of hydration of the product, as well as its behaviour in the initial stages of processing such as the filtering and drying. This has direct implications for the large scale processing of these materials. The focus of this work was to further develop the understanding of the process behaviour of zirconia powders at different pH values. The methods used have been reported previously.[4]

The calcination of hydroxides to oxides is a common industrial process, as is the use of calcination temperature to control the specific surface area (SSA) of the powder. The lower the temperature needed to obtain the required parameters the lower the cost of production.

A number of authors have noted differences in the calcination properties of zirconia dependent on its processing route each often contradicting others [5-13]. Contradictory findings are also obtained for the final phase distribution of the calcined powder. The work of Garvie [14] best demonstrates the link between crystallite size and the formation of the tetragonal or monoclinic phase of zirconia .

The particle size distribution (PSD) of the powder is extremely important and must be matched to the desired characteristics of the advanced ceramic and its processing route.[15] To achieve the required PSD size reduction processes are often used.[16] It is common to use attrition mills in the processing as they are highly efficient, thereby reducing the chances of contamination of the ceramic powder.[15]

2. MATERIALS AND METHODS

Powders of hydrated zirconium were precipitated from 0.81 M zirconyl chloride starting solutions at pHs of 3 and 12 as described previously.[4] Filtering and washing was carried out as previously reported[4] with the exception that all samples were left on the filter under vacuum for 2 hours.

Loss on Drying (LOD) was calculated from samples of filter cake dried in an oven at 110 ^{o}C for 24 hours (in alumina crucibles) and then cooled in a desiccator for a further 1 hour. The Loss On Ignition (LOI) was developed from the LOD samples by calcination in a muffle furnace for 2 hours at 1100 ^{o}C, after which the samples were cooled in a desiccator for 2 hours. The values reported are the mean of five samples.

Specific surface area of the powder (5 point BET) was established using a Micromeretics Gemini instrument with *Flow Prep* ©. The results are the mean of 5 determinations with the uncertainty being the standard deviation.

The samples were milled in a 01HD Union Process (Akron Ohio). Szegvari Attritor system. The attritor had a 500 ml volume with 0.8 mm diameter partially stabilised zirconia (PSZ) milling media, agitation was achieved using a PSZ attritor arm. Mill slip was made from 500 g of calcined powder obtained from 5 consecutive precipitation runs and milli-q water, the solids content was 45%. A flow through system was used with the mill slip being gravity fed to the top of the attritor from an external tank. The slip then passed through the milling chamber and a pump with an inlet at the bottom of the attritor, delivered mill slip back to the top of the external tank closing the loop. Pump speed and gravity feed rate were matched so a constant level was kept in the attritor. Sampling and testing were conducted on slip collected from the gravity feed discharge. The samples were milled until two consecutive PSD tests taken hourly returned a D90 of approximately 2μm. The use of statistical measures in particle sizing is common within the chemical powder industry the three most common measures that are used are the D90 being the 90th percentile, D50 and D10 which are both the 50th and 10th percentile respectively.

Mill slip solids content was 45% and was made from 500 g of calcined powder obtained from 5 consecutive precipitation runs and milli-q water.

Viscosity was measured using a Brookfield RV-4 viscometer at 50 RPM.

Particle sizing was obtained using a Coulter LS 320 laser particle sizing instrument.

Diffraction patterns were obtained using an in-situ powder X-Ray Diffraction (XRD) system. Oven dried samples were placed on a platinum sample well measuring 20.0 x 7.0 x 0.4 mm. The X-ray data were obtained using a X-ray diffractometer incorporating an Inel CPS-120 curved, position-sensitive detector. The angular range of the detector is 120 deg 2θ. Data were collected in the reflection mode using Cu Kα radiation operated at 35 kV and 30 mA. The XRD patterns were interpreted with the aid of Jade 6.0.3 analytical software (MDI 2003) for peak match. Phase composition and crystallite sizing was determined using Rietveld method with TOPAS Ver. 3.0 software. Crystallite size, or more correctly coherent scattering domain size, was determined from the width at half height of the [1-1-1] peaks using the Scherrer method [17]

Sample pellets for green and sintered density were formed by uniaxially pressing the powders to 200 MPa in stainless steel die using stearic acid dissolved in methanol as a die lubricant. Green and sintered densities were measured according to ASTM C20 (1992).

All samples were sintered at 1500 ^{o}C for 1 hour using a heating rate of 300 C.hr^{-1} over the range 400-1500 ^{o}C.

The sample buttons were made using the formulation and batching procedure of Mistler and Twiname [18]. Tape was made on silicon coated Mylar film

Photographs of sample disks were taken using Pentax K10D camera with a Sigma 100 mm Macro lens. The image contrast was enhanced using Photoshop CS-Z.

3. RESULTS

The LOI and LOD (Table 1) show a remarkable consistency within each sample set and are consistent with values obtained by micro-combustion and DTA/TGA.[3] Previous work by the authors [3] reported that the pH 3 sample had better filtering however the ammonium chloride (NH$_4$Cl PDF# 07-007) was not washed out of the sample. It is evident from the present work that while it filters faster, the pH 3 sample retains more ammonium chloride and that the LOI for the pH 3 sample is higher.

SSA analysis of the dried powder prior to calcination showed clear differences; Sample pH 3 returned a SSA of 238 m^2/g and the pH 12 sample 312 m^2/g. The SSA for the two powders with increasing calcination temperature is shown in Figure 1. The pH 12 powder has a higher SSA prior to calcination and through the 600 ^{o}C to 1000 ^{o}C temperature range. At 1000 ^{o}C the SSA of the two powders converged. The pH 12 sample showed a more linear decrease in SSA with calcination temperature than the pH 3 sample. The calcined powders had different textures, the pH 3 sample was quite coarse yet friable and the pH 12 sample was mostly fine with some coarser material that broke apart in a mortar and pestle with little difficulty (Figure 2).

Phase composition and crystallite size determination using XRD are shown in Table 2. The uncertainties developed for both the phase composition and crystallite size are estimated standard deviation (ESD) and are related to parameter fits of the model and not the variation within a given data set[19]. The uncertainties quoted in Table 2 are rounded to the nearest whole number. The two XRD data sets are shown for comparison (Figure 3) and the plot of the Rietveld refinement showing the XRD data set, refined pattern difference plot and phase identification markers is in Figure 4. The spurious peaks evident in Figure 4 are from the platinum sample holder (PDF# 65-2868). Within the experimental limits the data sets are very similar. The crystallite sizes of the monoclinic and tetragonal forms were determined to be 36 nm and 25 nm for the pH 3 powder and 30 nm and 20 nm for the pH 12. These values are comparable with those of Garvie [14] for the occurrence of metastable tetragonal zirconia and its martensitic transformation to monoclinic above a crystallite size of 30 nm.

Table 1. LOD and LOI for pH 3 and 12 samples (all values rounded to whole numbers).

	pH 3	pH 12
LOD	56 (2)%	54 (2) %
LOI	33 (1)%	21 (1)%
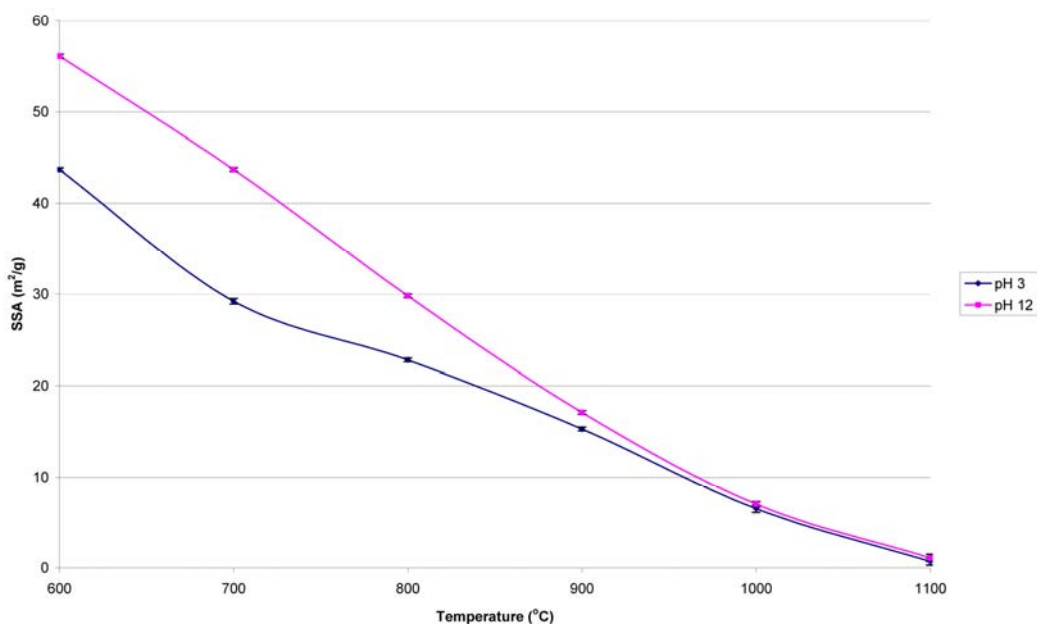
Figure 1. Specific Surface Area with calcination temperature for sample pH 3 and pH 12 (error bars are too small to be clearly seen, and indicate 1 standard deviation).

(a) (b)
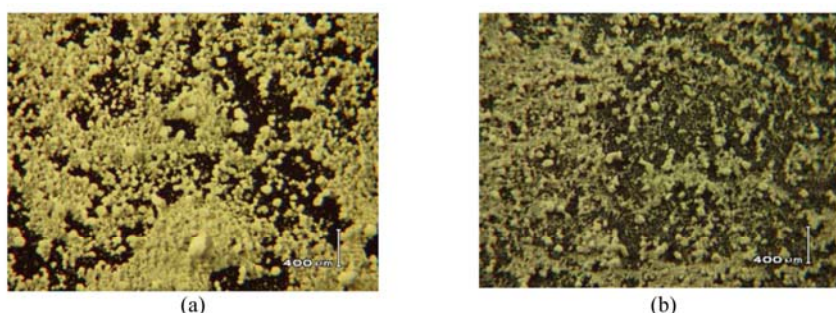
Figure 2. Optical micrograph of powder calcined at 700 °C (a) pH 3, (b) pH 12.
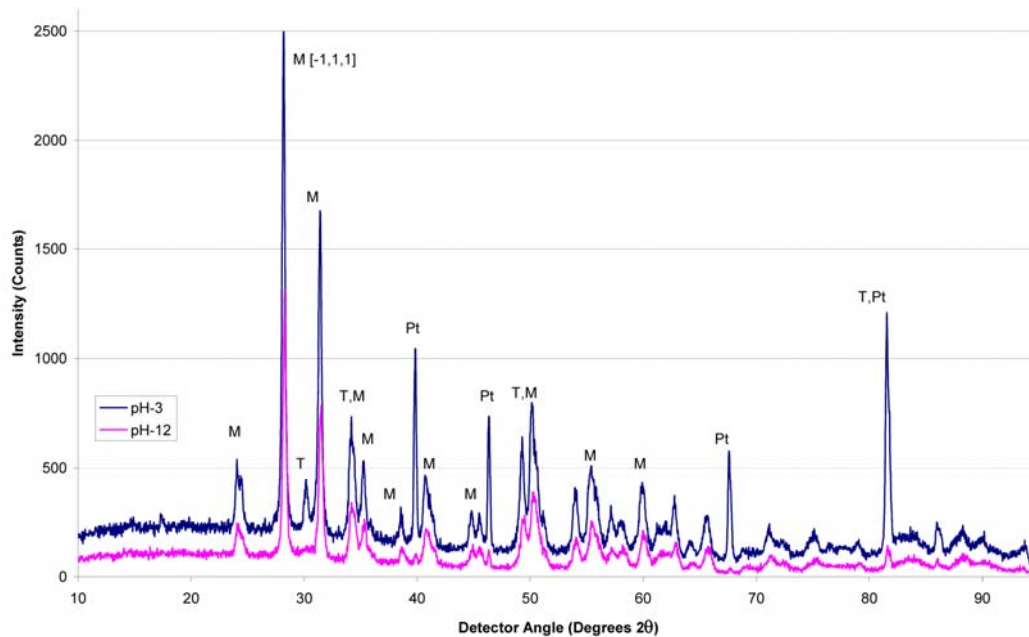
Figure 3. X-ray diffraction pattern of calcined powder both pH-3 and 12 showing mostly monoclinic zirconia.
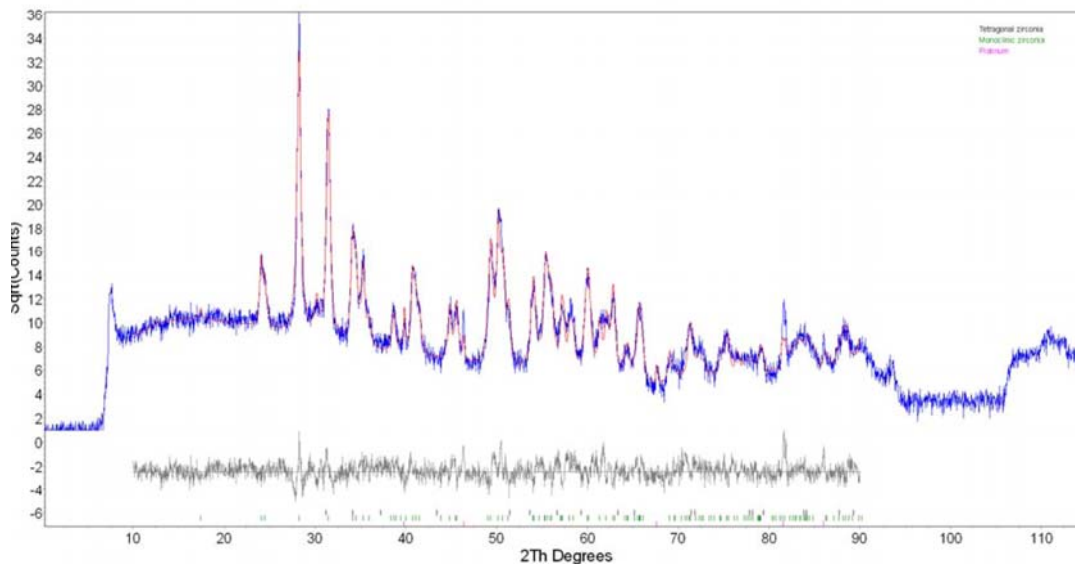
Figure 4. Topas Plot file showing refined pattern vs. data set, difference plot and phase peak markers for the Ph 12 Regions of exclusion exist above 90° 2θ and below 10.

Table 2. Phase % and Crystallite size for pH 3 and pH 12 (uncertainties are rounded to nearest whole number and are ESD)

Sample	% Phase composition		Crystallite size nm	
	Monoclinic	Tetragonal	Monoclinic	Tetragonal
pH 3	93(3)	7(4)	36(1)	25(1)
pH 12	96(5)	4(4)	30(1)	20(1)

85

69

Milling trials showed the pH 3 sample required 29 hours to reach the target D90 of 2 μm and the pH 12 sample required 26 hours (Figure 5 and Figure 6). While the difference of only three hours in the time taken to reach the target D90 appears small the overall milling responses for the two powders were significantly different. The D10 seems to plateau at 13 hours for pH 3 whilst it plateaus at 6 hours for pH 12. After 9 hours of milling the pH 12 powder has a D50 less than 5 μm with a small distribution in the particle size. This particle size is not achieved until after 16 hours for the pH 3 sample. This would suggest that the pH 12 sample would offer lower milling times for a range of target PSD in comparison too the pH 3 sample.

The viscosities of the mill slips were also measured every 4 hours (Figure 7) and are also significantly different. For the pH 12 powder the viscosity begins to increase significantly after approximately 8 hours of milling, which matches the point were the D90 drops below 5 μm. The viscosity increased until the milling was stopped. The viscosity of the pH 3 slip rises above 60 centipoises only after 24 hours of milling, even though the D90 reaches 5 μm after 16 hours. This would suggest that PSD is not the main contributing factor in the viscosity changes.
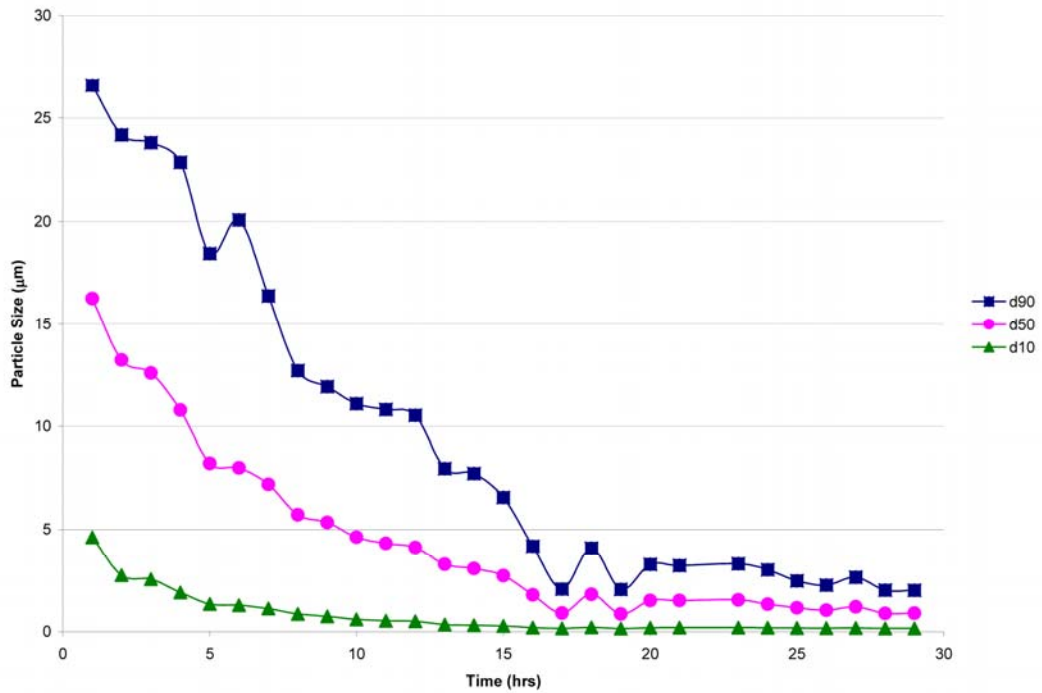
Figure 5. PSD vs Mill time for pH 3 sample.

The final sintered density and linear shrinkage of the two zirconia powders were investigated. The pH 3 sample reached 83% of its theoretical density and the pH 12 sample 88%. Theoretical density was taken to be 5560 kg.m^{-3} .[1] No distinction can be made between the two samples within the limits of the uncertainty (Table 3). However, the pH 3 sample had a higher variability for both its density and linear shrinkage. Tape cast buttons (Figure 8) were made from each of the powders. Tape casting is common in the manufacture of electronic components that contain zirconia, such as multi-layer ceramic capacitors (MLCC) and lead zirconate titanate (PZT) piezoelectric ceramics, Although the tape casting system was kept consistent, the pH 3 sample produced opaque samples with an uneven surface flatness and striations and reduced in size less than the translucent pH 12 sample (Figure 8).
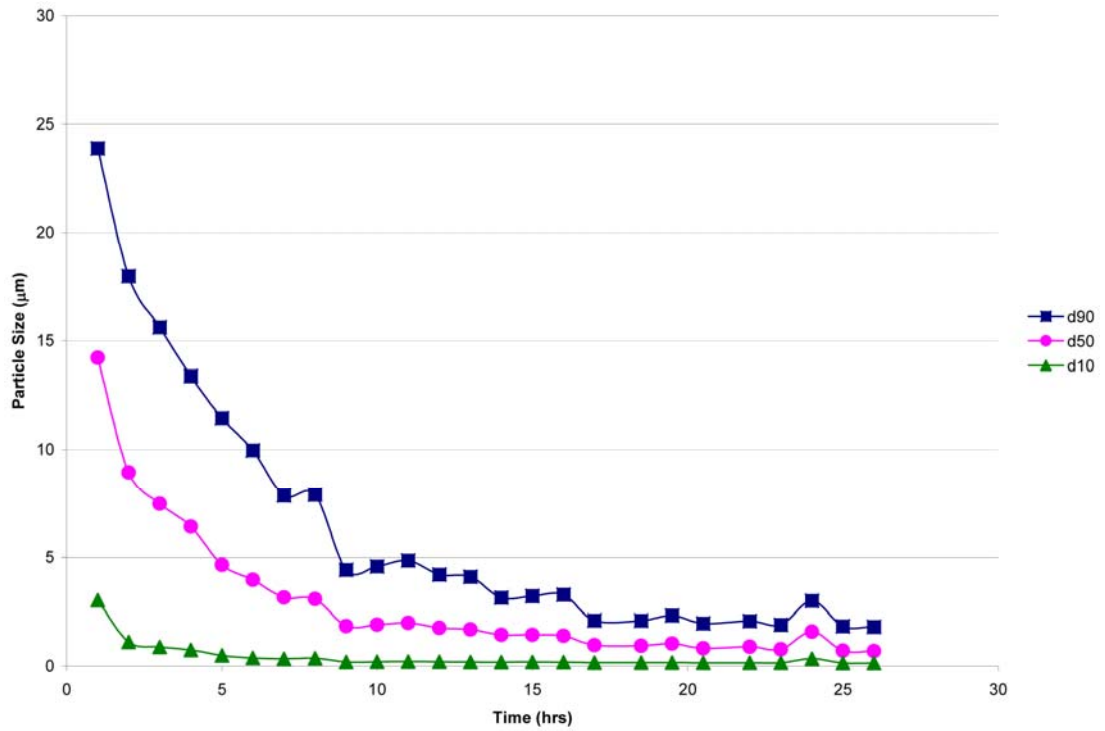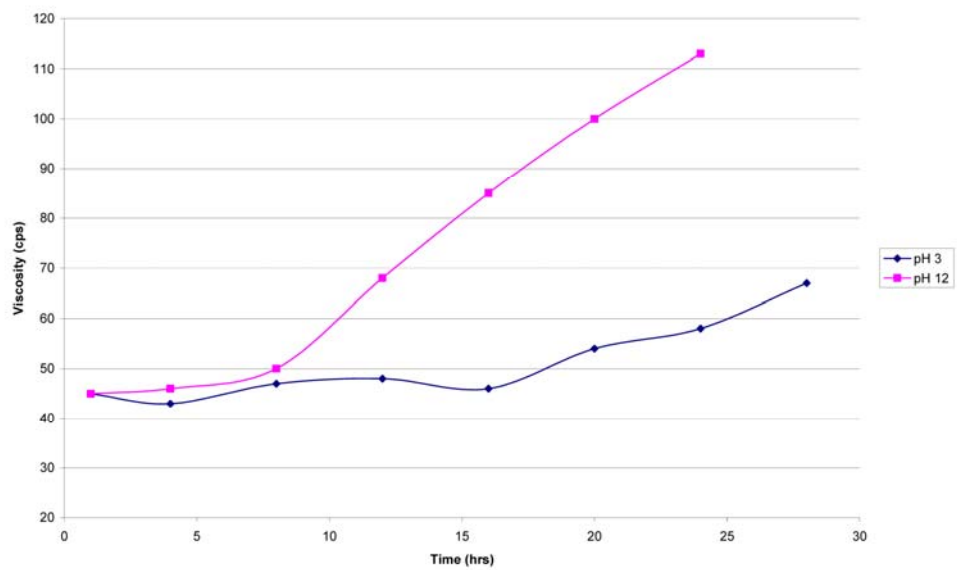
Figure 6. PSD vs Mill time for pH 12 sample.

Figure 7. Viscosity with milling time for both pH 3 and 12 mill slip.

Table 3. % Theoretical Density and linear shrinkage for pH 3 and pH 12 sample powders.

	pH 3	pH 12
% Theoretical density	83 (5)	88 (2)
% Linear shrinkage	18 (3)	21 (1)

87
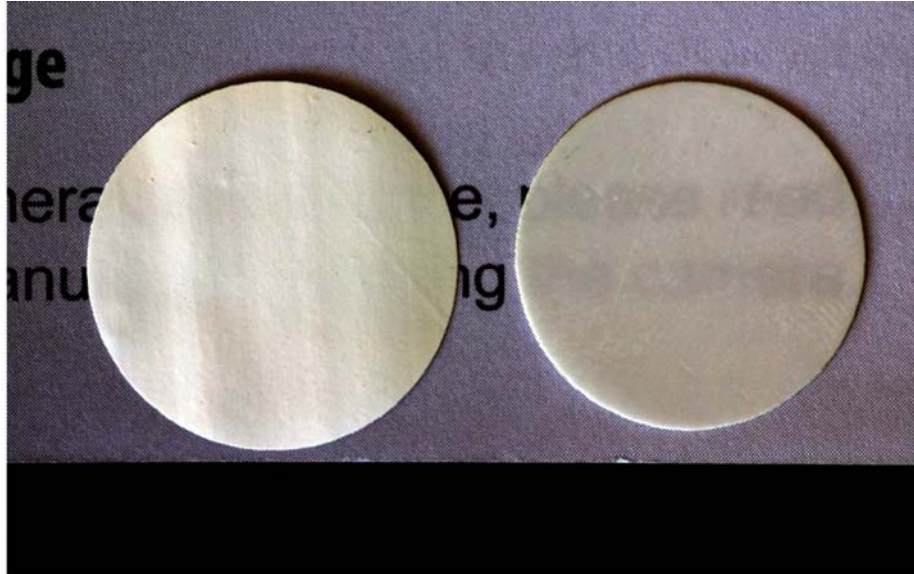
Figure 8. Photograph of pH 3 (on the left) and pH 12 (on the right) sample disks (original lettering is 3 mm high).

4. CONCLUSION

The zirconia powders produced at different pH values of 3 and 12 behave differently throughout processing from hydrous zirconium precipitate to sintered ceramic. The two precipitates have almost the same LOD after filtering and vacuum drying but the pH 3 product has a higher LOI. This would have a negative effect on plant operations as the additional energy required to drive off the water increases the cost of production.

The SSA response to calcination temperature has the two powders overlapping at approximately 1000 °C. However the response by the pH 12 product is more linear and may allow for simpler fine tuning of temperature when trying to achieve a target SSA.

X-ray diffraction demonstrated that essentially the two powders were very similar once calcined, with a crystallite size in the order of 35 nm and +90% of the phase being monoclinic zirconia.

The milling curves for the pH 12 sample show a more orderly size reduction as the milling progresses that may allow target PSD to be reached in a more uniform and predictable fashion with reduced time, offering cost reduction and reduced complexity in large scale processing.

Whilst both powders produced ceramics with similar average values for theoretical density and linear shrinkage, the variability of the pH 3 samples was greater than for the pH 12 samples. This suggests that either the processing needs greater control or refinement for pH 3 materials or less predictable results will be obtained using this precursor powder. This trend was mirrored in the tape casting of the two powders with the pH 12 sample producing a better ceramic, while the pH 3 sample produced a ceramic with striations and different opacity despite the use of identical processing conditions.

References

1. R. Stevens, *Introduction to Zirconia*, Magnesium Elektron, Swinton Manchester, 1986.
2. R.H.J. Hannink, P.M. Kelly and B.C. Muddle, *J. Am. Ceram. Soc.*, 2000, vol. 83(3), pp. 461-487.
3. G.A. Carter, R.D. Hart, M.R. Rowles, C.E. Buckley and M.I. Ogden, *manuscript in preparation*, 2008.
4. G.A. Carter, M.I. Ogden, C.E. Buckley, C. Maitland and M. Paskevicius, *Powder Technol.*, 2008, accepted. doi:10.1016/j.powtec.2008.1004.1087.
5. K. Matsui, H. Suzuki, O. Michiharu and *Journal of American Ceramic Society*, 1995, 78(1), 146-152.

88

6. K. Matsui and O. Michiharu, *Journal of American Ceramic Society*, 1997, 80(8), 1949-1956.

7. K. Matsui and O. Michiharu, *Journal of American Ceramic Society*, 2000, 83(6), 1386-1392.

8. K. Matsui and O. Michiharu, *Journal of American Ceramic Society*, 2001, 84(10), 2303-2313.

9. C.D. SagelRansijn, A.J.A. Winnubst, B. Kerkwijk, A.J. Burggraaf and H. Verweij, *Journal of the European Ceramic Society*, 1997, 17(6), 831-841.

10. C.D. SagelRansijn, A.J.A. Winnubst, A.J. Burggraaf and H. Verweij, *Jounal of the European Ceramic Society*, 1996, 16(759-766.

11. S. Rajendran, *Materials Forum*, 1993, 17(333-350.

12. G.-Y. Guo, Y.-L. Chen and W.-J. Ying, *Materials Chemistry and Physics*, 2004, 84(2-3), 308-314.

13. G.-Y. Guo and Y.-L. Chen, *Journal of Solid State Chemistry*, 2005, 178(5), 1675-1682.

14. R.C. Garvie, *Journal of Physical Chemestry*, 1965, 69 (4), 6.

15. M.N. Rahaman, *Ceramic Processing and Sintering Second Edition*, Marcel Dekker, New York, 2003.

16. R. Perry and D. Green, *Perry's Chemical Engineers Handbook Seventh Edition*, McGraw-Hill New York, 1997.

17. B.D. Cullity, *Elements of X-Ray Diffraction Second Edition*, Addison-Wesley Publishing Company, Reading Massachusetts, 1978.

18. R. Mistler and E. Twiname, *Tape Casting Theory and Practice*, American Ceramic Society, Westervill OH, 2000.

19. R.A. Young, *The Rietveld Method*, International Union Of Crystallography Oxford University Press, West st Oxford, 1993.

5. Industrial Precipitation of Zirconyl Chloride: The Effect of pH and Solution Concentration on Calcination of Zirconia.

Carter G., Hart R., Rowles M., Ogden M., Buckley C., 2009 '*Industrial Precipitation of Zirconyl Chloride: The Effect of pH and Solution Concentration on Calcination of Zirconia',* Materials Chemistry and Physics Doi: 10.1016/j.matchemphys.2009.05.014

ARTICLE IN PRESS

Industrial precipitation of zirconyl chloride: The effect of pH and solution concentration on calcination of zirconia

G.A. Carter[a,b], M. Rowles[c], M.I. Ogden[a,*], R.D. Hart[b], C.E. Buckley[b]

[a] Nanochemistry Research Institute, Department of Chemistry Curtin University of Technology, PO Box U1987, Perth, Western Australia 6845, Australia
[b] Centre for Materials Research, Curtin University of Technology, PO Box U1987, Perth, Western Australia 6845, Australia
[c] Commonwealth Scientific, Industrial Research Organisation (CSIRO), Minerals Division, Clayton, Vic, Australia

ARTICLE INFO

ABSTRACT

In situ and ex situ X-ray diffraction, and transmission electron microscopy were used to investigate the calcination of four samples of zirconia manufactured using two different zirconia reactant solution concentrations (0.81 M and 1.62 M) with precipitation carried out at pH 3 and 12. The calcinations were investigated over the temperature range from room temperature to 1000 °C. It was found that varying the precipitation conditions resulted in differing calcination routes; it is believed that variations in particle size and initial degree of hydration are responsible for these differences. It was also found that the initial phase produced after calcination was tetragonal zirconia, which underwent a process of crystallite growth to a size of ~30 nm before transformation from tetragonal to monoclinic.

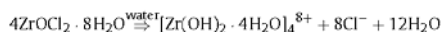© 2009 Elsevier B.V. All rights reserved.

1. Introduction

Zirconia is of increasing interest for diverse applications including high temperature engine components, ceramic hip replacements, catalysts and solid oxide fuel cells (SOFC) [1]. We are currently studying the aqueous processing of zirconyl chloride to zirconia under conditions relevant to local industrial manufacturers of zirconia products. Investigations have been concerned with the solution chemistry, as well as changes in precipitate particle size when the input parameters are varied [2–4]. It has been shown that the processing parameters used during the wet chemistry stage can have an effect on the particle growth during the process; TGA/DTA demonstrated differences in the responses to heat and micro-combustion and TEM revealed different structures were produced when precipitation was carried out at different pH values. These results coupled with the differences noted in the ceramics produced indicated a more in depth investigation into the calcination process was required [3,4]. This work describes the use of in situ XRD during calcination of the zirconium hydroxide produced using two concentrations of starting solutions (0.81 M and 1.62 M zirconyl chloride) precipitated at two different pH values of 3 and 12.

A full discussion of the literature of the chemical processing of zirconia can be found in previous publications by the authors [2–5]. In brief the processing can be broken down into the following steps:

(1) mixing of solutions, hydrolysis; (2) precipitation, washing and filtering; (3) calcination; followed by milling and packaging.
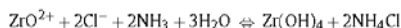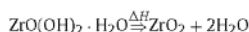
(1) Hydrolysis:

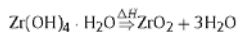$$4ZrOCl_2 \cdot 8H_2O \overset{water}{\Rightarrow} [Zr(OH)_2 \cdot 4H_2O]_4^{8+} + 8Cl^- + 12H_2O$$

(2) Precipitation:
For a pH of 12

$$ZrO^{2+} + 2Cl^- + 2NH_3 + 2H_2O \Leftrightarrow ZrO(OH)_2 + 2NH_4Cl$$

or for a pH of 3

$$ZrO^{2+} + 2Cl^- + 2NH_3 + 3H_2O \Leftrightarrow Zr(OH)_4 + 2NH_4Cl$$

(3) Calcination:

$$ZrO(OH)_2 \cdot H_2O \overset{\Delta H}{\Rightarrow} ZrO_2 + 2H_2O$$

or

$$Zr(OH)_4 \cdot H_2O \overset{\Delta H}{\Rightarrow} ZrO_2 + 3H_2O$$

The exact form of the zirconium hydroxide precipitate, $ZrO(OH)_2$ or $Zr(OH)_4$, is dependent on the pH at which it was formed [3]. It has also been shown that pH 3 precipitates have a higher concentration

* Corresponding author. Tel.: +61 9266 2483; fax: +61 9266 4699.
E-mail address: m.ogden@curtin.edu.au (M.I. Ogden).

of retained NH_4Cl than those produced at pH 12 along with significant differences in particle size and re-dispersion after filtering. These differences may also affect the calcination of the zirconium hydroxide to zirconia.

The available literature of zirconium solution chemistry is often contradictory ([4] and references therein). The interrelationship of chemical processing and crystallisation through calcination is no different; hydrothermal treatment of zirconyl nitrate has been reported to produce tetragonal zirconia [6], however in similar experiments Bleier and Cannon [7] produced both tetragonal and monoclinic zirconia. In situ and ex situ XRD calcination studies on zirconia manufactured from precipitates, sol–gel and hydrothermal processes have all indicated variable results depending upon the production method [8–21].

Burtron [16] indicated the pH of precipitation can change the monoclinic to tetragonal ratio after calcination, although no reasons for the differences were given. It has been suggested that the key factors affecting the phase produced are the chemical methods and the starting materials used in the production of the zirconia [10,22,23]. Garvie [24,25] showed that the tetragonal form of zirconia could occur at room temperature as long as the crystallite size did not exceed the critical size of 30 nm. This was attributed to the surface energy effects. Murase [18,19] suggested that water increases the rate of crystal growth and aided the tetragonal to monoclinic phase transition. In contrast, domain boundaries were suggested to inhibit the tetragonal to monoclinic transformation [26,27]. It was proposed that the crystallisation of tetragonal zirconia occurred on amorphous zirconia by a topotactic process [28,29]. Other studies proposed that tetragonal zirconia was due to the initial nucleation being favoured by trapped electrons due to anionic vacancies [30]. Shukla and Seal [31] cover all of the above proposed reasons for the stabilisation of the tetragonal zirconia with the addition of: macro- and micro-strain, internal and external hydrostatic energy, water vapour and lattice defects and propose that it is the oxygen ion vacancies that govern the phase stability. Irrespective of the proposed cause, what the literature does show is that the chemical route used in the formation and subsequent heat treatment behaviour are correlated and can lead to a different tetragonal to monoclinic phase ratios in the calcined powder.

This work was undertaken to further investigate zirconia calcination, with defined parameters that are relevant to the industrial manufacture of zirconia. We have previously demonstrated [4] that the processing parameters used in the production of zirconia influence the particle size of the precipitates generated as well as the filtration rates and agglomeration and subsequent dispersion. In this work the impact of the same variables on the calcination process was investigated using in situ XRD and ex situ TEM.

2. Experimental procedure

2.1. Sample preparation

Solutions of 0.81 M and 1.62 M of $ZrOCl_2$ (100 g l^{-1} and 200 g l^{-1} of ZrO_2) were prepared by dissolving zirconyl chloride crystals in milli-q water. All solutions were aged for 10 days and used within 12 h of the 10 day time frame. The aging time used was consistent with previous work [4]. Ammonia solution, 28% AR, grade was used to modify the pH of the solutions.

2.2. Precipitation

Precipitation was conducted as a continuous double jet injection that overflowed into an alcohol bath. The overflow product was filtered using a Büchner funnel and subsequently washed using a mixture of methanol, ethanol and water. Washed filtered cake was then dried in an oven at 55 °C for 5 days. The process has been comprehensively described previously [4].

Powders for ex situ XRD investigations were prepared by placing 10 g of oven-dried zirconium hydroxide powder in a platinum crucible in a preheated equilibrated muffle furnace for 45 min. Samples were obtained from 500 to 1000 °C in 100 °C increments. The powder was removed and cooled in a desiccator to room temperature.
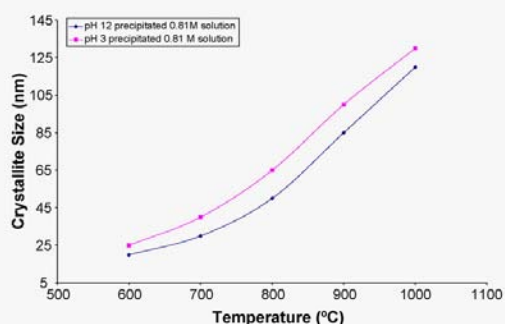

Fig. 1. Crystallite size with increasing maximum calcination temperature obtained via ex situ TEM.

2.3. Diffraction

Ex situ powder diffraction data were collected using Cu K_α radiation (α_1, α_2, weighted average $\lambda = 1.54178$ Å), at an accelerating voltage of 40 kV and filament current of 30 mA on samples with 10 wt% corundum as an internal standard using a Siemens D500 Bragg-Brentano X-ray diffractometer. The use of an internal standard allowed phase composition determination to 1% accuracy [32].

Powder diffraction data collected in situ during the calcinations were obtained using an in situ powder XRD system with a platinum resistance-strip heater. The Pt strip contained a 20.0 mm × 7.0 mm × 0.4 mm sample well. Each sample was hand ground with added ethanol and applied directly to the strip heater as a thick slurry. Diffraction patterns were obtained at 10 °C increments during heating and at 20 °C decrements during cooling. The X-ray diffractometer incorporated an Inel CPS-120 curved, position-sensitive detector with an angular range of 120° 2θ, facilitating rapid, simultaneous data accumulation. Datasets of 60 s duration were collected in reflection mode using Cu K_α radiation operated at 35 kV and 30 mA. Pattern interpretation and modelling was completed using Diffract plus TOPAS Version 3. Print files were made using Traces v 5.2.0 (Diffraction Technologies 1999).

Samples for TEM were prepared by hand grinding approximately 2 mg of powder in an agate mortar and pestle and dispersing the powder in 50 mL of water using ultrasound. The dispersion was added to a 100 mL volumetric cylinder, the heavy aggregate particles were allowed to settle and the dispersed fine fraction collected. TEM samples were prepared by placing a drop of this onto a 3.05 mm holey carbon TEM grid. The particles were examined using a JEOL 2011 Transmission electron microscope fitted with a LaB$_6$ electron gun and operated at 200 kV. The JEOL 2011 TEM is equipped with an Oxford INCA system Energy Dispersive X-ray Spectrometer (EDS) and has Gatan CCD digital image capture.

Energy dispersive spectra were collected at 2000–7000 counts per second for 100 live seconds. Elemental compositions of these crystals were calculated using the thin film method [33,34]. The k-factors used were derived from the spectra of standard minerals and confirmed by reference to the spectra of well-characterised zircon and yttria stabilised zirconia crystals. Camera length determinations for selected area diffraction analyses were determined by reference to aluminium and gold foils.

3. Results

The average crystallite sizes of samples produced from a 0.81 M zirconyl chloride solution precipitated at a pH of 12 and 3 and calcined at 600, 700, 800, and 1000 °C are shown in Fig. 1. Typical micrographs, Fig. 2(A–E), are shown for the pH 12 sample used to develop Fig. 1. It is clear that the crystallite sizes for the pH 3 sample are larger at all of the data points than those of the pH 12. The series of images (Fig. 2(A–E)) show in dramatic terms the coarsening of particle size with increasing temperature. Both powders exhibit a crystallite size that is close to the maximum 30 nm suggested by Garvie [24] that allows for the metastable tetragonal zirconia to be present when calcined at 600 °C. For temperatures greater than 600 °C the crystallite size is above the maximum listed by Garvie [24]. Selected area diffraction was conducted on each sample and it was found that all samples consisted of a mixture of monoclinic and tetragonal phases (see Fig. 2(F)).
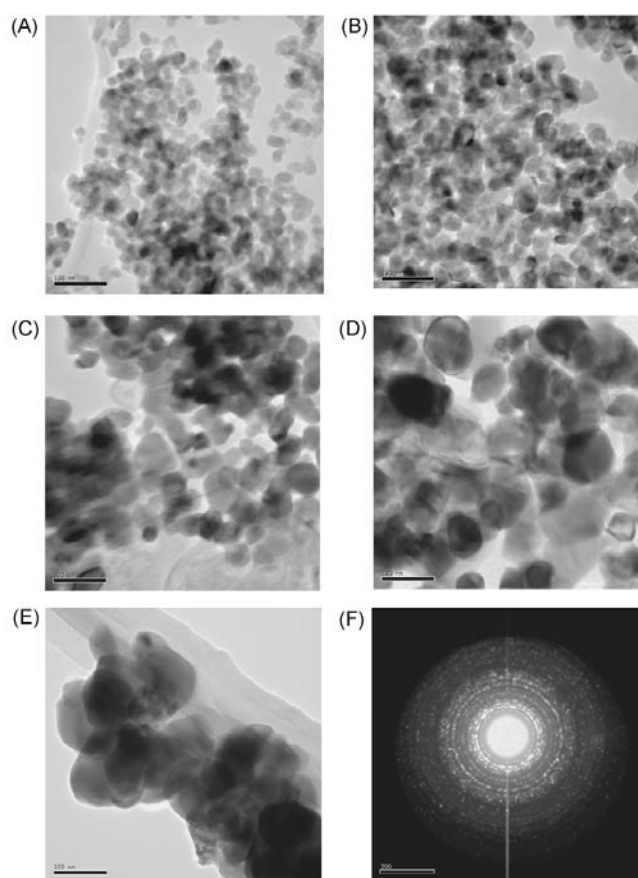
Fig. 2. TEM micrographs of samples precipitated from pH 12, 0.81 mol% solutions calcined at (A) 600°C, (B) 700°C, (C) 800°C, (D) 900°C, (E) 1000°C, and (F) TEM selected area diffractogram diffraction for 600°C sample.

Monoclinic versus tetragonal phase composition determined by XRD investigations of the calcined powder using 10% corundum as an internal standard is shown in Table 1.

Fig. 3 shows a typical XRD data plot with a Topas model (depicted pH 12, 600°C). Typical XRD plots for the pH 12 sample coinciding with the TEM images (Fig. 2) are shown in Fig. 4(A–E). The figures show the phase changes with increasing temperature above 600°C, with the intensity of the tetragonal (1 1 1) peak decreasing and the monoclinic (1 1 1) and (1 1 $\bar{1}$) peaks intensities increasing.

Also observable are the shape changes of these peaks, for example as the crystallite size increases the FWHM decreases.

Table 1 gives the phase composition analysis derived from *ex situ* powder XRD for the two powders at each temperature. Garvie has indicated that tetragonal zirconia is stable at room temperature if the crystallite size is less than 30 nm [24]. A comparison of Table 1 and Fig. 1 shows that even when the crystallite size is smaller than 30 nm there is considerable monoclinic phase present. Similarly there is tetragonal phase present when the crystallite size

Table 1
Phase composition (wt%) for *ex situ* investigation of calcined powder for 0.81 M solution precipitates (numbers in parentheses are the estimated standard deviations (ESD) from the Rietveld modelling [35]).

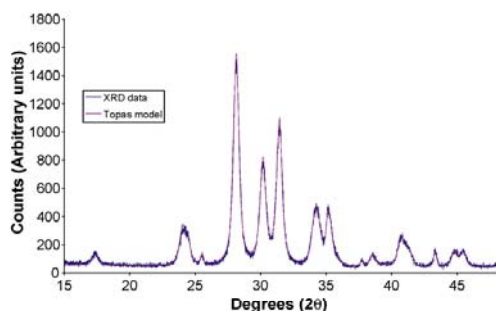| Temperature (°C)	pH 3 Phase composition			pH 12 Phase composition		
	Corundum (%)	Monoclinic (%)	Tetragonal (%)	Corundum (%)	Monoclinic (%)	Tetragonal (%)
600	10 (1)	72 (2)	19 (4)	10 (1)	65 (3)	25 (6)
700	10 (1)	86 (2)	4 (5)	10 (1)	76 (1)	14 (5)
800	10 (1)	88 (2)	2 (3)	10 (1)	83 (1)	7 (5)
900	10 (1)	87 (1)	3 (4)	10 (1)	87 (1)	3 (5)
1000	10 (1)	88 (2)	2 (4)	10 (1)	87 (1)	3 (5)

Fig. 3. XRD data and Topas model for 600 °C calcined powder *ex situ* investigation.

has increased above this threshold. However, this evidence does not directly contradict Garvie's [24] assertions; Garvie used the crystallite size determined in XRD/neutron diffraction or, more correctly, the coherently scattering domain size, whereas the direct measurement by TEM may result in slightly different size domains as individual grains observed in the TEM may consist of multiple scattering domains. In addition, the low percentage of tetragonal zirconia present does not represent a significant contradiction of Garvie's work [19,24].

Fig. 1 and Table 1 demonstrate that the differences in response to heating between samples produced at differing pHs are consistent with those reported previously [2,3]. In particular, the levels

of tetragonal phase in the pH 12 sample are significantly higher at lower temperatures.

Fig. 5 shows a subset of the XRD plots during calcination of the 0.81 M solution precipitated at pH 12, Fig. 6 is a subset of the XRD patterns for the same sample during cooling. For comparison Figs. 7 and 8 are the corresponding subsets for the 0.81 M solution precipitated at pH 3. These plots demonstrate clearly peak intensity changes corresponding to phase composition changes with temperature and also the variation in peak shapes corresponding to changes in crystallite size. Fig. 9 shows another representation of the results for the samples.

The calcination process is illustrated in Fig. 9. In A, the hydrous zirconia produced from 0.81 molar concentration ZrOCl₂ starting solution and precipitated at pH 12 is transformed to tetragonal zirconia (circle) at approximately 500 °C. This material remains stable and suddenly transforms to predominantly monoclinic zirconia between 700 and 500 °C. An initial small amount of monoclinic zirconia (ticks) transforms to tetragonal zirconia and rapidly decreases until the bulk of the tetragonal material is transformed. The crystallite size of the tetragonal zirconia (square) is initially stable at <20 nm up to about 620 °C then increases with increasing temperature to >80 nm. The monoclinic material shows crystallite growth starting at 900 °C (triangle) to become constant at 20 nm. The initial noise displayed in the graphs for the monoclinic crystallite size determination is expected and is due to the initial low concentrations of the phase at the start of transformation of the tetragonal phase back to monoclinic and so that transformation of only several particles has a large impact on the determined size.

In B, the hydrous zirconia produced from 1.62 molar concentration ZrOCl₂ starting solution and precipitated at pH 12 is similarly
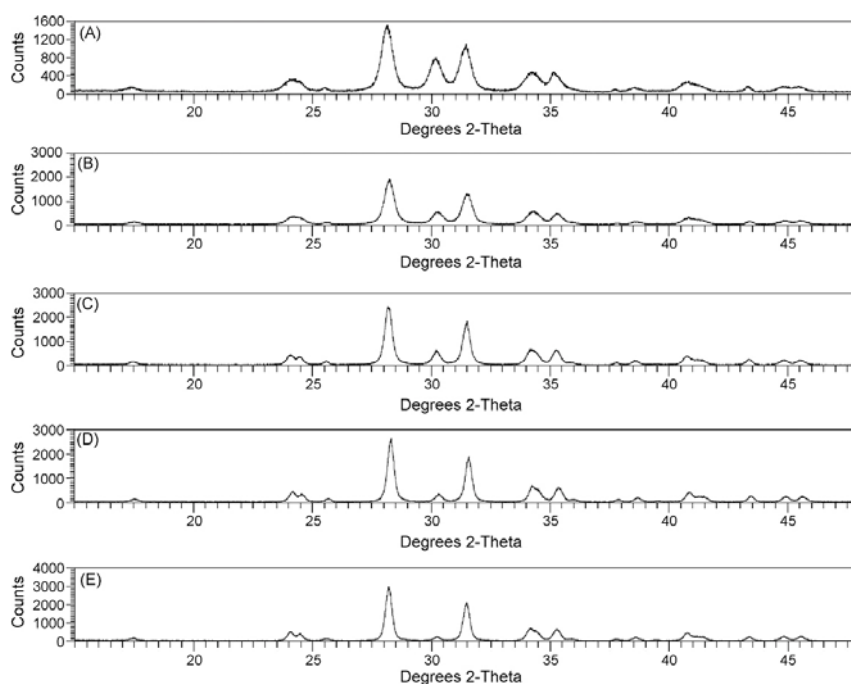

Fig. 4. XRD plots for precipitates from pH 12, 0.81 mol% solution calcined at (A) 600 °C, (B) 700 °C, (C) 800 °C, (D) 900 °C, and (E) 1000 °C.
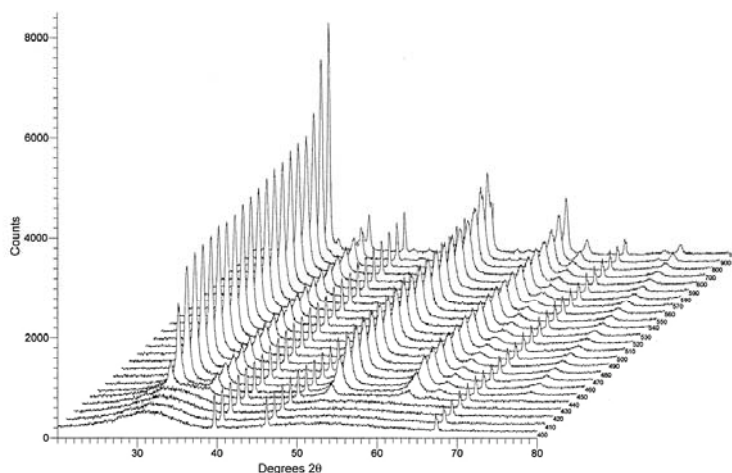
Fig. 5. XRD plots of precipitate from pH 12, 0.81 M solution heating 400 to 1000 °C.

transformed to tetragonal zirconia at approximately 500 °C but commences transformation to monoclinic zirconia at approximately 800 °C. The slope of the curve representing the decreasing concentration of tetragonal material is much more gradual than in A. The particle size of the tetragonal material when formed starts at approximately 30 nm and increases from 800 °C with increasing temperature and decreasing tetragonal phase before falling as cooling commences, eventually stabilising at 20 nm. The monoclinic crystallite size starts at 23 nm for a low concentration of material and increases with temperature and monoclinic phase concentration before falling on cooling and stabilising at 35 nm.

The two pH 3 precipitated materials behave similarly to B with the addition of distinct plateaus in both tetragonal to mono-

clinic transformation and crystallite size changes in the cool down between 1000 °C and 700 °C.

4. Discussion

The XRD results from the *in situ* experiments are consistent with *ex situ* calcination of the zirconia. and show almost exclusively monoclinic zirconia after heating to 1000 °C and cooling (Fig. 9) irrespective of the starting solution concentration or the pH at which precipitation was carried out. However, the advantage of the *in situ* experiments is that the phase progression can be tracked from the amorphous hydrous zirconia to the monoclinic phase. In all samples, there is some initial monoclinic material in the dried filter cake that decreases as the tetragonal phase concentration
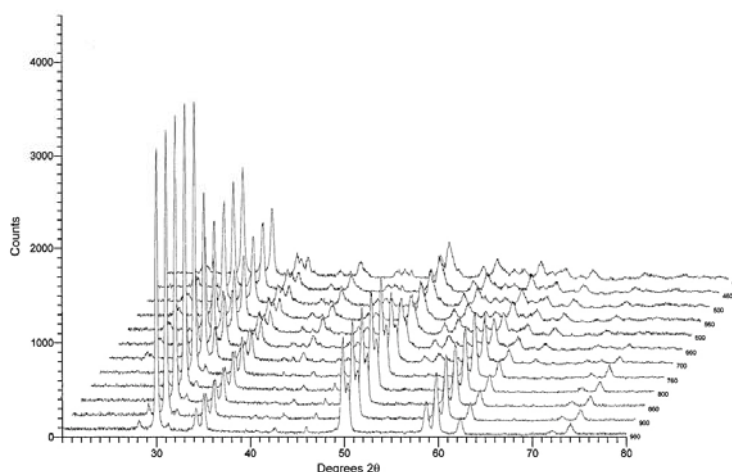

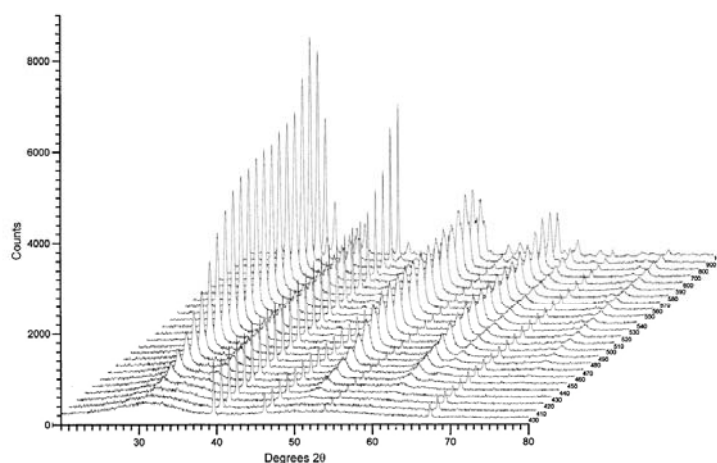**Fig. 6.** XRD plots of precipitate from pH 12, 0.81 M solution cooling from 980 to 400 °C.

Fig. 7. XRD plots of precipitate from pH 3, 0.81 M solution, heating from 400 to 1000 °C.

increases with heating, the actual amount is difficult to quantify due to the masking effect of the amorphous hump in the diffraction patterns. Observation of the crystallite size of the tetragonal phase supports Garvie's premise that crystallite size and the formation of metastable tetragonal zirconia are related [24]. The monoclinic phase concentration does not increase again until after the tetragonal crystallite size has increased to approximately 30 nm. The final crystallite size of the monoclinic material is smaller than the initial tetragonal phase, which contradicts the expected 4.6% growth due to the phase (lattice) change. This may be because the crystallites are breaking apart during the calcination process as was also observed by the authors in previous work using TEM and SEM [4].

The two samples manufactured at pH 3 (Fig. 9C and D) have slightly lower levels of tetragonal zirconia during the process. The two pH 3 samples display a plateau stage in the transformation of tetragonal to monoclinic during the calcination, Murase suggests that the presence of water during calcination and other processing steps [17,18] reduces the amount of tetragonal zirconia present. Carter et al. [3] has shown that the hydrous zirconia produced at pH 3 is best formulated as $Zr[OH]_4$, whereas at pH 12 the product is more consistent with $ZrO(OH)_2$. The different observed transformation behaviours may be due to the differences in the structures.

Fig. 9 also shows that the pH 12, 0.81 M sample has a significantly different transformation path to the other samples. The tetragonal phase material is stable above the 750 °C temperature whereas most of the other samples commenced transformation at this temperature. It has a final monoclinic crystallite size of 20 nm while the other three samples are well above this. This is believed
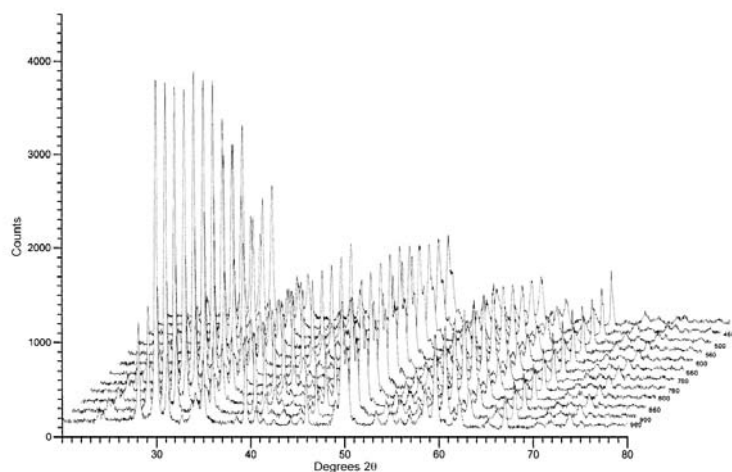

Fig. 8. XRD plots of precipitate from pH 3, 0.81 M solution cooling from 980 to 400 °C.

80

to be due to the initial particle size of the precipitates. As previously reported, zirconia produced under these conditions (pH 12 and 0.81 M solution) contain approximately 49 nm particles, significantly smaller than those produced under the other conditions studied (pH 12/1.62 M = 743 nm, pH 3 0.81 M and 1.62 M = 1130 and

2160 nm, respectively) [3]. The small particle size results in a higher surface area that would allow for more rapid dehydroxylation. The difference seen in the rates of the transformation between the zirconia powders produced from 0.81 M and 1.62 M $ZrOCl_2$ solutions at pH 12 are also believed to be due to particle size differences.
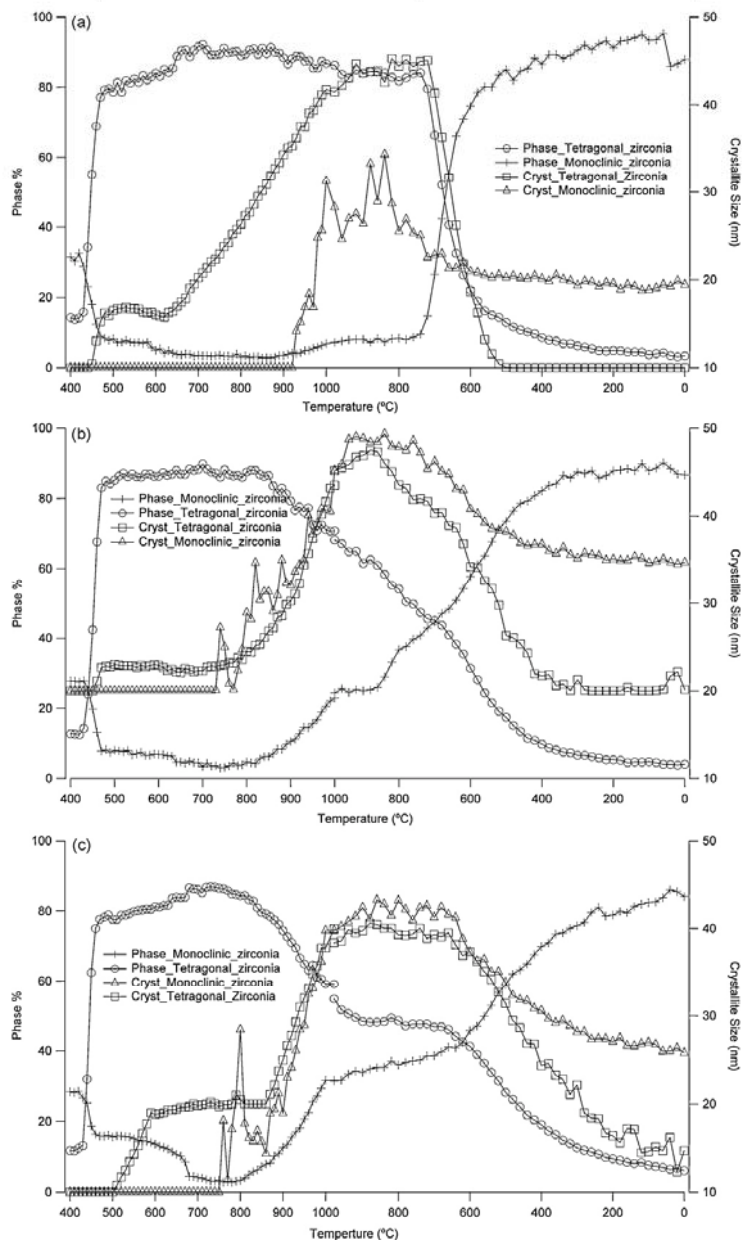

Fig. 9. Crystallite size and phase composition (wt%) changes for calcinations of powders obtained from (A) pH 12, 0.81 M solution, (B) pH 12, 1.62 M solution, (C) pH 3, 0.81 M solution, and (D) pH 3, 1.62 M solution.
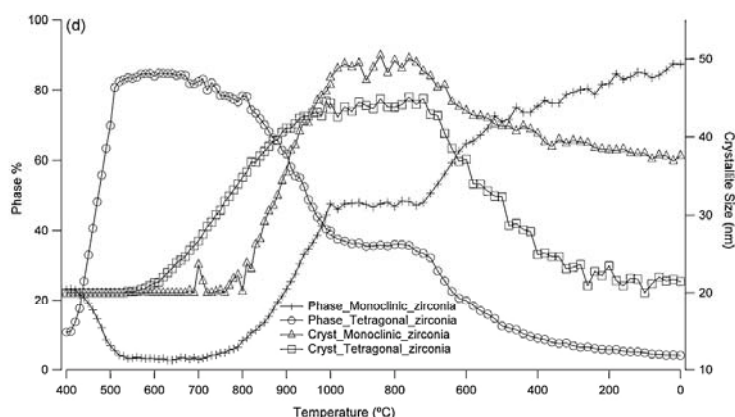
Fig. 9. (*Continued*).

5. Conclusions

In situ and *ex situ* XRD along with TEM has been used to study the calcination of zirconia precipitated from zirconyl chloride solutions of different concentrations and pH. The path taken during calcination was found to vary depending on the precipitation conditions. These differences are strongly related to the initial particle size and the structure of the precipitated hydrous zirconia. The sample made at pH 12 and a concentration of 0.81 M has a distinctly different response to temperature than the other three samples, consistent with the small particle size and composition of this sample. The *in situ* XRD experiments provided clear evidence that increases in particle size of tetragonal zirconia with increasing temperature precedes the transformation to the monoclinic phase.

References

[1] R. Stevens, Introduction to Zirconia, vol. 13, Magnesium Elektron, Swinton Manchester, 1986.
[2] G. Carter, M. Rowles, R. Hart, M. Ogden, C. Buckley, Mater. Forum 32 (2008) 82.
[3] G.A. Carter, R.D. Hart, M.R. Rowles, C.E. Buckley, M.I. Ogden, Powder Technol. 191 (2009) 218.
[4] G.A. Carter, M.I. Ogden, C.E. Buckley, C. Maitland, M. Paskevicius, Powder Technol. 188 (2009) 222.
[5] G.A. Carter, R.D. Hart, N.M. Kirby, D. Milosevic, A.N. TiTkov, J. Australas. Ceram. Soc. 39 (2003) 149.
[6] R.P. Denkewicz, K.S. Ten huisen, J.H. Adair, J. Mater. Res. 5 (1990) 2698.
[7] A. Bleier, P.F. Becher, K.B. Alexander, C.G. Westmoreland, J. Am. Ceram. Soc. 75 (1992) 2649.

[8] X. Turrillas, P. Barnes, A.J. Dent, S.L. Jones, C.J. Norman, J. Mater. Chem. 3 (1993) 583.
[9] D.D. Upadhyaya, A. Ghosh, G.K. Dey, R. Prasad, A.K. Suri, J. Mater. Sci. 36 (2001) 4707.
[10] R. Srinivasan, H. Burtron, O. Davis, B.C. Camden, R. Hubbard, J. Am. Ceram. Soc. 75 (1992) 1217.
[11] C.L. Ong, J. Wang, L.M. Gan, S.C. Ng, J. Mater. Sci. Lett. 15 (1996) 1680.
[12] C.L. Ong, J. Wang, S.C. Ng, L.M. Gan, J. Am. Ceram. Soc. 81 (1998) 2624.
[13] W.Z. Zhu, Ceram. Int. 24 (1998) 35.
[14] G.J. Callon, D.M. Goldie, M.F. Dibb, J.A. Cairns, J. Paton, J. Mater. Sci. Lett. 19 (2000) 1689.
[15] L. Lopato, A.V. Shevchenko, V.P. Red'ko, V.V. Pasichnyi, Powder Metall. Metal Ceram. 45 (2006) 1.
[16] H.D. Burtron, J. Am. Ceram. Soc. 67 (1984), C.
[17] Y. Murase, E. Kato, J. Am. Ceram. Soc. 62 (1979) 527.
[18] Y. Murase, E. Kato, J. Am. Ceram. Soc. 66 (1983) 196.
[19] Y. Murase, E. Kato, K. Daimon, J. Am. Ceram. Soc. 69 (1986) 83.
[20] A. Clearfield, Pure Appl. Chem. 14 (1964) 91.
[21] A. Clearfield, J. Mater. Res. 5 (1990) 161.
[22] R. Srinivasan, R.J. De Angelis, B.H. Davis, J. Mater. Res. 1 (1986) 483.
[23] L. Rice, B.H. Davis, R. Srinivasan, J. Am. Ceram. Soc. 73 (1990) 3528.
[24] R.C. Garvie, J. Phys. Chem. 69 (1965) 6.
[25] R.C. Garvie, J. Phys. Chem. 82 (1978) 218.
[26] Y. Fujiki, T. Mitsuhashi, J. Am. Ceram. Soc. 56 (1973) 493.
[27] M. Ichihara, U. Taksuke, T. Mitsuhashi, J. Am. Ceram. Soc. 57 (1974) 97.
[28] M. Yoshimura, S. Somiya, E. Tani, J. Am. Ceram. Soc. 64 (1981), C.
[29] M. Yoshimura, S. Somiya, E. Tani, J. Am. Ceram. Soc. 66 (1983) 11.
[30] M.I. Osendi, J.S. Moya, C.J. Serna, J. Soria, J. Am. Ceram. Soc. 68 (1985) 135.
[31] S. Shukla, S. Seal, Int. Mater. Rev. 50 (2005) 45.
[32] B.H. O'Connor, D.Y. Li, Adv. X-ray Anal. 43 (2000) 305.
[33] G.W. Lorimer, Mineral. Mag. 51 (1987) 49.
[34] W.B. Jepson, J.B. Rowse, Clay Clay Miner. 23 (1975) 310.
[35] R.A. Young, The Rietveld Method, International Union of Crystallography Oxford University Press, New York, 1993.

6. Industrial Precipitation of Yttria Partially Stabilised Zirconia

Carter G., Hart R., Rowles M., Ogden M., Buckley C., 2009 '*Industrial Precipitation of Yttria Partially Stabilised Zirconia',* Journal of Alloys and Compounds, DOI:10.1016/j.jallcom.2009.02.005.

Industrial precipitation of yttrium chloride and zirconyl chloride: Effect of pH on ceramic properties for yttria partially stabilised zirconia

G.A. Carter[a,b], R.D. Hart[b], M. Rowles[c], M.I. Ogden[a,*], C.E. Buckley[b]

[a] Nanochemistry Research Institute, Curtin University of Technology, PO Box U1987, Perth, Western Australia 6845, Australia
[b] Centre for Materials Research, Curtin University of Technology, PO Box U1987, Perth, Western Australia 6845, Australia
[c] Commonwealth Scientific, Industrial Research Organisation (CSIRO), Minerals Division, Clayton, Vic, Australia

ARTICLE INFO

ABSTRACT

Two 3 mol% partially stabilised zirconia (P-SZ) samples suitable for the SOFC market were manufactured from solutions through to ceramics using a method similar to a known industrial process. The only difference in preparation of the two 3 mol% P-SZ samples was the pH of precipitation which was set at pH 3 or 12. Particle size measurements by dynamic light scattering were used to characterise the precipitate and the filtration rates were investigated. Five point N_2-BET was used to investigate the specific surface area before and after calcination with the response to temperature tracked. Similarly TGA/DTA investigation was used to determine the calcination point during all of these tests and it was found that both powders behaved similarly. XRD-Rietveld analysis incorporating in situ and ex situ calcination revealed that the pH 3 sample had more monoclinic phase present after calcination and sintering as a ceramic. Ceramic testing incorporating hardness (Vickers), toughness (K_{1C}), MOR, density and grain sizing was carried out, all determined that the material produced at pH 12 was superior for SOFC applications than the pH 3 sample. Further investigation using TEM-EDS revealed that the processing of the pH 3 powder had allowed a lower concentration of the yttrium which was incorporated at approximately 2 mol% instead of the required 3. ICP-OES of the after filter liquor indicated that high concentrations of yttrium (797 ppm) were found in the solution with the wash solution having 149 ppm yttrium. In contrast the pH 12 samples had 7 ppm in both the after filter liquor and wash indicating that the yttrium is bound within the matrix more completely at the higher pH.

© 2009 Elsevier B.V. All rights reserved.

1. Introduction

Zirconia and yttria-doped zirconia are important technological ceramic materials. As part of an on-going research program we have been investigating the fundamental chemistry of the processing of these materials, with a core focus on industrially relevant aqueous processing. Here we are using zirconyl chloride and investigating how the aqueous processing changes might affect the ceramic performance.

Previous publications by the group have highlighted differences in the aqueous processing of both un-doped and doped zirconia in the through-processing of the wet chemistry. Small Angle X-ray Scattering (SAXS) of zirconyl chloride solution speciation demonstrated changes with solution concentration and doping levels. This work found few changes were evident by increasing the solution concentration from 0.81 to 1.62 M, however a trend was noticed with increasing yttrium chloride concentration from 3 to 10 mol% [1]. Dynamic light scattering (DLS) characterising the precipitates

obtained at pH 6 demonstrated that significant particle growth was observed upon doubling the concentration and enhanced particle growth was also seen upon the introduction of doping elements, in particular yttrium [1].

Further work focused on process changes found that significant differences in precipitated particle size were caused by both the pH of precipitation and the agitation level. Investigations of materials produced at pH 3 and 12, using TGA/DTA, micro-combustion and TEM EDS, found that the precipitated zirconium hydroxide had different structures, with the pH 3 sample giving results consistent with a formulation of $Zr[OH]_4$ while the pH 12 sample was consistent with $ZrO[OH]_2$ [2]. Previous work conducted on the through-processing has in the main concentrated on un-doped zirconia and demonstrated that there were differences evident in the ceramics made from zirconia produced at the different pH values [3]. Carter et al. [1–3] outline a number of authors who have similarly found the performance of zirconia dependent on the process used in its manufacture.

The major focus of this research was to facilitate the industrial processing of zirconia for Solid Oxide Fuel Cell (SOFC) applications and therefore we have focused on the through-processing and ceramic properties of a 3 mol% yttria zirconia which is commonly

---

* Corresponding author. Tel.: +61 8 9266 2483; fax: +61 8 9266 4699.
E-mail address: m.ogden@curtin.edu.au (M.I. Ogden).

called 3 mol% yttria partially stabilised zirconia (3 mol% Y-PSZ). The current work follows the processing steps from precipitation through to general ceramic testing to compare the differences between ceramics obtained from powders manufactured at pH 3 with those produced at pH 12.

The engineering/physical properties of zirconia have been thoroughly reviewed [4,5]. SOFC are devices for converting hydrogen (or natural gas) and oxygen into water with a resulting generation of electrical power. The obvious difference between a SOFC and other fuel cells is that the major component in the anodes, cathodes and electrolytes are entirely or partially made from an oxide ceramic. Badwal and Foger [6] detail that SOFC electrolytes must not only have high oxygen-ion ionic conductivity but must also be stable with respect to other cell components, and have the mechanical properties such as strength, toughness, creep and thermal shock resistance. SOFC place high demands on both the materials that they are manufactured from and the manufacturing method. In addition, the components themselves are required to have good ionic/electrical properties and be able to withstand high operating temperatures while maintaining the mechanical properties required for typical life times of 40,000–50,000 h [6].

Most SOFC manufacturers/developers are using zirconia doped with yttria as the electrolyte with variations in the amount of yttria [7]. The physical characteristics of precursor powders for the manufacture of a planar SOFC have been discussed by Bellon et al. and Ahmed et al. [8,9]. Carter et al. [10] showed that the process of co-precipitation of three initially mixed chlorides, alumina chloride, yttrium chloride and zirconium chloride, can produce an oxide powder that has a homogeneous distribution of all three constituents. This homogeneity in solid solution allows for greater control of the zirconia polymorphs, leads to better processing ability in the manufacture of the parts of the SOFC, and because of a lack of concentration gradients in the finished material is likely to lead to better lifetimes.

McEvoy [11] states that the ideal solid electrolyte was identified by Nernst as zirconium oxide with a mixture of di- or trivalent substitutes in solid solution, with the 8% yttria–zirconia being preferred. 3 mol% Y-PSZ has subsequently been found to be better due to its inherent mechanical strength [12,6]. SOFC manufacturers have investigated a range of novel formulations often with other elements substituting for yttria [12–18]. Ciacchi et al. [7] supply comparative chemical, XRD phase composition, sintered density, grain size and conductivity data for five commercially produced 3 mol% Y-PSZ, providing bench mark information for any prospective commercial producer of 3 mol% Y-PSZ for SOFC applications, although no information as to how they are made are given.

2. Experimental procedures

Solution preparation, precipitation, milling and particle sizing by DLS, were carried out as reported previously [1,3], with further details contained in the Supplementary information. It is of note that precipitation was carried out in line with a local manufacturer's technology that is of a proprietary nature [10].

After milling to a particle size ranging from 15 to 42 μm the slip was spray-dried using a binder.

Sintered sample characterisation as well as in situ calcination studies were conducted using X-ray diffraction (XRD) with the patterns being analysed using Rietveld refinement (full experimental details are contained in the Supplementary information).

The physical testing of the 3 mol% yttria–zirconia matrix was carried out using a range of standard or well known tests, as described in the Supplementary information.

3. Results

We have previously studied the precipitation of zirconia in the absence of yttrium, and found that pH has a significant impact on

Table 1
Wet chemistry conditions and physical properties (PS is mean diameter by peak intensity).

pH	Concentration of starting solutions	Agitation level	PS (μm)	Filtration rate minutes	SSA (m² g⁻¹)
3	0.81	High	2.7(1)	5	197(5)
12	0.81	High	1.8(2)	7	215(3)

the nature of the precipitate [1,2]. The conditions used here (Table 1) are based on this earlier work. It was immediately noted that with the added yttrium, the differences in particle size (Table 1) as a function of pH are much smaller than found for the pure zirconia system [2].

Fig. 1 shows the TGA/DTA trace for both the pH 3 and 12 samples. The calcination point for both samples was approximately 400 °C with a weight loss of around 43% (pH 3, 405 °C, 42.4 wt% and pH 12, 393 °C and 44.2 wt%). Once again, the change in pH is found to induce a much smaller change than found in the pure zirconia system; previously the authors reported that a marked difference exists between zirconium hydroxide precipitated at differing pH values [2]. For a non-stabilised zirconia system the maximum weight loss was 32.5 wt% assigned to a transformation of ZrO[OH]$_2$ to ZrO$_2$. In this case the mass loss is significantly greater for what in relative terms is a small amount of added yttrium. One explanation for this is that the additional yttrium has changed the surface charge such that less water is driven off during the drying process prior to the TGA/DTA analysis.

Fig. 2 shows the X-ray diffraction patterns for the pH 12 sample during the calcination; Fig. 3 shows the plots for the pH 3 sample. The transformation temperature differences observed between
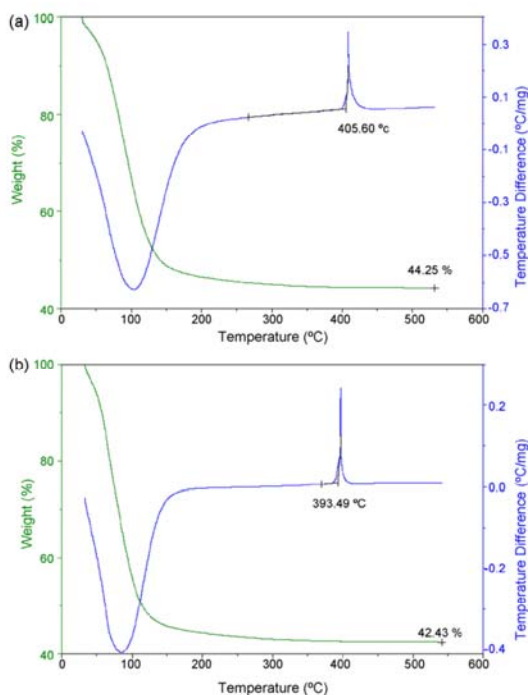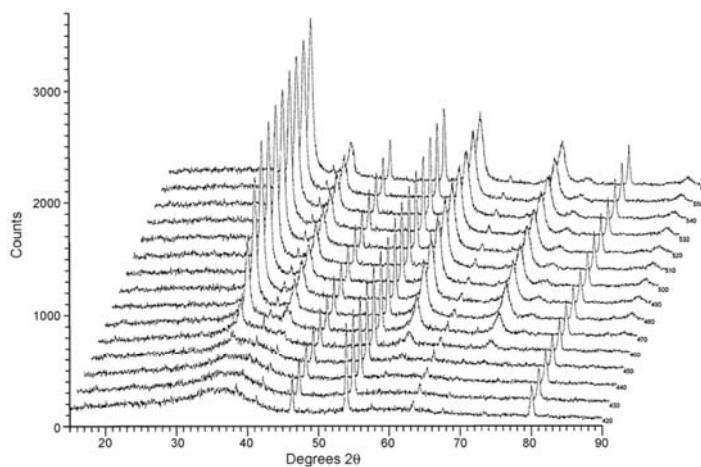

Fig. 1. TGA/DTA trace (a) pH 3 sample; (b) pH 12 sample.

85

Fig. 2. XRD plots with increasing temperature through calcination, pH 12 sample.
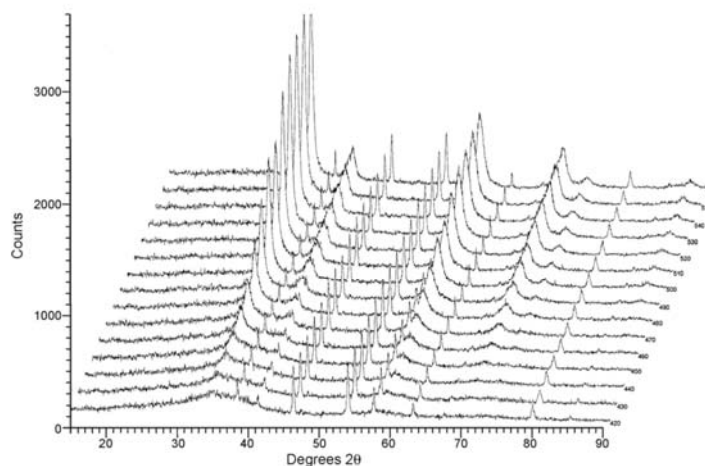

Fig. 3. XRD plots with increasing temperature through calcination, pH 3 sample.

the TGA/DTA and the X-ray diffraction are assumed to be due to experimental differences, with sample size, temperature steps with holds and temperature measuring systems all contributing. A typical pattern fit from the Rietveld analysis to determine the phase compositions of the samples with temperature is shown in Fig. 4. The results of the phase analysis are shown in Fig. 5, the phase composition % does not appear to change once the maximum tetragonal phase has been obtained. Here some differences with pH are observed; for the pH 3 precipitated samples the maximum is approximately 75%, while for the pH 12 samples it is approximately 90%.

TEM microscopy (Fig. 6) found that a crystallite size of 18 ± 5 nm within a larger aggregate was typical for both powders. The specific surface area (SSA) response with calcination was also similar, showing a linear decrease from approximately 700 °C until 1100 °C (Fig. S 3).

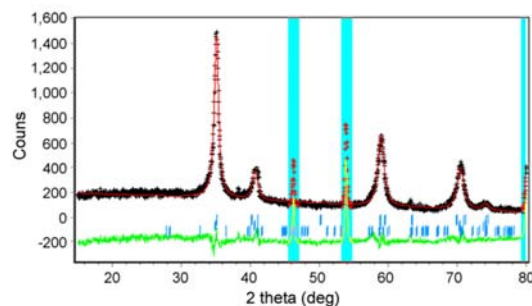**Fig. 4.** Rietica plot pH 12 sample @ 580 °C (the regions of exclusion are peaks due to Pt strip heater/sample holder).
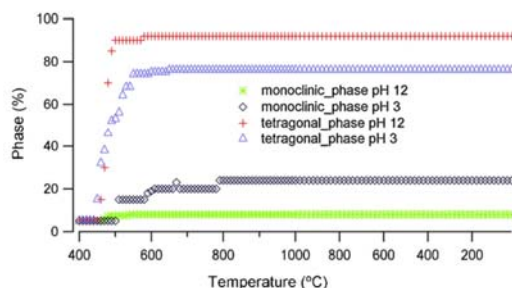
Fig. 5. Phase composition for both samples with temperature (all uncertainties for both phases are 3%).
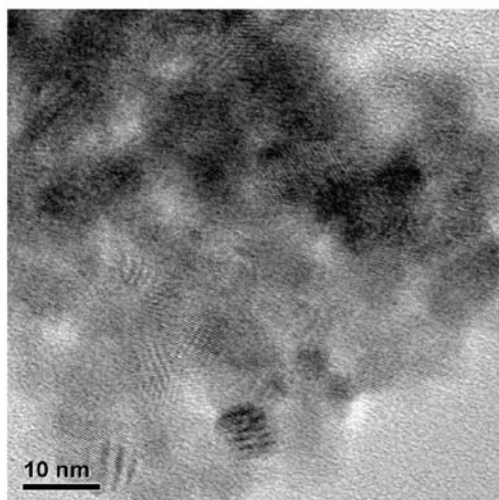

Fig. 6. pH 12 sample TEM image showing lattice planes.

Attrition milling curves for samples of powders calcined at 1000 °C were similar for the last 7 h of milling with the total time of 22 h in both cases. The responses in the first 10 h do vary, with the pH 3 sample D90 reducing more slowly than that of the pH 12, as also found for unstabilised zirconia [3]. Full milling curves are contained in the supplementary information (Figs. S 1 and 2).

The sintered density of 3 mol% Y-PSZ samples is reported to be between 6.04 and 6.08 g cm^{-3} [7,13]. Varying densities have been reported for commercial samples sintered at 4 different temperatures [14] and a similar firing regime was used here. The results (Table 2) show that the sintered densities for the pH 3 samples are between 5.88 and 5.80 g cm^{-3} with those of the pH 12 samples between 6.01 and 6.08 g cm^{-3}, depending on thermal treatment.

The density of the pH 3 sample was considerably lower than literature values, and various causes for this were considered. It has

Table 3
Physical properties of ceramics (fired at 1550 °C).

	pH 3	pH 12
Grain size (μm)	2(2)	2(2)
Hardness (GPa)	12.60(8)	12.46(3)
Toughness (MPa m$^{1/2}$)	6.32(9)	6.78(7)
MOR (GPa)	0.81(7)	1.02(3)
Weibull modulus	9.68	13.34

been suggested that less than optimal densities can be caused by the powder compacts containing hard agglomerates from the powder processing [15]. The strength of the spray-dried agglomerates was investigated using a literature method [16] and the powders were found to be the same (a SEM micrograph of a typical spray-dried agglomerate can be seen in Fig. S 4). Another explanation could be the porosity in the ceramic but the grain sizing micrographs showed little evidence of this (see Fig. S 5 for typical grain sizing micrograph). Investigations of the porosity of yttria–zirconia ceramics have been conducted to good effect in this manner previously [17].

The linear shrinkage for 3 mol% Y-PSZ is reported to be 27% [18]. The values listed in Table 2 for the maximum density are slightly lower at 24 and 25% for the pH 3 and 12 samples respectively.

Table 3 shows the other physical properties obtained from the testing of the samples. The grain size of the two samples revealed that the two powders (pH 3 and 12) are similar. Grain size is linked with surface flatness of tape cast parts, with grain sizes up to 10 μm producing "excellent" flatness [8]. SEM micrographs of the powders produced here show grain sizes well below the 10 μm range. A reported generalisation is that the grain size of YSZ materials with less than 8.5 mol% yttria is usually larger than 5 μm [12]. Other reports, however, give grain sizes of approximately 0.6 μm [7,14,19]. A rather novel but simple experiment [20] showed that exaggerated growth of grains can be attributed to variation in yttria concentrations within the system, and hence the relatively small particle size distribution within the two samples in this work may indicate a relatively uniform or homogenous yttria distribution, which is an advantage of the co-precipitation method used to prepare the samples.

Hardness of the Y-SZ determined using Vickers indentation is shown in Table 3. Fig. S 6 shows a typical optical micrograph of an indentation observed in this work. The resulting values are consistent with literature [6,21,22]. Kondoh et al. [23] lists lower densities and higher hardness and toughness values for ceramics with lower yttrium levels. In Hsieh and Tuan [20] the value for the hardness and toughness for 3 mol% Y-PSZ is 13.1 ± 0.2 GPa and 4.5 ± 0.2 MPa m$^{1/2}$ for a mixture of co-precipitated 8 mol% YSZ with pure zirconia powder co-milled to form 3 mol% Y-PSZ. The increased hardness is suggested to be a result of the uneven distribution of yttria [20], the materials examined in the present work have lower hardness values but have higher toughness values. Hsieh and Tuan [20] used the K_{1C} method to determine the hardness, which is the same method employed here following literature procedures [24]. However, Kruzic and Ritchie [25] suggest that this may not be suitable due to secondary cracking which is evident in Fig. S 6. The K_{1C} method has nevertheless been used for this work as results using the method suggested by Kruzic and Rictchie [25] are rarely reported.

Table 2
Sintering temperature vs density and % linear shrinkage (uncertainties are std. deviation of 5 samples).

Sintering temperature	pH 3 density (g cm^{-3})	% Linear shrinkage	pH 12 density (g cm^{-3})	% Linear shrinkage
1650	5.85(1)	20(3)	6.04(2)	20(2)
1550	5.88(1)	24(1)	6.08(2)	25(1)
1450	5.86(2)	21(3)	6.03(2)	20(4)
1350	5.80(5)	19(2)	6.01(4)	20(3)

87
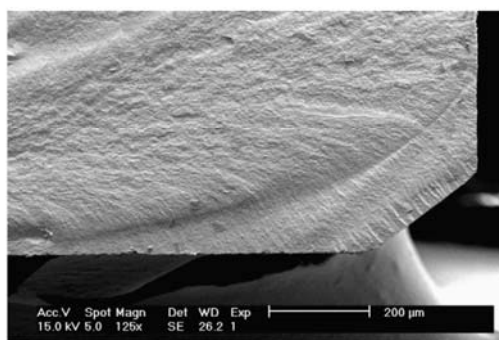
Fig. 7. MOR bar broken surface showing chamfer (pH 12).

Table 4
ICP-OES results of liquor and wash for yttrium.

Sample	Y (ppm)
pH 3 liquor	797
pH 3 wash	149
pH 12 liquor	7
pH 12 wash	7

Kondoh et al. [23] list tensile strength against the yttria content for commercially available Y-SZ and Y-PSZ. They found that the tensile strengths of 2.6, 3 and 4 mol% Y-PSZ were the same. They also found K_{1C} fracture toughness values of for the 2.6 and 3 mol% samples of 5 MPa m$^{1/2}$ and the 4 mol% had a value closer to 6 MPa m$^{1/2}$. These values are comparable with those determined here (Table 3).

A comparison of the bars manufactured for the Modulus of Rupture (MOR) test showed that their optical properties appeared to be different (Fig. S 7), although the reason for this is not apparent at this stage. The value of 1.02 GPa developed for the pH 12 sample exceeds that listed by Badwal and Foger [6]. However these authors also list 900 MPa as the lower limit, which the pH 3 sample does not reach. The minimum Weibull modulus requirement for a modern engineering ceramic is 9.7 which both samples achieved (pH 12 = 13.34, pH 3 = 9.86, Table 3) [26]. Fig. 7 is a typical micrograph of the fractured surface of the MOR bars showing there were no indications of poor forming or sintering in either sample.

Fig. 8 shows the XRD traces for the sintered ceramics of both samples, the differences are mainly the presence of higher concentrations of monoclinic phase in the pH 3 sample compared to the pH 12 sample. The hump at 28.44° 2θ in Fig. 8 is similar to the literature result for a 2.6% sample [27] suggesting the pH 3 sample may have this composition. This hypothesis was tested by TEM EDS analysis.

TEM EDS determined yttria values for the two samples were 3.3(8) wt% for pH 3 and 5.5(4) wt% for pH 12 (equivalent to 1.8 and 3 mol%; figures in brackets are the uncertainties in the last decimal place from the standard deviation of 20 sample points). The dif-
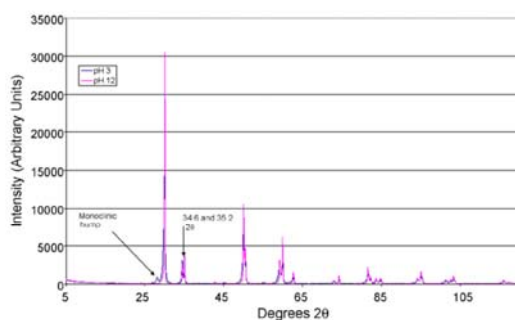
ference was unexpected as both samples were produced from the same initial solution compositions.

Literature values [13] for the densities of 1.7, 2.2, 2.8 and 3.1 mol% Y-PSZ are given as 5.842, 6.044, 6.085 and 6.077 g cm^{-3} (measured). In this work, the pH 3 sample returned a density of 5.88 g cm^{-3} and the pH 12 gave 6.08 g cm^{-3}. This would suggest that the pH 3 sample had between 1.7 and 2.2 mol% yttria consistent with the TEM EDS result of 2 mol%.

Subsequent testing of the liquor after passing through the filter and of the wash solution using ICP-OES indicated that minimal yttrium is lost from the pH 12 processing, however the pH 3 sample had high levels of yttrium in the liquor as well as the wash (Table 4). This would indicate that the yttrium is not precipitating out under the acidic conditions in such a way as to be tightly bound within the zirconium matrix thus allowing it to be lost in the subsequent processing steps. This is a significant finding as the industrially relevant process that this research is based upon uses formation in the acidic region.

4. Conclusions

Two Y-PSZ powders were produced using the same initial chemical mix and the same processing with the exception of pH of precipitation, and both were processed through to ceramics. The two pH values used were 3 and 12 and throughout the processing the two samples behaved remarkably similarly. The precipitated particle sizes, filtration rate and SSA for the pH 3 sample was found to be 2.7(1) μm, 5 min and 197(5) m^2 g^{-1} while the pH 12 sample had 1.8(2) μm, 7 min and 215(3) m^2 g^{-1}, both samples calcining at approximately 400 °C. In situ XRD used to determine the phase evolution with temperature from 350 °C through to 1000 °C and returning to room temperature which showed that the pH 3 sample obtained approximately 75% tetragonal phase while the pH 12 sample obtained 90% tetragonal phase. The total milling time for both samples was 22 h although slight differences were noted in the milling curves. The spray-dried mill slip produced a free flowing powder for both samples that when investigated using SEM and powder compaction methods showed a well formed and regular powder.

The mechanical properties of the final sintered ceramics showed differences in the results for density, hardness, toughness and MOR measurements. The pH 3 sample was harder but had lower toughness and MOR than the pH 12 sample. Differences in the XRD patterns of the final sintered ceramic were noted with the pH 3 sample having higher levels of the monoclinic phase. The similarity of the pH 3 sample to that in literature for a 2.6 mol% Y-PSZ suggested that the yttrium level was lower than expected from the starting solution concentrations. TEM-EDS investigation revealed that the pH 3 precipitated sample had 3.3(8) wt% and pH 12 = 5.5(4) wt% (≈2 and 3 mol% respectively). This difference in yttria content explains the differences in the mechanical properties with the density of the pH 3 sample matching well to the theoretical density of a powder made from 1.7 to 2.2 mol% Y-PSZ.

Subsequent testing using ICP-OES indicated that when the processing is conducted at pH 3, high levels (797 ppm) of yttrium are found in the liquor after filtering with lower levels (149 ppm) found in the wash solution after filtering. In contrast only 7 ppm was found

Fig. 8. XRD of the sintered ceramics.

88

G.A. Carter et al. / Journal of Alloys and Compounds xxx (2009) xxx–xxx

in both the liquor and wash for the pH 12 precipitated sample. Precipitation at such low pH for Y-PSZ powders is not feasible as the loss of yttrium in the filtering and washing of precipitate adversely affects the final properties of the ceramic.

Comparisons made to products currently available in the market for use in SOFC manufacture indicate that the process used to produce the pH 12 sample would be suitable for the manufacture of SOFC.

Acknowledgements

Appendix A. Supplementary data

Supplementary data associated with this article can be found, in the online version, at doi:10.1016/j.jallcom.2009.02.005.

References

[1] G.A. Carter, M.I. Ogden, C.E. Buckley, C. Maitland, M. Paskevicius, Powder Technol. 188 (2009) 222.
[2] G. Carter, M. Rowles, R. Hart, M. Ogden, C. Buckley, Powder Technol. 191 (2009) 218.
[3] G. Carter, M. Rowles, R. Hart, M. Ogden, C. Buckley, Mater. Forum 32-2008 (2008) 82.
[4] R.H.J. Hannink, P.M. Kelly, B.C. Muddle, J. Am. Ceram. Soc. 83 (2000) 461.
[5] D.J. Green, R.H.J. Hannink, M.V. Swain, Transformation Toughening of Ceramics, CRC Press, Inc., Florida, 1989.
[6] S.P.S. Badwal, K. Foger, Mater. Forum 21 (1997) 187.
[7] F.T. Ciacchi, K.M. Crane, S.P.S. Badwal, Solid State Ionics 73 (1994) 1994.
[8] O. Bellon, R. Ratnaraj, D. Rodrigo, 10YSZ based electrolyte materials for electrolyte supported SOFCs, in: Presented at 5th European SOFC Forum, Proceedings, 2002.
[9] K. Ahmed, J. Love, R. Ratnaraj, High performance cell development at CFCL, in: Presented at Electrochemical Society Proceedings, 2001.
[10] G.A. Carter, R.D. Hart, N.M. Kirby, D. Milosevic, A.N. TiTkov, J. Aust. Ceram. Soc. 39 (2003) 149.
[11] A.J. McEvoy, J. Mater. Sci. 36 (2001) 1087.
[12] S.P.S. Badwal, F.T. Caicchi, Ionics 6 (2000) 1.
[13] R. Ingel, D. Lewis, J. Am. Ceram. Soc. 69 (1986) 325.
[14] S.P.S. Badwal, F.T. Ciacchi, K.M. Giampietro, Solid State Ionics 176 (2005) 169.
[15] O.C. Standard, C.C. Sorrell, Key Eng. Mater. 153–154 (1998) 251.
[16] R.L.K. Matsumoto, J. Am. Ceram. Soc. 69 (1986) C246.
[17] A.G. Mawson, G.A. Carter, R.D. Hart, N.M. Kirby, A.C. Nachmann, Mater. Forum 30 (2006) 148.
[18] S.K. Tadokoro, E.N.S. Muccillo, J. Alloys Compd. 344 (2002) 186.
[19] S.P.S. Badwal, F.T. Ciacchi, V. Zelizko, Ionics 4 (1998) 25.
[20] G.H. Hsieh, W.H. Tuan, J. Mater. Sci. Lett. 21 (2002) 391.
[21] N. Gupta, P. Mallik, B. Basu, J. Alloys Compd. 379 (2004) 228.
[22] N. Gupta, P. Mallik, M.H. Lewis, B. Basu, Euro. Ceram. Viii, Pts 1-3 vol. 264–268 (2004) 817.
[23] J. Kondoh, H. Shiota, K. Kawachi, T. Nakatani, J. Alloys Compd. 365 (2004) 253.
[24] G.R. Anstis, P. Chantikul, B.R. Lawn, D.B. Marshall, J. Am. Ceram. Soc. 64 (1981) 533.
[25] J.J. Kruzic, R.O. Ritchie, J. Am. Ceram. Soc. 86 (2003) 1433.
[26] D.R. Askeland, P.P. Phule, Essentials of Materials Science and Engineering, Thomson, Toronto, Ontario, Canada, 2004.
[27] J. Kondoh, J. Alloys Compd. 375 (2004) 270.

89

7. Conclusions and Further Work

7.1.   Conclusions

This work investigated some of the fundamental processing of Zirconium into zirconia for value-added markets, the peak of this market being the SOFC market. This work was based on the proprietary process as used by Doral Specialty Chemicals and the aim throughout has been to optimise this process; this precondition led to the experimental design being laid out in a relatively linear fashion. The focus has thus been to develop a greater understanding of the science underlying the Doral process and the hope is that this translates into success in the market place. It has been mentioned previously that the process can be divided into stages and that is how this research has been conducted. Figure 14 is a schematic of the research process used for the monoclinic type zirconia with the main tools used in the investigation of each stage.
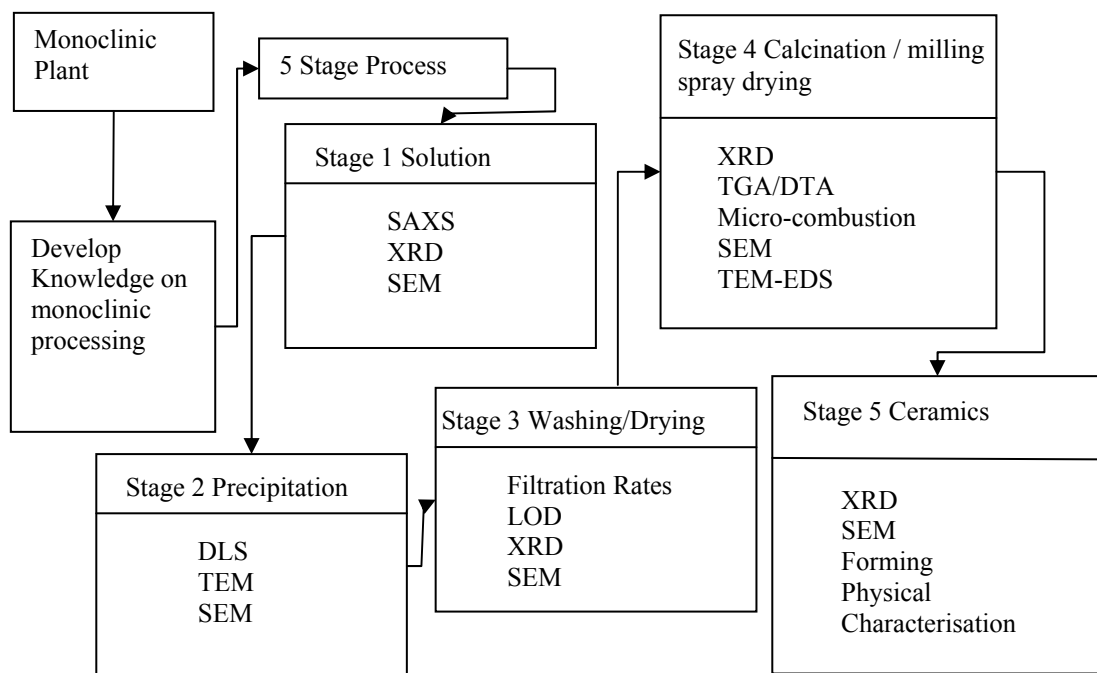

Figure 14. Schematic of Monoclinic Zirconia Research Process.

The aim after developing the understanding of the monoclinic process was then to transfer that knowledge to the production of the yttrium stabilised zirconia. As stated in the introduction the key points of interest in undertaking this research were;

i) Study of the solution phase structure of the zirconyl chloride system under industrially relevant conditions.

ii) Study of the precipitation process, characterising the products formed as a function of the precipitation conditions.

iii) Investigate links between the solution phase structure and the precipitated products through to sintered ceramics.

Each published paper clearly addresses one or more of these three key research objectives.

7.1.1.   Overview Conclusion

Industrial manufacturing typically involves finding compromises in the optimum parameters for individual parts of the process to achieve the best product. Thus taking any one part of the process in isolation may lead to developing inelegant solutions. This work demonstrates this. For example, if one looks at the filtration rates vs. pH of precipitation to achieve the best through-put for the process then one would be precipitating at low pH. As was shown in this work, however, such precipitation conditions produce inherently inferior ceramics. The lesson therefore from this project is to develop fundamental understanding for industry, the work must not only develop the basic knowledge but should further integrate that basic knowledge with the whole framework.

It is evident from this work that by targeting a particular concentration of starting solutions, and having a pH of precipitation that develops a particular speciation of zirconium hydroxide, the ceramic properties of any subsequently manufactured pieces can be influenced. Thus consideration must be given to the process to optimise such inputs. Applying what has been learnt in this work would suggest that optimum conditions may be pH 12 precipitation with high agitation and solution

concentration that is between the two used in this work. This system may also offer the most controllable calcination process and it appears the better ceramic properties.

The following sections hold the conclusions drawn in each paper contained in this work and highlight assertions such as those made in the previous paragraph.

7.1.2.   *Solution Chemistry/Precipitation of Zirconyl Chloride*

Samples of industrially available crystalline zirconium oxychloride octahydrate were investigated. ICP-OES found that the major trace elements were only present at the limit of detection. SAXS investigation of solutions at two concentrations of zirconyl chloride (0.81 and 1.62 M) suggested that the zirconyl speciation was unchanged. Addition of yttrium chloride also had little effect on the SAXS measurement particle radii.

Precipitation was performed using aqueous ammonia as the base. The precipitate particle sizes were measured by DLS with the 1.62 M solution found to have a significantly larger particle size than the 0.81 M solution (4.2 μm , 1.0 μm). The particle sizes were confirmed by electron microscopy, and were found to be in reasonable agreement. The effect on particle size of adding yttrium chloride was also investigated. Samples of 3, 5, 8 and 10 mole% yttrium-zirconium were found to have increasing particle size with increasing yttrium concentration (2.0, 3.7, 4.5, and 4.9 μm respectively). Experiments were carried out to determine if the change in particle size was predominantly a result of the added cations, or anions. Precipitations were performed with added cesium chloride and calcium chloride, such that the chloride concentration matched that of the 8 mole% yttrium-zirconium solution in each case. The precipitate particles sizes increased with the cation charge (ZrCs13, 1.8 μm; ZrCa4 2.6 μm; ZrY8, 4.5 μm), all being larger than the system with no additives (1.0 μm), despite the fact that the chloride concentration is constant. Thus, it appears from these data that the particle size increase is dependent on the charge of the added cation, and less so on the chloride concentration.

From this work it is evident that the growth rate of precipitated particles for zirconyl chloride solutions is dependent on the concentration of the starting solution as well as

the concentration of added cation and the type of cation present. Controlling these factors may enable optimisation of the precipitate particle size. The impact of added cations on properties such as particle surface charge, and on downstream processing of the zirconia is under investigation.

7.1.3. *Precipitation Effects of Processing Parameters*

Concentration of starting solutions, agitation levels and the pH that the precipitation is conducted at all affect the particle size distribution for the hydrous zirconium that is produced. The largest change is due to pH with the smallest change occurring when comparing a pH 12 sample with low agitation and a starting concentration of 1.62 M (PS of 743 nm) with a pH 3 sample with the other processing parameters remaining the same (3390 nm); this is an increase by 4.5 times. The largest change occurred when comparing a pH 12 precipitation with high agitation and 1.62 M solution concentration (PS 73 nm) with the same processing parameters except for the precipitation being carried out at pH 3 (2160 nm) which is an increase of greater than 29 times. The effect of the pH of precipitation is most remarkable in that it overshadows all of the other processing parameters with the PS being smaller by 1 to 2 orders of magnitude for those samples precipitated at a pH 12 in comparison to those produced at pH 3. From an industrial processing perspective, the small PS of the precipitate at pH 12 (743 to 49 nm dependent on processing parameters) leads to significant difficulty in filtering which is an important issue.

An order of magnitude change in PS is not limited to pH changes however as within those precipitations tests carried out at pH 12 changes in the level of agitation also produced order of magnitude differences. The higher agitation in all cases produced smaller PS. As expected lower solutions concentrations were found to produce smaller PS.

The differences seen in the filtering and subsequent differences in morphology of the dried powders, was investigated initially using XRD which showed that those powders produced at pH 3 had retained greater amounts of ammonium chloride. To further investigate the composition of the precipitates TGA/DTA and TGA-MS along with micro-combustion analysis were used with the results suggesting that the

pH of precipitation causes differences in the structure of the hydrated zirconium. The pH 3 powders are thought to have a structure most closely resembling $Zr[OH]_4$ whilst those produced at pH 12 are consistent with a formulation of $ZrO[OH]_2$.

TEM with EDS was used to investigate the zirconium to oxygen content of powders produced at both pH values as well as a zirconia sample. It was found that the pH 3 sample had almost 43 wt% O while the pH 12 sample had approximately 32 wt% O. The difficulty in using TEM EDS for light elements precludes detailed analysis but the results returned are in accordance with the different degrees of hydration suggested by the TGA/DTA, and micro-combustion work. The effect that the differing degrees of hydration has on the ceramic process further down stream in the manufacturing process is unclear.

It makes some sense, however, in operational situations to use lower pH precipitation as this will have the double benefit of allowing for lower base input with associated cost reduction and the PS that allows for the most economical filtering. The tuning of both solution concentration and agitation may allow for the targeting of specific PS. In all cases, however, the final ceramic properties must be considered. The structural differences and or other differences between the manufacture systems may impact on the final ceramics.

7.1.4.   *Non-Stabilised Zirconia Ceramics*

The two zirconia powders produced at differing pH's namely pH 3 and 12 behave differently through the processing from hydrous zirconium precipitate to sintered ceramic. The two precipitates have almost the same physically bound water content after filtering and vacuum drying as shown by the LOD values while the pH 3 product has more chemically bound water. The SSA of the dried precipitates show a further difference with the pH 3 sample having a lower SSA; the SSA response to calcination temperature has the two powders overlapping at approximately 1000 $^{\circ}$C. The response by the pH 12 product is more linear however, and may allow for simpler fine tuning of temperature to achieve a target SSA.

X-ray diffraction revealed that the two powders once calcined were essentially the same from a crystallographic stand point, with a crystallite size in the order of 35 nm and 90% of the phase being monoclinic zirconia.

The two calcined powders were attrition milled to a target D90 below 2 μm with the pH 3 powder taking 29 hours and the pH 12 sample 26 hours. The pH 12 sample had the D90 drop below 5 μm after approximately 9 hours as opposed to 16 hours for the pH 3. The milling curves for the pH 12 show a more orderly size reduction as the milling progresses which again may allow target PSD to be reached in a more uniform fashion in reduced time offering cost reduction and reduced complexity in a plant setting.

The two powders when uniaxially pressed and sintered produced in the order of 88% theoretical dense samples, that underwent approximately 20% linear shrinkage. Whilst both powders produced similar values the variability that the pH 3 sample displayed was more marked than that of the pH 12 sample, suggesting that the processing needs to be refined or that less predictable results can be achieved using such powder. This trend was mirrored in the tape casting of the two powders with the pH 12 sample producing a ceramic that was more in line with what was expected, whilst the pH 3 sample produced a ceramic with striations and different opacity despite the use of the same processing conditions.

7.1.5.   *In-Situ XRD of Non-Stabilised Zirconia*

In situ and *ex situ* XRD along with TEM has been used to study the calcination of zirconia precipitated from zirconyl chloride solutions of different concentrations and pH. The path taken during calcination was found to vary depending on the precipitation conditions. These differences are strongly related to the initial particle size and the structure of the precipitated hydrous zirconia. The sample made at pH 12 and a concentration of 0.81 M has a distinctly different response to temperature than the other three samples, consistent with the small particle size and composition of this sample. The *in situ* XRD experiments provided clear evidence that increases in particle size of tetragonal zirconia with increasing temperature precedes the transformation to the monoclinic phase.

7.1.6. Yttrium Stabilised Zirconia

Two Y-PSZ powders were produced using the same initial chemical mix and the same processing with the exception of pH of precipitation, and both were processed through to ceramics. The two pH values used were 3 and 12 and throughout the processing the two samples behaved remarkably similarly. The precipitated particle sizes, filtration rate and SSA for the pH 3 sample was found to be 2.7(1) μm, 5 minutes and 197(5) m^2/g while the pH 12 sample had 1.8(2) μm, 7 minutes and 215(3) m^2/g, both samples calcining at approximately 400ºC. In situ XRD used to determine the phase evolution with temperature from 350 ºC through to 1000 ºC and returning to room temperature which showed that the pH 3 sample obtained approximately 75% tetragonal phase whilst the pH 12 sample obtained 90% tetragonal phase. The total milling time for both samples was 22 hours although slight differences were noted in the milling curves. The spray dried mill slip produced a free flowing powder for both samples that when investigated using SEM and powder compaction methods showed a well formed and regular powder.

The mechanical properties of the final sintered ceramics showed differences in the results for density, hardness, toughness and MOR measurements. The pH 3 sample was harder but had lower toughness and MOR than the pH 12 sample. Differences in the XRD patterns of the final sintered ceramic were noted with the pH 3 sample having higher levels of the monoclinic phase. The similarity of the pH 3 sample to that in literature for a 2.6 mol% Y-PSZ suggested that the yttrium level was lower than expected from the starting solution concentrations. TEM-EDS investigation revealed that the pH 3 precipitated sample had 3.3(8) wt% and pH 12 = 5.5(4) wt% (≈ 2 and 3 mol% respectively). This difference in yttria content explains the differences in the mechanical properties with the density of the pH 3 sample matching well to the theoretical density of a powder made from between 1.7 to 2.2 mol% Y-PSZ.

Subsequent testing using ICP-OES indicated that when the processing is conducted at pH 3, high levels (797 ppm) of yttrium are found in the liquor after filtering with lower levels (149 ppm) found in the wash solution after filtering. In contrast only 7 ppm was found in both the liquor and wash for the pH 12 precipitated sample.

Precipitation at such low pH for Y-PSZ powders is not feasible as the loss of yttrium in the filtering and washing of precipitate adversely affects the final properties of the ceramic.

Comparisons made to products currently available in the market for use in SOFC manufacture indicate that the process used to produce the pH 12 sample would be suitable for the manufacture of SOFC.

7.2. Further Work

It is possible to break down the further work into sections relating to each individual section.

7.2.7. Solution Chemistry/Precipitation of Zirconyl Chloride

The starting place for further work would be to investigate the speciation changes during hydrolysis of zirconyl chloride with time. Literature indicates that there are changes but these have not been quantified. As the work that was completed here shows that SAXS and subsequent data analysis of the solutions is possible, this would not be experimentally difficult. The only issue is that laboratory-based SAXS instruments do not have the intensity of photons required to achieved small enough time increments, but this of course can be resolved by the use of synchrotron facilities.

The other area of fundamental research would be to determine the mechanism behind the size increase in precipitated particle size with cation charge. This would also involve the determination of the role that the chloride ions play in the solution chemistry of zirconyl chloride which is still poorly understood within the available literature.

7.2.8. Precipitation Effects of Processing Parameters

Whilst this work determined that precipitation of zirconyl chloride under the acidic or basic regimes developed different structures assigned as $ZrO[OH]_2$ or $Zr[OH]_4$ these studies could be extended to determine the structure changes at specific pH values, and also to find the specific bonding arrangements of each structure.

7.2.9. Non-Stabilised Zirconia Ceramics

The mechanisms behind the differences seen in the two ceramics produced from the powders which were manufactured at different pH is unclear. The *in-situ* calcination work indicated differences in crystallite size, however strain data was not available from this work and this may give some indications of the underlying causes of the differences seen. A full investigation into micro-cracking, grain growth, strain and other microstructure effects due to the differences seen in the calcination between the different zirconia products is warranted.

7.2.10. In-Situ XRD of Non-Stabilised Zirconia

Incorporating a mass spectrometer to analyse the evolved gas whilst the calcination process is underway would deliver significant insight regarding the mode of transformation and would allow differences seen to be related back to the degree of hydration of the zirconia species.

7.2.11. YSZ

This work only investigated the 3 mol% YSZ from solutions to ceramics, the obvious extension would be to further investigate the 5, 8 and 10 mol% YSZ which are used in SOFC manufacture.

8. Appendix A:- Supplementary Information for Publications

8.1. Appendix A-1: Supplementary Information for '*Ammonia-Induced Precipitation of Zirconyl Chloride and Zirconyl-Yttrium Chloride Solutions Under Industrially Relevant Conditions*'

Carter G. A., Ogden M. I., Buckley C. E., Maitland C., Paskevicius M., 2009, '*Ammonia-Induced Precipitation of Zirconyl Chloride and Zirconyl-Yttrium Chloride Solutions Under Industrially Relevant Conditions*', Journal of Powder Technology, vol. [188], pp 222-228.

Ammonia-induced precipitation of zirconyl chloride and zirconyl-yttrium chloride solutions under industrially relevant conditions. Part 1.

Geoffrey. A. Carter, Mark I. Ogden and Craig E. Buckley, Clinton Maitland and Mark Paskevicius.
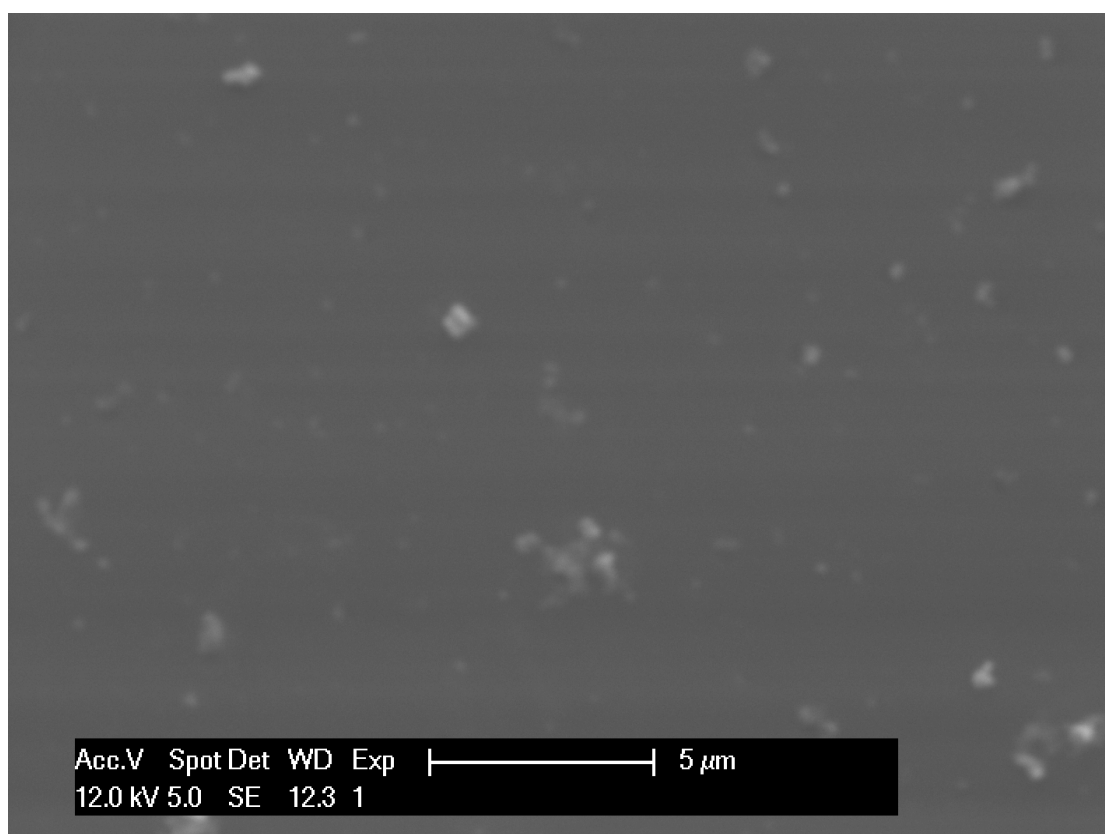
Supporting Information

Fig. S1 SEM micrograph of spun coated 0.81 M precipitates.

Small Angle X-ray Scattering – Data Analysis

The UFM was applied to the data from SAXS for the 0.81 M solutions using Irena. In Irena, the data is fitted using the following model (Beaucage and Schaefer 1994),

$$I(q) = I_U(q)S(q) \qquad (1)$$

where $I_U(q)$ is intensity due to the unified model given by

$$I_U(q) \approx G_1 \exp\left(-q^2 R_{g1}^2/3\right) + B_1 \left\{ \left[erf\left(q k R_{g1}/\sqrt{6}\right) \right]^3 \middle/ q \right\}^{P_1}$$

$$+ \sum_{i=2}^{n} \left(G_i \exp\left(-q^2 R_{gi}^2/3\right) + B_i \exp\left(-q^2 R_{g(i-1)}^2\right) \left\{ \left[erf\left(q k R_{gi}/\sqrt{6}\right) \right]^3 \middle/ q \right\}^{P_i} \right) \tag{2}$$

G_i is the Guinier law prefactor, P_i is the power law, B_i is the power law prefactor, $k = 1.06$ for mass fractals or $k = 1$ for every other case, i is the level and $S(q)$ is the structure factor for spherical particles given by

$$S(q) = \frac{1}{1+k\phi} \tag{3}$$

where $k = 8V_H/V_o$ is the packing factor, V_H is the hard core volume of a domain and V_o is the average volume available to a domain (for face centred Cubic (FCC) packing of spheres $k = 5.92$).

$$\phi = 3\frac{\sin(q\eta) - q\eta\cos(q\eta)}{q^3 \eta^3} \tag{4}$$

where η is the average radial distance between particles. Equations 1, 3 & 4 are for weakly correlated systems and for these equations to be applicable the value of k must be less than four (Beaucage 1995).

For the 1.62 M solutions the structure factor $S_1(K_1)$ for spherical particles used in the HPMSA model (Hayter and Penfold 1981) is given by (5)

$$S_1(K_1) = \frac{1}{1 - 24\xi\, a(K_1)} \tag{5}$$

where ξ is the volume fraction and $a(K_1)$ is a dimensionless quantity described in full detail in the literature (Hayter and Penfold 1981).

Fig. S2 shows the fit to the scattering data achieved using the UFM for the 0.81 M solution (sample Zr1). This is a typical fit to the data for all the 0.81 M solutions measured and represents close agreement between the experimental intensities and that of the model. From Table S2, $k < 4$ for samples Zr1, Zr23 & Zr3, and hence the application of equation (1) is appropriate for these samples. Fig. S3 displays the scattering data for the same starting raw material, with the solution concentration at 1.62 M (sample Zr6). The model doesn't fit as neatly as for the 0.81 M solutions, particularly at low q. From Table S2, $k < 4$ for samples Zr5 & Zr6, but only just ($k = 3.8$ and 3.7 respectively) and since $k > 4$ for sample Zr4 the criteria to

use equation 1 is not satisfied, therefore the HPMSA model was used for the 1.62 M solutions (Fig. S4). The HPMSA model offers a more refined method than the UFM in the case of the 1.62 M solutions as it takes into account the particle to particle interactions using a screened coulomb approach. When the 0.81 M solutions were modelled using the HPMSA the method failed to converge, which makes sense since in general the mean spherical approximation fails at low density (Hayter and Penfold 1981; Hansen and Hayter 1982). This result coupled with the success of the UFM for the 0.81 M solutions and the success of the HPMSA for the 1.62 M solutions validates the analysis method.
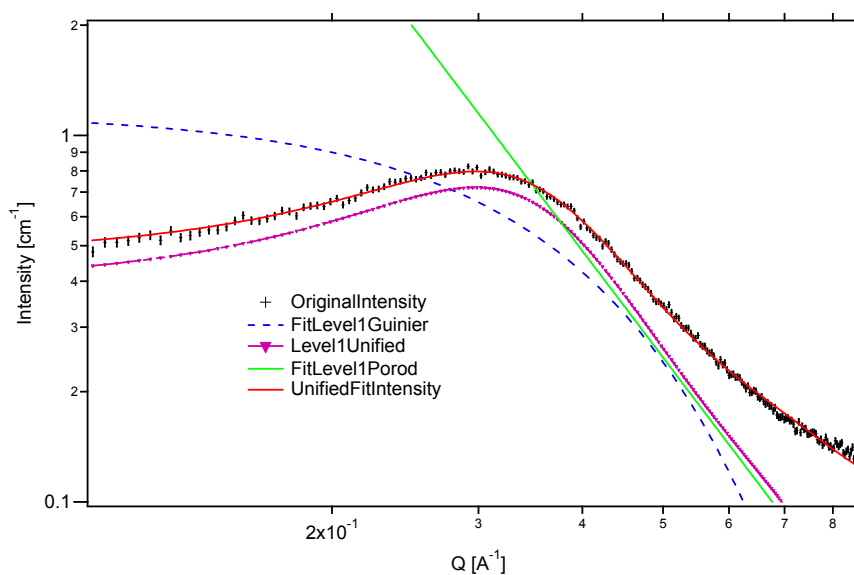
Fig. S2 Data and fitted model for sample Zr1 concentration of 0.81 M. The plot shows the contribution from the Guinier and the power law parts of the UFM equation.

Fig. S5 displays the fit to a similar scattering pattern, for a 0.81 M solution with 8 mol % yttrium-zirconium mixture. Samples ZrY3, ZrY5, ZrY8 & ZrY10 all have values of $k < 4$, therefore η (Table S2) will be a more accurate representation of the average radial particle to particle distance than d_p. The result for all of the 0.81 M solutions, are essentially identical irrespective of yttrium levels.
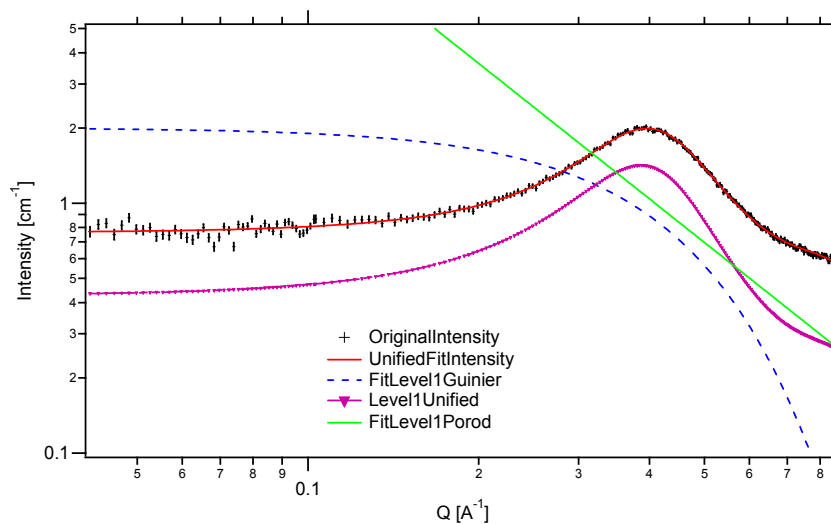
102

Fig. S3 Data and fitted model using the UFM for sample Zr67, concentration 1.62 M. The plot shows the contribution from the Guinier and the power law parts of the UFM equation.
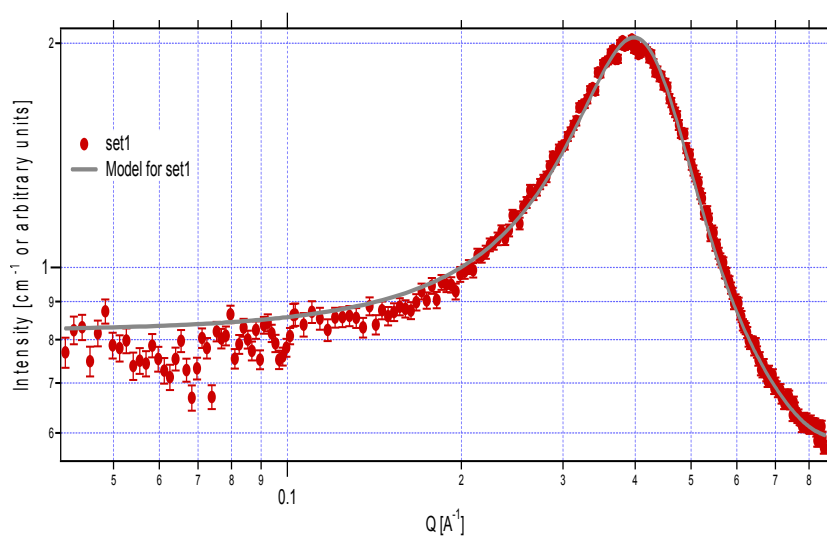

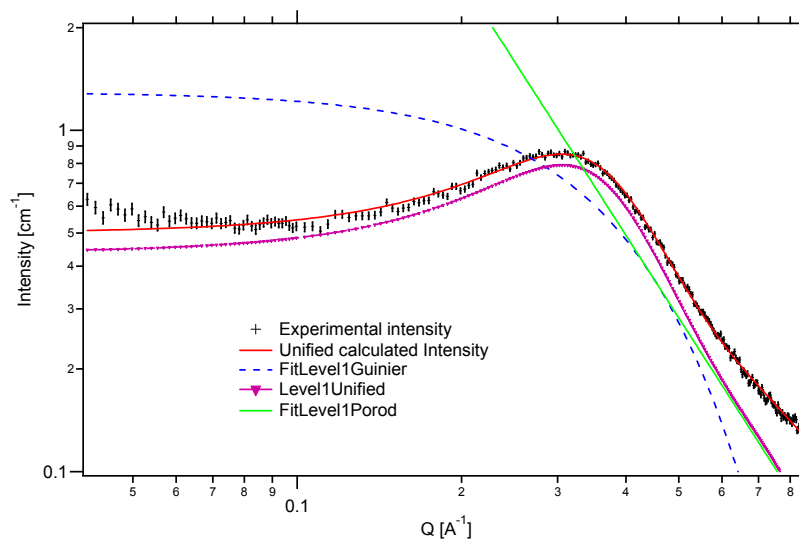**Fig. S4** Data and Fitted model using the HPMSA for sample Zr6, concentration 1.62 M.

Fig. S5 Data and model (UFM) for sample ZrYy8 concentration 0.81 M with 8 mole % yttrium added. The plot shows the contribution from the Guinier and the power law parts of the UFM equation.

Table S2. Results of SAXS and precipitate particle size analyses, including pH, concentration, radius of gyration *Rg* (Å), particle radius *R* (Å), packing factor *k* and particle to particle interaction distance *dp* (Å) and η (Å), and precipitate particle size mean diameter *p* (μm).

Sample	Conc. (M)	Added Cations	pH	R_g ±0.3 Å	η ±1.0 Å	k	R ±0.4 Å	d_p (Å)	p (μm)
Zr1	0.81		0.74	4.4	16.1	1.64	5.7	21	1.0(1)
Zr2	0.81		0.74	4.3	15.9	1.80	5.6	21	
Zr3	0.81		0.73	4.4	16.0	1.62	5.7	21	1.1(1)
Zr4	1.62		0.45	3.9	14.9	5.24	5.1	14	
Zr5	1.62		0.46	3.9	15.0	3.80	5.1	15	
Zr6	1.62		0.47	4.1	15.2	3.70	5.3	16	4.2(1)
ZrY3	0.81	YCl$_3$ (3 mol%)	0.77	4.3	16.3	1.60	5.6	22	2.0(1)
ZrY5	0.81	YCl$_3$ (5 mol%)	0.76	4.3	15.7	1.31	5.6	21	3.7(2)
ZrY	0.81	YCl$_3$ (8 mol%)	0.77	4.3	15.6	1.70	5.6	22	4.5(1)
ZrY10	0.81	YCl$_3$ (10 mol%)	0.72	4.3	15.2	1.74	5.6	20	4.9(2)
ZrCa4	0.81	CaCl$_2$ (4.2 mol%)							2.6(1)
ZrCs13	0.81	CsCl (12.7 mol%)							1.8(1)

Anstis, G. R., P. Chantikul, et al. (1981). "A Critical Evaluation of Indentation Techniques for Measuring Fracture toughness: I, Direct Crack Measurements." Journal of the American Ceramic Society **64**(9): 533-538.

ASTM (1990). ASTM E 384-89 1990, 'Standard Test Method for Microhardness of Materials', , ASTM Standards.

ASTM C 112-96 1999 (1999). ASTM C 112-96 1999, 'Standard Test Method for Determining Average Grain Size', .

ASTM C 1161-94 1996 (1996). <u>ASTM C 1161-94 1996, 'Stanard test method for flexural strength of advanced ceramics at ambient temperature'</u>, ASTM Standards.

Beaucage, G. (1995). "Approximations leading to a unified exponential power-law approach to small-angle scattering." <u>Journal of Applied Crystallography</u> **28**: 717-728.

Beaucage, G. and D. W. Schaefer (1994). "Structural Studies of Complex-Systems using Small-Angle Scattering - A Unified Guinier Power-Law Approach." <u>Journal of Non-Crystalline Solids</u> **172**: 797-805.

Callister, J., W.D. (1997). <u>Materials Science and Engineering: An Introduction 4th edn</u>. New York., John Wiley & Sons, Inc.

Hansen, J. P. and J. B. Hayter (1982). "A Rescaled MSA Structure Factor for Dilute Charged Colloidal Dispersions." <u>Molecular Physics</u> **46**(3): 651-656.

Hayter, J. B. and J. Penfold (1981). "An Analytic Structure Factor for Macroion Solutions." <u>Molecular Physics</u> **42**(1): 109-118.

Mahdjoub, H., P. Roy, et al. (2003). "The effect of slurry formation upon the morphology of spray-dried yttria stabilised zirconia particals." <u>Journal of the European Ceramic Society</u> **23**: 1637-1648.

8.2. Appendix A-2: Supplementary Information for *'Industrial Precipitation of Yttria Partially Stabilised Zirconia'*

Industrial precipitation of yttrium chloride and zirconyl chloride: Effect of pH on ceramic properties for yttria partially stabilised zirconia

G. A. Carter,[a+b*] R. D. Hart[b], M. Rowles[c] M. I. Ogden[a] and C. E. Buckley[b]

[a] Nanochemistry Research Institute, Curtin University of Technology, PO Box U1987, Perth, Western Australia, 6845, Australia

[b] Centre for Materials Research, Curtin University of Technology, PO Box U1987, Perth, Western Australia, 6845, Australia

[c] Commonwealth Scientific, Industrial Research Organisation (CSIRO), Minerals Division, Clayton Vic

Sintered samples where investigated using a Siemens D500 Bragg-Brentano X-ray diffractometer with Cu K_α with α_1 and α_2 weighted average radiation ($\lambda = 1.54178$ Å). The instrument was operated with an accelerating voltage of 40 kV and a filament current of 30 mA. The goniometer settings were 20 - 120° 2θ with a step size of 0.02° 2θ, the slit size (1/2/3) used were 1°/1°/1°. Pattern investigation and Rietveld analysis was conducted using the software package Rietica 1.7.7 (1997). Powder diffraction of the hydrous cake through calcination up to 1000ºC were obtained using an X-ray diffractometer incorporating a platinum resistance-strip heater, with an Inel CPS-120 curved, position-sensitive detector. The angular range

Corresponding Author current affiliation Nanochemistry Research Institute, Curtin University of Technology, PO Box U1987, Perth, Western Australia, 6845, Australia Tel:- +61 8 9266, Fax:- +61 8 9266 4699 Email:-

of the detector is 120 deg 2θ, facilitating rapid, simultaneous data accumulation. Data were collected in the reflection mode using Co K radiation operated at 35 kV and 30 mA. Datasets of 60 s in duration were collected in 10ºC increments as the temperature was increased from room temperature to 1000ºC and every 20ºC whilst cooling. The Pt strip of the heater contained a small sample well measuring 20.0 x 7.0 x 0.4 mm. Each sample was hand ground in a mortar and pestle with ethanol and was applied directly onto the Pt strip heater as a thick slurry.

The samples were milled in a 01HD Union Process (Akron Ohio) Szegvari Attritor system. The attritor had a 500 ml volume with 0.8 mm diameter partially stabilised zirconia (PSZ) milling media, agitation was achieved using a PSZ attritor arm. Mill slip was made from 1 kg of calcined powder and milli-q water, the solids content was 45%. A flow through system was used with the mill slip being gravity fed to the top of the attritor from an external tank. The slip then passed through the milling chamber and a pump, with an inlet at the bottom of the attritor, delivering the mill slip back to the top of the external tank closing the loop. Pump speed and gravity feed rate were matched so a constant level was kept in the attritor. Sampling and testing were conducted on a slip collected from the gravity feed discharge. The samples were milled until two consecutive PSD tests taken hourly returned a D90 of approximately 2 μm. The use of statistical measures in particle sizing is common within the chemical powder industry; the three most common measures that are used are the D90 being the 90th percentile, D50 and D10, which are both the 50th and 10th percentile respectively.
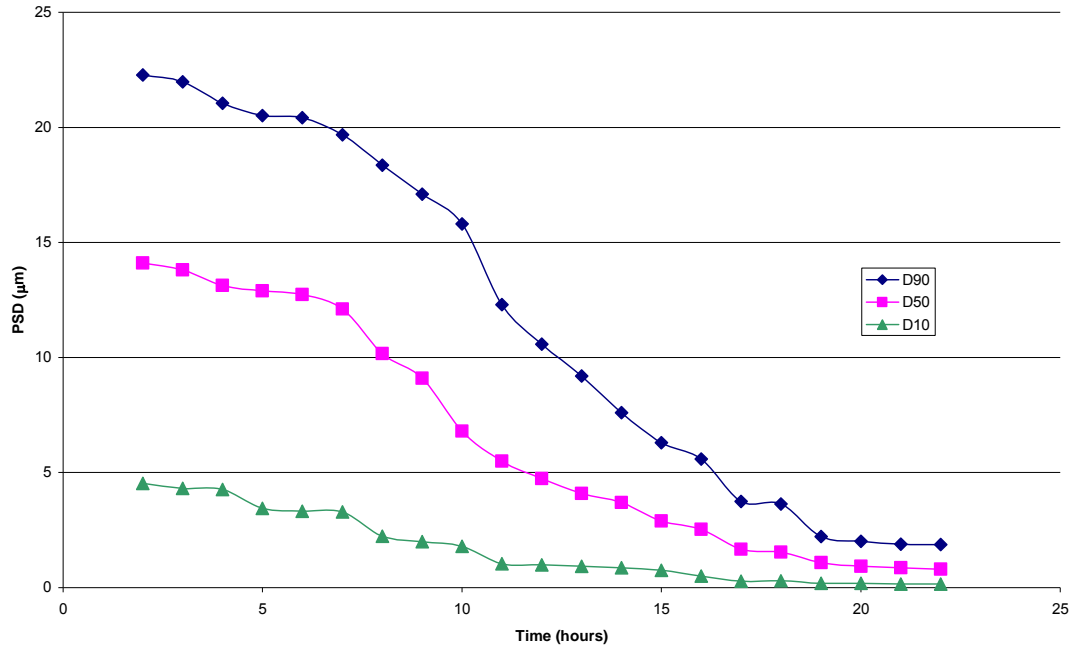
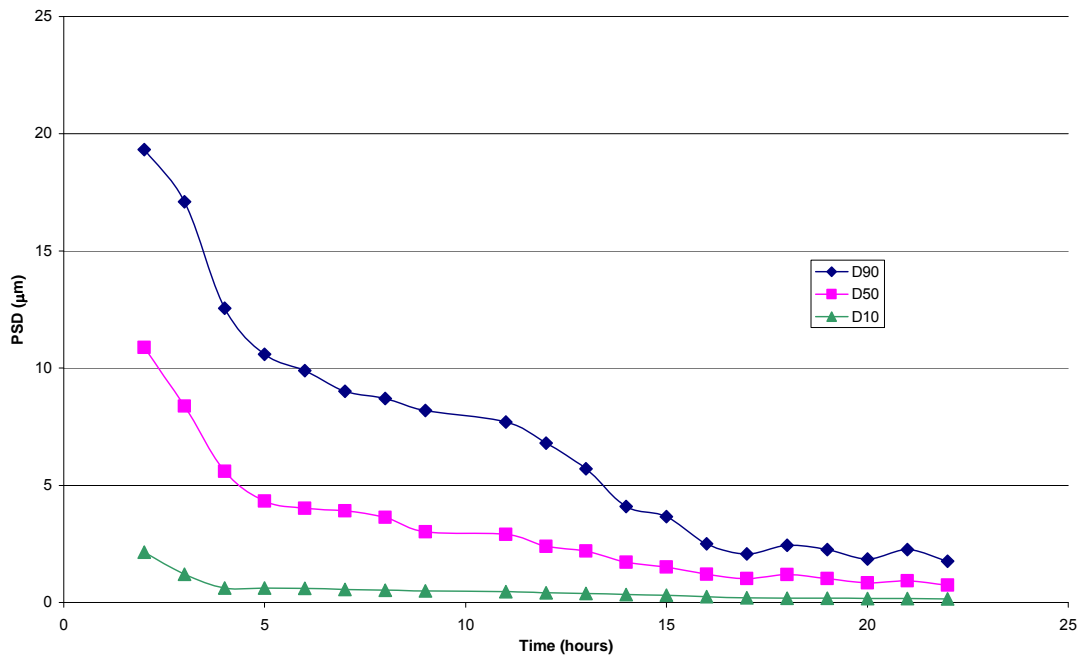**Figure S 1 pH 3 milling Curve**

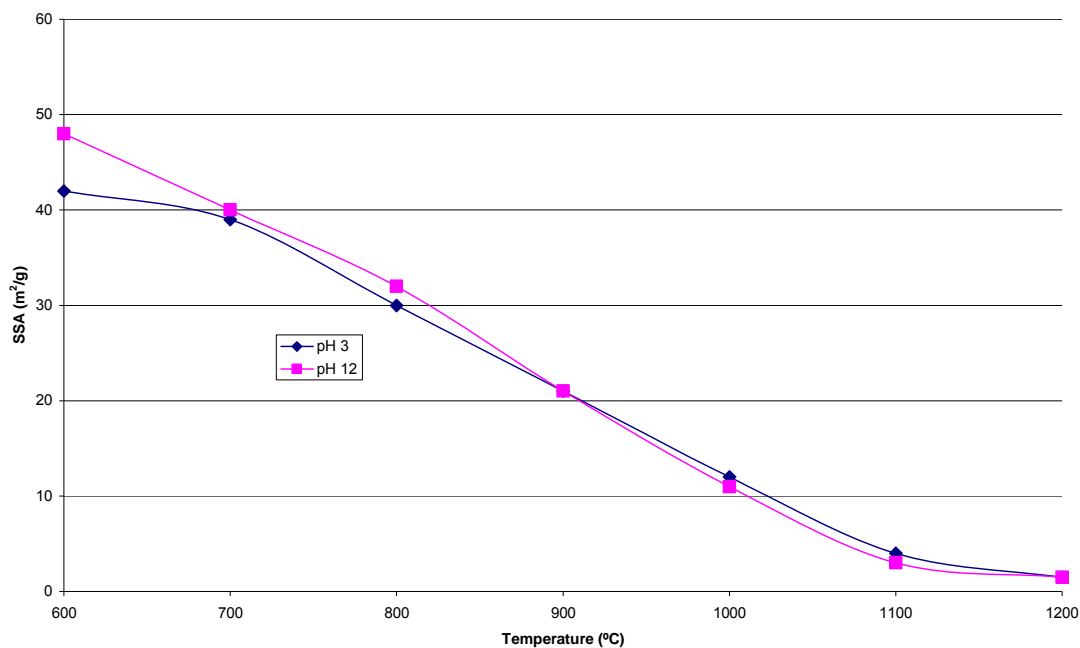

Figure S 2 pH 12 milling curve

Figure S 3   SSA Variation with Calcination Temperature for pH 3 and pH 12 samples

Slurry suitable for spray drying was formed using the constituents listed in Table S 1. The products were mixed together using a TABULAR shaker mixer for 40 minutes then rolled for 24 hours in a plastic drum with alumina beads to break up any aggregates. The slurry was then spray dried with a Niro Mobile Minor using a two fluid nozzle. Spray drying is a method for drying slurries into homogeneous free flowing powders. It also allows the final spherical agglomerate particle size to be controlled.

Table S 1 Spray drying slurry constituents

Material	wt%
Zirconia powder	45
Distilled water	52
Dispex	1
Glycerol	1
Polyvinyl acetate	1

The feed slurry was mixed to produce a solids content of approximately 47% which was fed into the system at a controlled rate so that an outlet temperature of 105 ºC was retained for an inlet temperature of 350 ºC. The atomising air rate was set to the mid point of the rotameter with an air pressure of 7 Bar (0.7 MPa).

Mahdjoub *et. al.* (Mahdjoub, Roy et al. 2003) discusses the effect of slurry formation upon the morphology of spray-dried zirconia yttria composites and lists conditions that produce misshapen agglomerates that result in powders that are not free flowing and are difficult to compact in subsequent processing. An investigation of the spray-dried powder shape was undertaken using SEM they both were found to be spherical with Figure S 4 being typical.
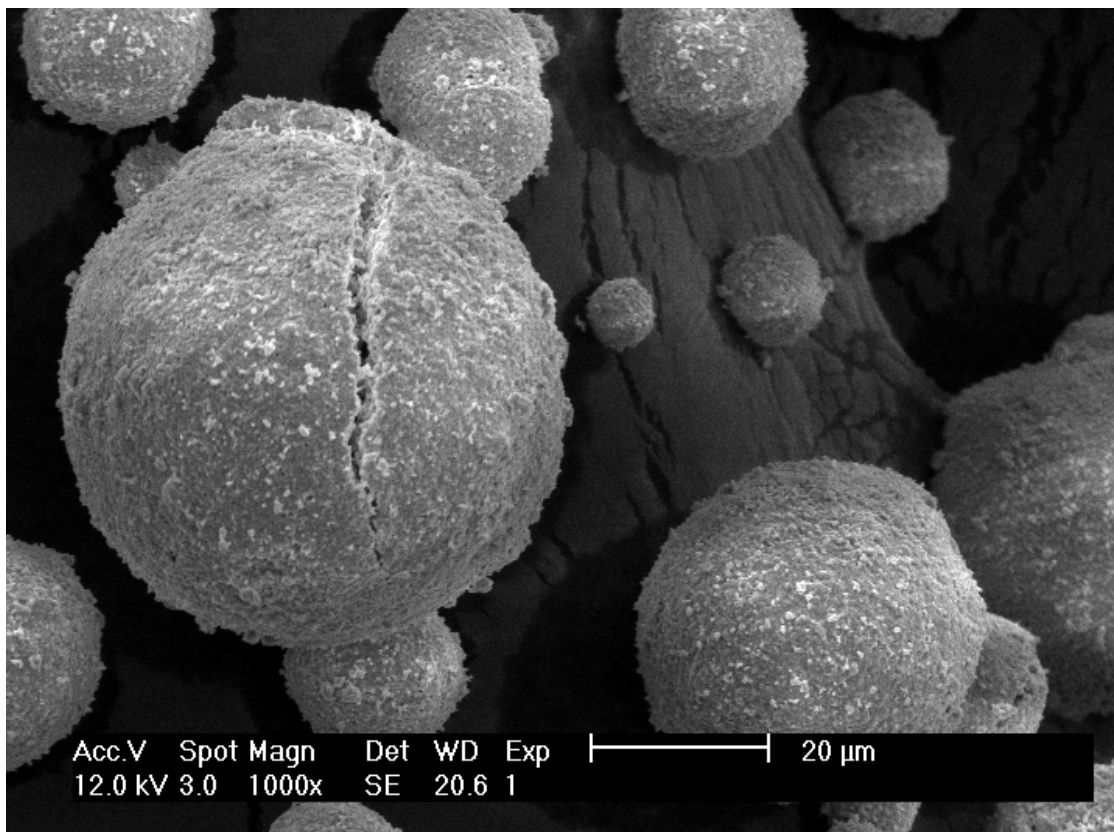

Figure S 4 SEM of spray-dried agglomerate (pH 3)

The following is a brief account of the procedures used in the testing.

All pellets and bars used in this testing were initially formed using a 316 SS die with stearic acid dissolved in methanol as a die lubricant. The die and powder was pressed at 30 MPa with a dwell of approximately 30 seconds. The powder was removed from the die and bagged in standard balloons for cold isostatic pressing at 200 MPa.

All samples tested were fired using the same sintering regime, the firing regime used is a standard regime used for comparative testing and has not been optimised to find the best conditions for firing. The sintering profile is described in Table S 2.

Table S 2 Sintering regime

Temperature	Time Taken	Rate
0ºC to 30ºC	10 mins	3ºC/min
30ºC to 400ºC	6 hrs 10 mins	1ºC/min
Dwell at 400ºC	30 mins	
400ºC to 1550ºC	9 hrs 35 mins	2ºC/min
Dwell at 1550ºC	3 hrs	
1550ºC to 30ºC	8 hrs 27 mins	3ºC/min

The sintering was conducted in a muffle furnace with molybdenum di-silicide ($MoSi_2$) heating elements in a standard air atmosphere.

All physical characterisation was conducted using the following well documented procedures

1) Hardness (Vickers indentation ASTM E 384-89 (1997)) (ASTM 1990)

2) Toughness (K_{1c} Vickers crack propagation method as per Anstis *et al.*)(Anstis, Chantikul et al. 1981)

3) Modulus Of Rupture (MOR ASTM method C1161-94 (1996))(ASTM C 1161-94 1996 1996)

4) Grain sizing (Abrahm's three ring method with ASTM E-112)(ASTM C 112-96 1999 1999)

5) Linear Shrinkage

6) Green and sintered density (ASTM C20 (1992))

Samples used in Hardness, toughness and grain sizing after pressing/firing were polished to 1 μm finish using a Struers Pedimat with diamond polish. The polishing consisted of mounting in epoxy resin and grinding using a 40 μm Pedimat pad until flat. The remaining polishing at 9, 6, 3 and 1 μm was for 30 minutes with a force of 20 N.

MOR test pieces were diamond machined parallel to the specimen axis to an approximately 6 μm, then polished to a 3 μm finish with diamond polish using a Struers Pedimat.

The Vickers microhardness test defined in ASTM E 384-89 (1997) was used to determine the hardness of the ZY3. A Zwick hardness tester type 3212B was used for hardness measurements. Indentations were made with a 1 kg load applied for 20 seconds. The indentation was inspected using the optical and digital system of a Nikon Eclipse ME600 materials microscope. The objective lens used was 50x magnification resulting in an effective magnification of 500x. Five replicates of each composition were tested with each sample being tested a number of times. An Asahi standardised block for hardness (Test certificate number 75308) was used prior to testing the zirconia samples the values returned were within the calibration range (hardness value of 964.3 ± 4%).

Toughness is defined as a measure of the energy that a material is able to absorb before fracture (Callister 1997). By measuring the crack length initiated by a hardness test indentation and using the formula below the value of the fracture toughness can be determined.

$$k_c = 0.16 Hv \sqrt{\frac{d}{2}} \left(\frac{c}{d} \right)^{-\frac{3}{2}}$$

Where Hv is the hardness and d is the mean distance of the indent diagonals and c is the mean distance of the fracture diagonals (Anstis, Chantikul et al. 1981).

Modulus of rupture (MOR), preformed to ASTM Designation C1161-94 (1996) also known as the bend strength, is the maximum stress or stress at fracture was developed using the four point bending test. Samples were 55 mm x 3 mm x 4 mm with a chamfer on one of the corners as per the ASTM. Breaks were made using a Lloyds 6000R test instrument.

The grain sizing was conducted using the Abrams three circle method in line with ASTM E-112. The samples were thermally etched by heating with a ramp rate of 1 ^{o}C/minute to 1500 ^{o}C with a dwell of 30 minutes. Imaging was conducted using a Phillips XL30 tungsten filament SEM. The SEM was operated at 25kV secondary electron imaging at a magnification of either 1000 or 1500x dependent on particle size.

The green density of a pressed pellet was determined by a measurement of its dimensions to ascertain its volume and a measurement of its weight. Dividing the pellets weight by its volume allows the density to be calculated. The radius and height of the pellet was ascertained by the use of vernier callipers or a micrometer. The measurements of the dimensions of the pellet were taken at three different places on the pellet and an average used for the calculation. The pellet was weighed to four decimal places on a balance.

The samples were fired in accordance with the firing regime as specified in the relevant section of this document. The sintered density of the pellet was obtained by Archimedes principle.

The linear shrinkage, a measure of the linear dimensional change during firing, was developed by measuring the green powder dimensions and then measuring dimensions of the fired part.
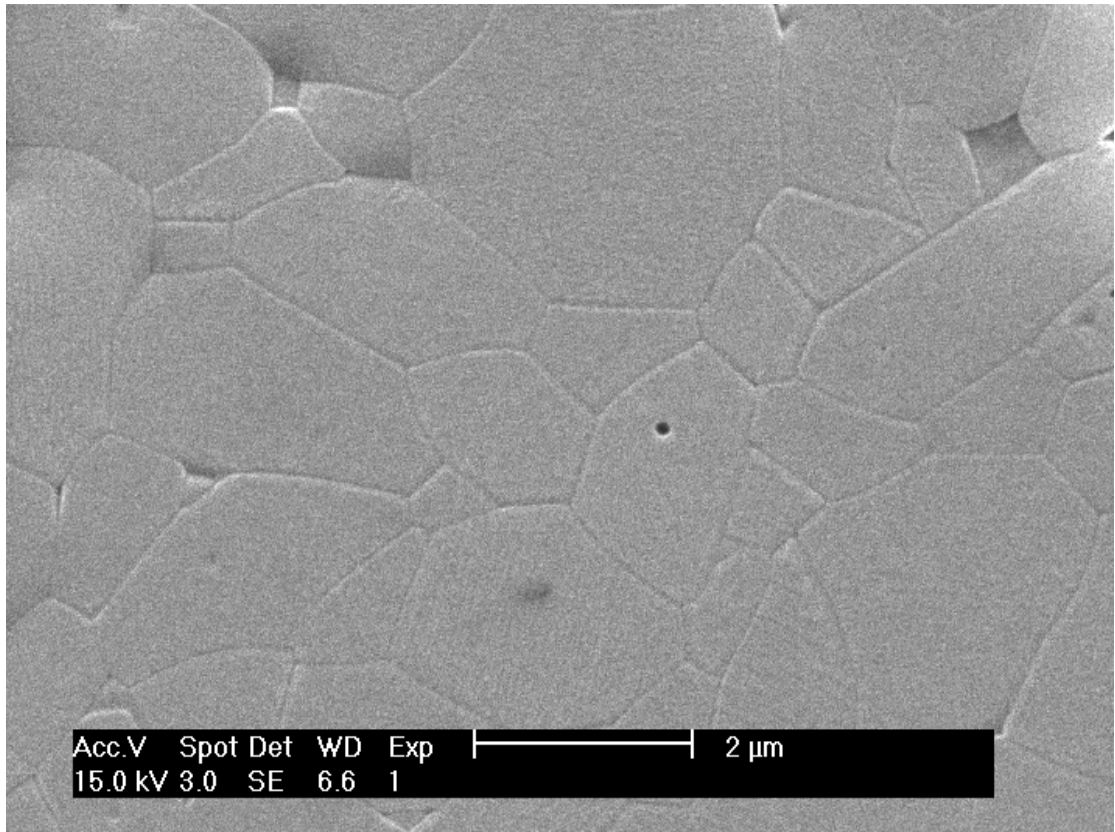
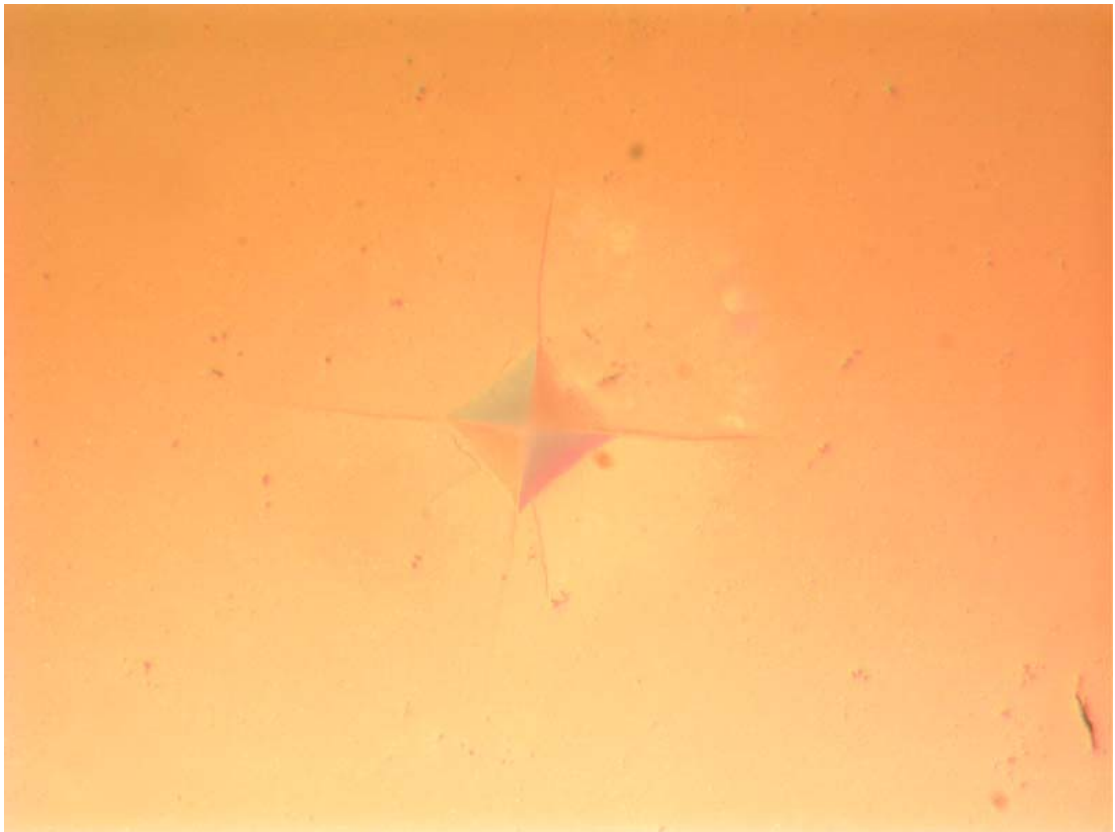**Figure S 5 SEM micrograph used for grain sizing pH 12 Typical.**

Figure S 6 Optical micrograph showing a Vickers indentation.

Figure S 7 Optical Micrograph of 2 MOR bars showing difference in optical properties

[28]   H. Mahdjoub, P. Roy, C. Filiatre, G. Bertrand, C. Coddet, *J. Eur. Ceram. Soc.* **2003**, *23*, 1637.

[29]   ASTM, *ASTM E 384-89 1990, 'Standard Test Method for Microhardness of Materials',* , Vol. 1990, ASTM Standards, **1990**.

[30]   ASTM C 1161-94 1996, *ASTM C 1161-94 1996, 'Stanard test method for flexural strength of advanced ceramics at ambient temperature'*, Vol. 03.01, ASTM Standards, **1996**.

[31]   ASTM C 112-96 1999, *ASTM C 112-96 1999, 'Standard Test Method for Determining Average Grain Size',* , Vol. 03.01, **1999**.

[32]   J. Callister, W.D. , *Materials Science and Engineering: An Introduction 4th edn*, John Wiley & Sons, Inc., New York. **1997**.

# 9. Appendix B:- Experimental Information – Small Angle Scattering

Most materials scientists if not all know the Brag equation $\lambda = 2d\sin\theta$ for diffraction and its derivation. What is less understood is that for the majority of the observed lattice spacing's are of the same order of magnitude as the X-ray wave lengths that are in the most cases used, this thus leads to the angle θ being relatively large (Guinier, Fournet 1955). With the need to study macromolcules the study of small angle X-ray diffraction was introduced to allow the detection of large lattice spacing's (Guinier, Fournet 1955).

The obvious place to start such a discussion on theory would be to describe the interaction of the neutrons and x-rays with the sample, this will be a simplistic version of that that will move into some of the basic mathematical discussions.

For neutrons the interaction is with the nucleus of the particle in question, this is termed nuclear interaction, neutrons can also interact with the electronic structure by way of the dipole, as such is known as magnetic interaction. Neutrons are particles (as defined in the physical sciences when dealing with quantum type objects). There energy is kinetic and can be determined by the standard equation of $E = \frac{1}{2}mv^2$ this is well known equation and the elements are E being the energy, m and v being the mass and velocity respectively.

Electromagnetic interaction is the term used to describe the interaction that x-rays undergo. This is due to the interaction with the x-rays be contributed to by the electron cloud. As is well known x-rays energy of an x-ray can be defined by $\lambda = \frac{h}{mv}$ where λ is the wave length, h is Plank's constant with the momentum being mv which have been defined previously.

It is possible to define the following parameters to explain a scattering event; if we have a wave vector k in the direction of v that can be determined as $|k| = \frac{2\pi}{\lambda}$ which can then be related as below:
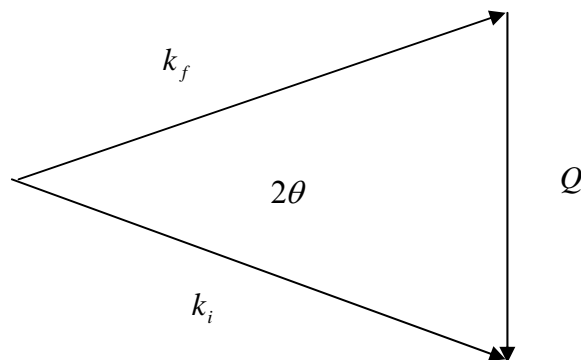

X-rays or neutrons

k_f

k_i

λ

Scattering angle

2θ

k_i

Sample
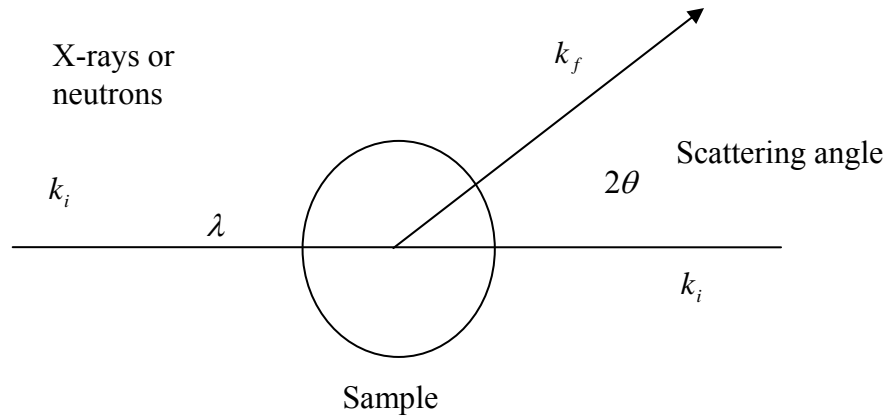
thus the term 2θ is the scattering angle.

The scattering vector Q can be related to this by $Q = k_i - k_f$ which can be understood diagrammatically by;

k_f

Q

2θ

k_i
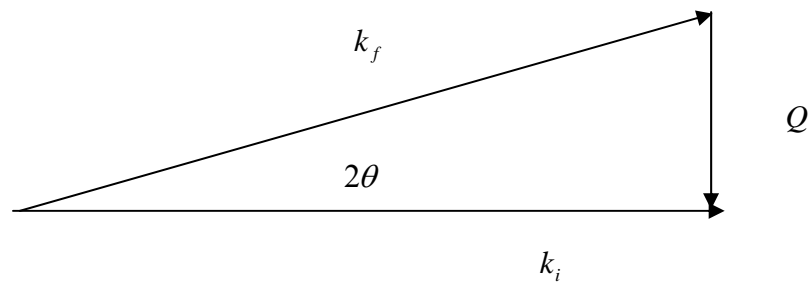
If we take the case of inelastic scattering we have a slightly different case as shown;

k_f

2θ

Q

k_i

Now if we introduce Bragg's law ($\lambda = 2d\sin\theta$) where d is conventionally thought of as the lattice plane spacing we can rearrange to make $d = \dfrac{\lambda}{2\sin\theta}$ and then substitute in for k we can end up with $d = \dfrac{2\pi}{\left(\dfrac{4\pi}{\lambda}\right)\sin\theta} = \dfrac{2\pi}{Q}$ which is thus moved to allow a relation ship between the scattering vector Q and d where as d increases Q decreases.

The scattering cross section is a measure of the ability of an object to remove photons from a direct beam and send them into new directions. This can be understood with the following diagram;
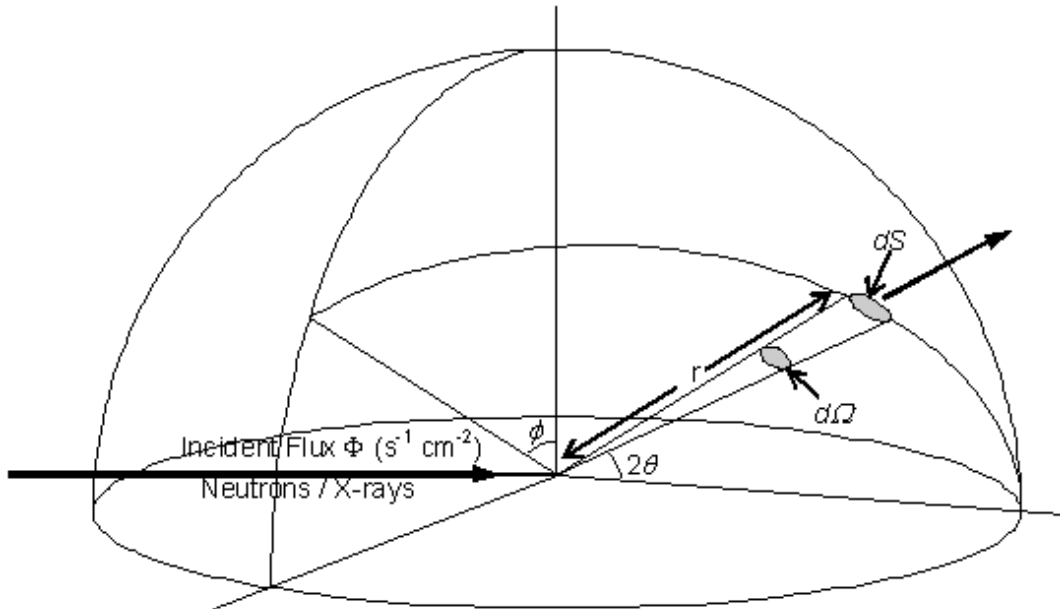

Figure 15. Scattering cross section line diagram.

The incident flux Φ has the units of (s^{-1} cm^{-1}) with dS being the scattered area and r the radius. These can be used to define the differential cross section;

$$\frac{d\sigma}{d\Omega} = \frac{\left(\text{No.Scattered}/\sec\cdot\text{in}\cdot\text{to}\cdot\left(d\Omega = dS/r^2\right)\right)}{\Phi d\Omega} \tag{B-1}$$

This can then become the total cross section (σ);

120

$$\sigma = \int \frac{d\sigma}{d\Omega} d\Omega$$

It is possible to define $\frac{d\sigma}{d\Omega}$ for a single electron using classical physics as

$$\frac{d\sigma}{d\Omega} = \left(\frac{r_e^2}{mc^2} \right) \left[\frac{1 + \cos^2(2\theta)}{2} \right]$$

The scattering length density can be calculated for a molecule from

$$\rho_s = r_e N_a \left(\frac{\rho_m}{MW} \right) \sum_{i=1}^{n} Z_j$$

In this ρ_s is the scattering length density of the species, ρ_m mass density of the species, MW is the molecular weight, N_a is Avogadro's number, Z_j is the atomic number of atom j in the molecule.

These parameters are all important as the most practical way to make use of the information generated by a SAXS experiment is to use the general equation;

$$I_m \propto \Phi \cdot \Delta\Omega \eta v \tau_s \frac{d\sigma}{d\Omega}(Q)$$

From equation B-5 it can be seen that the measured intensity (I_m) is proportional to the differential cross section, it does however have other factors involved. These are the solid angle ($\Delta\Omega$), the detector efficiency (τ_s), and the volume (v). These are mostly to do with the instrument used, thus they are instrument specific which includes the type of radiation used (in λ terms) (King 1995, Higgins and Benoit 1994, Buckley 2002).

If an alternate understanding is required then it is possible to take the most general case for dilute spherical particles in a vacuum and calculate through and develop a more practical approach. The most general equation for particles in a vacuum is given by Guinier and Fournet (1955) and the following equations and derivations where achieved with the assistance Kirby (2006) and Buckley (2004)

$$I_Q = I_{eQ} \overline{N} \overline{F_Q^2}$$

(B-6)

Here I_Q is the observed intensity of transmission (units = photons.cm^{-2}), whilst $\overline{N}$ is the average number of particles in the analysis volume (this has no units and is a number).

I_{eQ} is the scattering intensity of a single electron and can be determined by $I_{eQ} = R_e^2 I_0 p^{-2} \dfrac{1+\cos^2 2\theta}{2}$ this can be reduced for small angles to $I_{eQ} = R_e^2 I_0 p^{-2}$ within this equation I_0 is the incident intensity (units = photons.cm^{-2}), and p is the distance between the sample and detector.

$\overline{F}^2$ is a function of the form factor were and is equal too $\overline{F}^2 = n^2 i_Q$ here the form factor (i_Q) of the particles and can be determined for spherical particles by $i_Q = \left(3\dfrac{\sin(Qr) - Qr\cos(Qr)}{(Qr)^3} \right)^2$, with n^2 being the number of electrons in the particle which can be determined by $n = v\overline{\rho}$ with $\overline{\rho}$ being the average electron density and v being the volume of the particle and r being the real space radius.

If the whole thing is bought together we are left with equation B-7 for spheres

$$I_Q = \left[\frac{I_0 R_e^2}{p^2} \right] \overline{N} \left[\left(v^2 \Delta\rho^2 \right) \left(3\frac{\sin(Qr) - Qr\cos(Qr)}{(Qr)^3} \right)^2 \right]$$

(B-7)

This however neglects the practicalities of experimentation and dose not have a transmission factor (T) or the detector efficiency (E_d) and it also can be simplified some what. If we make use of the fact that $\overline{N} = V \cdot \dfrac{\phi}{v}$ where V is the volume of the sample in the beam, V is able to expressed as $V = A.D$ with A being the area of the beam and D being the thickness of the sample. ϕ is the volume fraction of particles in suspension and v is the volume of a single particle (same as previously used the volume of a sphere $v = \dfrac{4}{3}\pi r^3$).

If all of the components are bought together then equation B-7 becomes equation B-8;

$$I_Q = \left[\frac{\Phi R_e^2}{p^2} \right] \left[D\phi \right] \left[\left(\left(\frac{4}{3}\pi r^3 \right) \Delta\rho^2 \right) \left(3\frac{\sin(Qr) - Qr\cos(Qr)}{(Qr)^3} \right)^2 \right]$$

(B-8)

The incident flux (Φ) has been used as defined before but as a reminder can be seen to be $\Phi = I_0 A$.

One important factor to note is that all of the equations used above are working in units of photons.cm^{-2}

Typically in an experiment that uses counting detectors you will know the A_{pixel} which is the area subtended by each pixel of the detector, with the specimen to detector distance being known the solid angle for each pixel can be calculated ($d\Omega$). The number of photons on each pixel is then $J_Q = I_Q A_{pixel} d\Omega p^2$, therefore the fundamental equation can be written ; (after Kirby 2006, Buckley 2004)

$$J_q = I_0 AdT \frac{d\sigma}{d\Omega} d\Omega E_D$$

(B-9)

This can then be used along equation B-8 and rearranged to give absolute cross section of a colloid of spherical particles in solution.

$$\frac{d\sigma}{d\Omega} = R_e^2 \phi \left(\frac{4}{3} \pi r^3 \right) (\Delta\rho)^2 \left[3 \frac{\sin Qr - Qr \cos Qr}{Q^3 r^3} \right]^2$$

<div align="right">

(B-10)

</div>

This thus will give the observed pattern on an absolute scale assuming that the corrections for the transmission, absolute scaling and background have been accounted for.

9.1. References Appendix B

Buckley, C.E., Maitland C., Scott D., Carter G., Connolly J., 'Comparison of Specific Surface Area Determined from Small Angle X-ray Scattering (SAXS) and BET', Journal of the Australasian Ceramic Society, 2004, 40(2), 7-12.

Guinier, A., Fournet, G., 1955, 'Small Angle Scattering of X-Rays' John Wiley & Sons New York

Higgins, J. S., Benoit, H. C., 1994, 'Polymers and Neutron Scattering' Oxford Science Publications, Oxford.

King, S. M., 1995, 'Small Angle Neutron Scattering' Rutherford Appleton Laboratory, Didcot.

Kirby N., Australian Synchrotron SAXS/WAXS Beam Line Scientist private conversations

10. Appendix C:- Statements of Contributions of Others

10.2. Appendix C-1: Statements of Contributions of Others for *'Ammonia-Induced Precipitation of Zirconyl Chloride and Zirconyl-Yttrium Chloride Solutions Under Industrially Relevant Conditions'*

Carter G. A., Ogden M. I., Buckley C. E., Maitland C., Paskevicius M., 2009, *'Ammonia-Induced Precipitation of Zirconyl Chloride and Zirconyl-Yttrium Chloride Solutions Under Industrially Relevant Conditions'*, Journal of Powder Technology, vol. [188], pp 222-228.

7th April 2009

To Whom It May Concern

I, Prof. M. I. Ogden, contributed by project supervision and manuscript editing to the paper/publication entitled

Carter G. A., Ogden M. I., Buckley C. E., Maitland C., Paskevicius M., 2009, '*Ammonia-Induced Precipitation of Zirconyl Chloride and Zirconyl-Yttrium Chloride Solutions Under Industrially Relevant Conditions*', Journal of Powder Technology, vol. [188], pp 222-228.

undertaken with Geoffrey A Carter.

(Signature of Co-Author)

M. I. Ogden

Geoffrey A Carter

7th April 2009

To Whom It May Concern

I, Prof. C. E. Buckley, contributed by project supervision and manuscript editing to the paper/publication entitled

Carter G. A., Ogden M. I., Buckley C. E., Maitland C., Paskevicius M., 2009, '*Ammonia-Induced Precipitation of Zirconyl Chloride and Zirconyl-Yttrium Chloride Solutions Under Industrially Relevant Conditions*', Journal of Powder Technology, vol. [188], pp 222-228.

undertaken with Geoffrey A Carter.

.

(Signature of Co-Author)

C. E. Buckley

Geoffrey A Carter

7th April 2009

To Whom It May Concern

I, Mr C Maitland, contributed by Specialist technical advise to the paper/publication entitled

Carter G. A., Ogden M. I., Buckley C. E., Maitland C., Paskevicius M., 2009, '*Ammonia-Induced Precipitation of Zirconyl Chloride and Zirconyl-Yttrium Chloride Solutions Under Industrially Relevant Conditions*', Journal of Powder Technology, vol. [188], pp 222-228.

undertaken with Geoffrey A Carter.

C. Maitland

Geoffrey A Carter
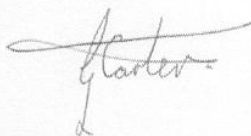
7th April 2009

To Whom It May Concern

I, Mr M. Paskevicius, contributed by Specialist technical advise to the paper/publication entitled

Carter G. A., Ogden M. I., Buckley C. E., Maitland C., Paskevicius M., 2009, '*Ammonia-Induced Precipitation of Zirconyl Chloride and Zirconyl-Yttrium Chloride Solutions Under Industrially Relevant Conditions*', Journal of Powder Technology, vol. [188], pp 222-228.

undertaken with Geoffrey A Carter.

M. Paskevicius

Geoffrey A Carter

10.3. Appendix C-2: Statements of Contributions of Others for '*The Effect of Processing Parameters on Particle Size in Ammonia-Induced Precipitation of Zirconyl Chloride Under Industrially Relevant Conditions*'

<u>Carter G.</u>, Hart R., Rowles M., Ogden M., Buckley C., 2009, '*The Effect of Processing Parameters on Particle Size in Ammonia-Induced Precipitation of Zirconyl Chloride Under Industrially Relevant Conditions*', Journal of Powder Technology, doi: 101016/j.powtec.200810.012.

7th April 2009

To Whom It May Concern

I, Dr R. D. Hart, contributed by specialist technical advise and instrument usage to the paper/publication entitled

> **Carter G.**, Hart R., Rowles M., Ogden M., Buckley C., 2009, '*The Effect of Processing Parameters on Particle Size in Ammonia-Induced Precipitation of Zirconyl Chloride Under Industrially Relevant Conditions*', Journal of Powder Technology, doi: 101016/j.powtec.200810.012.

undertaken with Geoffrey A Carter.

(Signature of Co-Author)

R. D. Hart

Geoffrey A Carter

7th April 2009

To Whom It May Concern

I, Dr M Rowles, contributed by specialist technical advise and instrument usage to the paper/publication entitled

Carter G., Hart R., Rowles M., Ogden M., Buckley C., 2009, '*The Effect of Processing Parameters on Particle Size in Ammonia-Induced Precipitation of Zirconyl Chloride Under Industrially Relevant Conditions*', Journal of Powder Technology, doi: 101016/j.powtec.200810.012.

undertaken with Geoffrey A Carter.

M. Rowles

Geoffrey A Carter

7th April 2009

To Whom It May Concern

I, Prof. M. I. Ogden, contributed by project supervision and manuscript editing to the paper/publication entitled

Carter G., Hart R., Rowles M., Ogden M., Buckley C., 2009, '*The Effect of Processing Parameters on Particle Size in Ammonia-Induced Precipitation of Zirconyl Chloride Under Industrially Relevant Conditions*', Journal of Powder Technology, doi: 101016/j.powtec.200810.012.

undertaken with Geoffrey A Carter.

(Signature of Co-Author)

M. I. Ogden

Geoffrey A Carter

7th April 2009

To Whom It May Concern

I, Prof. C. E. Buckley, contributed by project supervision and manuscript editing to the paper/publication entitled

    Carter G., Hart R., Rowles M., Ogden M., Buckley C., 2009, '*The Effect of Processing Parameters on Particle Size in Ammonia-Induced Precipitation of Zirconyl Chloride Under Industrially Relevant Conditions*', Journal of Powder Technology, doi: 101016/j.powtec.200810.012.

undertaken with Geoffrey A Carter.
.
(Signature of Co-Author)

C. E. Buckley

Geoffrey A Carter

10.4. Appendix C-3: Statements of Contributions of Others for '*From Zirconyl Chloride to Zirconia Ceramic, A Plant Operation Perspective*'

Carter G., Rowles M., Hart R., Ogden M., Buckley C., 2008, '*From Zirconyl Chloride to Zirconia Ceramic, A Plant Operation Perspective*', Materials Forum, vol. [32], pp. 82-89.

7th April 2009

To Whom It May Concern

I, Dr M Rowles, contributed by specialist technical advise and instrument usage to the paper/publication entitled

Carter G., Rowles M., Hart R., Ogden M., Buckley C., 2008, '*From Zirconyl Chloride to Zirconia Ceramic, A Plant Operation Perspective*', Materials Forum, vol. [32], pp. 82-89.

undertaken with Geoffrey A Carter.

M. Rowles

Geoffrey A Carter

7th April 2009
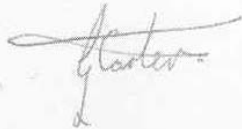
To Whom It May Concern

I, Dr R. D. Hart, contributed by specialist technical advise and instrument usage to the paper/publication entitled

Carter G., Rowles M., Hart R., Ogden M., Buckley C., 2008, '*From Zirconyl Chloride to Zirconia Ceramic, A Plant Operation Perspective*', Materials Forum, vol. [32], pp. 82-89.

undertaken with Geoffrey A Carter.

(Signature of Co-Author)

R. D. Hart

Geoffrey A Carter

7th April 2009

To Whom It May Concern

I, Prof. C. E. Buckley, contributed by project supervision and manuscript editing to the paper/publication entitled

Carter G., Rowles M., Hart R., Ogden M., Buckley C., 2008, '*From Zirconyl Chloride to Zirconia Ceramic, A Plant Operation Perspective*', Materials Forum, vol. [32], pp. 82-89.

undertaken with Geoffrey A Carter.
.
(Signature of Co-Author)

C. E. Buckley

Geoffrey A Carter

10.5. Appendix C-4: Statements of Contributions of Others for '*Industrial Precipitation of Zirconyl Chloride: The Effect of pH and Solution Concentration on Calcination of Zirconia*'

Carter G., Hart R., Rowles M., Ogden M., Buckley C., 2009 '*Industrial Precipitation of Zirconyl Chloride: The Effect of pH and Solution Concentration on Calcination of Zirconia*', Materials Chemistry and Physics Doi: 10.1016/j.matchemphys.2009.05.014

27th May 2009

To Whom It May Concern

I, Dr R. D. Hart, contributed by specialist technical advise and instrument usage to the paper/publication entitled

Carter G., Rowles M., Hart R., Ogden M., Buckley C., 2009, '*Industrial Precipitation of Zirconyl Chloride: The Effect of pH and Solution Concentration on Calcination of Zirconia*' Mater. Chem. Phys. (2009). Doi: 10.1016/j.matchemphys.2009.05.014

undertaken with Geoffrey A Carter.

(Signature of Co-Author)
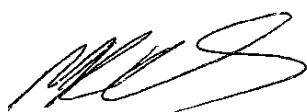
R. D. Hart

Geoffrey A Carter
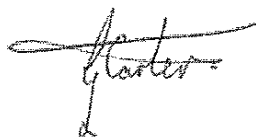
27th May 2009

To Whom It May Concern

I, Dr M Rowles, contributed by specialist technical advise and instrument usage to the paper/publication entitled

Carter G., Rowles M., Hart R., Ogden M., Buckley C., 2009, *'Industrial Precipitation of Zirconyl Chloride: The Effect of pH and Solution Concentration on Calcination of Zirconia'* Mater. Chem. Phys. (2009). Doi: 10.1016/j.matchemphys.2009.05.014

undertaken with Geoffrey A Carter.

M. Rowles

Geoffrey A Carter

27th May 2009

To Whom It May Concern

I, Prof. M. I. Ogden, contributed by project supervision and manuscript editing to the paper/publication entitled

<u>Carter G.</u>, Rowles M., Hart R., Ogden M., Buckley C., 2009, '*Industrial Precipitation of Zirconyl Chloride: The Effect of pH and Solution Concentration on Calcination of Zirconia*' Mater. Chem. Phys. (2009). Doi: 10.1016/j.matchemphys.2009.05.014

undertaken with Geoffrey A Carter.

(Signature of Co-Author)

M. I. Ogden

Geoffrey A Carter

27th Mayl 2009

To Whom It May Concern

I, Prof. C. E. Buckley, contributed by project supervision and manuscript editing to the paper/publication entitled
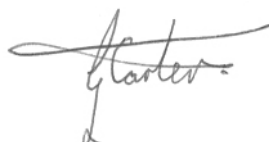
Carter G., Rowles M., Hart R., Ogden M., Buckley C., 2009, '*Industrial Precipitation of Zirconyl Chloride: The Effect of pH and Solution Concentration on Calcination of Zirconia*' Mater. Chem. Phys. (2009). Doi: 10.1016/j.matchemphys.2009.05.014

undertaken with Geoffrey A Carter.
.

(Signature of Co-Author)

C. E. Buckley

Geoffrey A Carter

10.6. Appendix C-5: Statements of Contributions of Others for '*Industrial Precipitation of Yttria Partially Stabilised Zirconia*'

<u>Carter G.</u>, Hart R., Rowles M., Ogden M., Buckley C., 2009 '*Industrial Precipitation of Yttria Partially Stabilised Zirconia*', Journal of Alloys and Compounds, DOI:10.1016/j.jallcom.2009.02.005.

7th April 2009

To Whom It May Concern

I, Dr R. D. Hart, contributed by specialist technical advise and instrument usage to the paper/publication entitled

Carter G., Hart R., Rowles M., Ogden M., Buckley C., 2009 '*Industrial Precipitation of Yttria Partially Stabilised Zirconia*', Journal of Alloys and Compounds, DOI:10.1016/j.jallcom.2009.02.005.

undertaken with Geoffrey A Carter.

.
(Signature of Co-Author)

R. D. Hart

Robert Hart.

G Carter

Geoffrey A Carter

7th April 2009

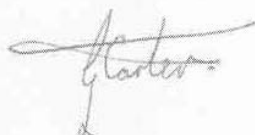To Whom It May Concern

I, Dr M Rowles, contributed by specialist technical advise and instrument usage to the paper/publication entitled

Carter G., Hart R., Rowles M., Ogden M., Buckley C., 2009 '*Industrial Precipitation of Yttria Partially Stabilised Zirconia*', Journal of Alloys and Compounds, DOI:10.1016/j.jallcom.2009.02.005.

undertaken with Geoffrey A Carter.

M. Rowles

Geoffrey A Carter

7th April 2009

To Whom It May Concern

I, Prof. M. I. Ogden, contributed by project supervision and manuscript editing to the paper/publication entitled

Carter G., Hart R., Rowles M., Ogden M., Buckley C., 2009 '*Industrial Precipitation of Yttria Partially Stabilised Zirconia*', Journal of Alloys and Compounds, DOI:10.1016/j.jallcom.2009.02.005.

undertaken with Geoffrey A Carter.

(Signature of Co-Author)

M. I. Ogden

Geoffrey A Carter

7th April 2009

To Whom It May Concern

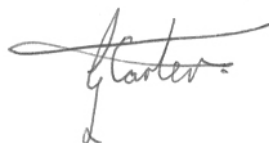I, Prof. C. E. Buckley, contributed by project supervision and manuscript editing to the paper/publication entitled

Carter G., Hart R., Rowles M., Ogden M., Buckley C., 2009 '*Industrial Precipitation of Yttria Partially Stabilised Zirconia',* Journal of Alloys and Compounds, DOI:10.1016/j.jallcom.2009.02.005.

undertaken with Geoffrey A Carter.
.
(Signature of Co-Author)

C. E. Buckley

Geoffrey A Carter

11.   Appendix D:- Copyright Forms

11.1.   Appendix D-1: Elsevier Journal Articles

Copyrights relating to Elsevier journal articles held by Authors; relevant point is underlined and in Bold type; 4 papers used in this Thesis are published in Elsevier Journals being;

Carter G. A., Ogden M. I., Buckley C. E., Maitland C., Paskevicius M., 2009, '*Ammonia-Induced Precipitation of Zirconyl Chloride and Zirconyl-Yttrium Chloride Solutions Under Industrially Relevant Conditions*', Journal of Powder Technology, vol. [188], pp 222-228.

Carter G., Hart R., Rowles M., Ogden M., Buckley C., 2009, '*The Effect of Processing Parameters on Particle Size in Ammonia-Induced Precipitation of Zirconyl Chloride Under Industrially Relevant Conditions*', Journal of Powder Technology, doi: 101016/j.powtec.200810.012.

Carter G., Hart R., Rowles M., Ogden M., Buckley C., 2009 '*Industrial Precipitation of Zirconyl Chloride: The Effect of pH and Solution Concentration on Calcination of Zirconia*', Materials Chemistry and Physics Doi: 10.1016/j.matchemphys.2009.05.014

Carter G., Hart R., Rowles M., Ogden M., Buckley C., 2009 '*Industrial Precipitation of Yttria Partially Stabilised Zirconia*', Journal of Alloys and Compounds, DOI:10.1016/j.jallcom.2009.02.005.

COPYRIGHT

What rights do I retain as a journal author*?

As a journal author, you retain rights for large number of author uses, including use by your employing institute or company. These rights are retained and permitted without the need to obtain specific permission from Elsevier. These include:

- the right to make copies (print or electric) of the journal article for their own personal use, including for their own classroom teaching use;
- the right to make copies and distribute copies (including via e-mail) of the journal article to research colleagues, for personal use by such colleagues (but not for Commercial Purposes**, as listed below);
- the right to post a pre-print version of the journal article on Internet web sites including electronic pre-print servers, and to retain indefinitely such version on such servers or sites (see also our information on electronic preprints for a more detailed discussion on these points);
- the right to post a revised personal version of the text of the final journal article (to reflect changes made in the peer review process) on the author's personal or institutional web site or server, incorporating the complete citation and with a link to the Digital Object Identifier (DOI) of the article;
- the right to present the journal article at a meeting or conference and to distribute copies of such paper or article to the delegates attending the meeting;
- for the author's employer, if the journal article is a 'work for hire', made within the scope of the author's employment, the right to use all or part of the information in (any version of) the journal article for other intra-company use (e.g. training), including by posting the article on secure, internal corporate intranets;
- patent and trademark rights and rights to any process or procedure described in the journal article;
- **the right to include the journal article, in full or in part, in a thesis or dissertation**;
- the right to use the journal article or any part thereof in a printed compilation of works of the author, such as collected writings or lecture notes (subsequent to publication of the article in the journal); and
- the right to prepare other derivative works, to extend the journal article into book-length form, or to otherwise re-use portions or excerpts in other works, with full acknowledgement of its original publication in the journal.

*__Please Note:__ The rights listed above apply to journal authors only. For information regarding book author rights, please contact the **Global Rights Department**

150

11.2. Appendix D-2: Material Forum Journal Article

Copyright information relating to;

<u>Carter G.</u>, Rowles M., Hart R., Ogden M., Buckley C., 2008, '*From Zirconyl Chloride to Zirconia Ceramic, A Plant Operation Perspective*', Materials Forum, vol. [32], pp. 82-89.

This publication is one of the 5 used as the body of this Thesis

PERMISSION TO USE COPYRIGHT MATERIAL AS SPECIFIED BELOW:

Carter G., et al., *From Zirconyl Chloride to Zirconia Ceramic, A Plant Operation Perspective.* Materials Forum, 2008. **32-2008**: p. 82-89.

I hereby give permission for Geoffrey Carter to include the abovementioned material(s) in his higher degree thesis for the Curtin University of Technology. This permission is granted on a non-exclusive basis and for an indefinite period.

I confirm that I am the copyright owner of the specified material.

Permission to use this material is subject to the following conditions: Full acknowledgement of the ownership of the copyright and the source of the material will be provided.

Signed:

Name: Helen Woodall

Position: Event and Training Manager, Materials Australia
Date: 27/1/09

Please return signed form to Geoff Carter.

11.3. Appendix D-3: 3rd Party Information/Reproduction

Copies of Copyright permission for use of 3rd party information/reproduction.

Dear Geoffrey Carter,

Thank you for your email request. Permission is granted for you to use the material below for your thesis/dissertation subject to the usual acknowledgements and on the understanding that you will reapply for permission if you wish to distribute or publish your thesis/dissertation commercially.

Best wishes,

Lina Kopicaite

Permissions Assistant
Wiley-Blackwell
9600 Garsington Road
Oxford OX4 2DQ
UK
Tel: +44 (0) 1865 476158
Fax: +44 (0) 1865 471158
Email: lkopicai@wiley.com

A01_First_Name: Geoffrey
A02_Last_Name: Carter
A03_Company_Name: Curtin Universityof Technology
A04_Address: Kent st
A05_City: Bently
A06_State: Western Australia
A07_Zip: 6845
A08_Country: Australia
A09_Contact_Phone_Number: +61 8 9266 3781
A10_Fax: +61 8 9266 4699
A11_Emails: g.carter@exchange.curtin.edu.au
A12_Reference:
A13_Book_Title: Journal of American Ceramic Society vol. 84, No. 7, pp.1637-1638, 2001
A40_Book_or_Journal: Journal
A14_Book_Author:
A15_Book_ISBN:
A16_Journal_Month:
A17_Journal_Year: 2001
A18_Journal_Volume: 84
A19_Journal_Issue_Number: 7
A20_Copy_Pages: Figure 1 and 2 page 1638
A21_Maximum_Copies: 6
A22_Your_Publisher: Curtin University of Technology
A23_Your_Title: G Carter Doctoral Thesis The Controlof the precipitation process of Value added Zirconia
A24_Publication_Date: November 2008
A25_Format: print
A41_Ebook_Reader_Type:
A26_If_WWW_URL:
A27_If_WWW_From_Adopted_Book:
A28_If_WWW_Password_Access:
A45_WWW_Users:

```
A29_If_WWW_Material_Posted_From:
A30_If_WWW_Material_Posted_To:
A42_If_Intranet_URL:
A32_If_Intranet_From_Adopted_Book:
A33_If_Intranet_Password_Access:
A48_Intranet_Users:
A34_If_Intranet_Material_Posted_From:
A35_If_Intranet_Material_Posted_To:
A50_If_Software_Print_Type:
A60_If_Other_Type:
A37_Comments_For_Request: It is my understanding that you/your
organisation holds copyrights in the following material:
```

Huang C., Tang Z., Zhang Z., ¡¥Differences between Zirconium
Hydroxide
(Zr(OH)4"ªnH2O) and Hydrous Zirconia (ZrO2"ªnH2O)¡¦ Journal of
American Ceramic Society vol. 84, No. 7, pp.1637-1638, 2001

I would like to reproduce an extract of this work in a Doctoral
thesis which I am currently undertaking at Curtin University of
Technology in Perth, Western Australia. The subject of my research
is the control of the precipitation process of value added zirconia.
I am carrying out this research as part of an Australian Research
Counsel linkage grant with Doral Specialty Chemicals as the
industrial sponsor.

The specific material / extract that I would like to use for the
purposes of the thesis is Figure 1 and 2 on page 1638.

Once completed, the thesis will be made available in hard-copy form
in the Curtin Library. The material will be provided strictly for
educational purposes and on a non-commercial basis.

```
A01_First_Name: Geoffrey
A02_Last_Name: Carter
A03_Company_Name: Curtin Universityof Technology
A04_Address: Kent st
A05_City: Bently
A06_State: Western Australia
A07_Zip: 6845
A08_Country: Australia
A09_Contact_Phone_Number: +61 8 9266 3781
A10_Fax: +61 8 9266 4699
A11_Emails: g.carter@exchange.curtin.edu.au
A12_Reference:
A13_Book_Title: Journal of American Ceramic Society vol. 78, No. 1, 146-52
1995
A40_Book_or_Journal: Journal
A14_Book_Author:
A15_Book_ISBN:
A16_Journal_Month:
A17_Journal_Year: 1995
A18_Journal_Volume: 78
A19_Journal_Issue_Number: 1
A20_Copy_Pages: Matsui K., Suzuki H., Michiharu O., 'Raman Spectroscopic
Studies on the Formation Mechanism of Hydrous-Zirconia Fine Particles'
Journal of American Ceramic Society vol. 78, No. 1, 146-52 1995 Figures
1,page 147 and Figure 2 page 147. Figures 4 and 5 page 148
A21_Maximum_Copies: 6
```

A22_Your_Publisher: Curtin University of Technology
A23_Your_Title: G Carter Doctoral Thesis The Controlof the precipitation process of Value added Zirconia
A24_Publication_Date: November 2008
A25_Format: print
A41_Ebook_Reader_Type:
A26_If_WWW_URL:
A27_If_WWW_From_Adopted_Book:
A28_If_WWW_Password_Access:
A45_WWW_Users:
A29_If_WWW_Material_Posted_From:
A30_If_WWW_Material_Posted_To:
A42_If_Intranet_URL:
A32_If_Intranet_From_Adopted_Book:
A33_If_Intranet_Password_Access:
A48_Intranet_Users:
A34_If_Intranet_Material_Posted_From:
A35_If_Intranet_Material_Posted_To:
A50_If_Software_Print_Type:
A60_If_Other_Type:
A37_Comments_For_Request: It is my understanding that you/your organisation
holds copyrights in the following material:

Matsui K., Suzuki H., Michiharu O., 'Raman Spectroscopic Studies on the Formation Mechanism of Hydrous-Zirconia Fine Particles' Journal of American
Ceramic Society vol. 78, No. 1, 146-52 1995

I would like to reproduce an extract of this work in a Doctoral thesis which I am currently undertaking at Curtin University of Technology in Perth, Western Australia. The subject of my research is the control of the precipitation process of value added zirconia. I am carrying out this research as part of an Australian Research Counsel linkage grant with Doral
Specialty Chemicals as the industrial sponsor.

The specific material / extract that I would like to use for the purposes of the thesis is Figure 1 and 2 on page 147 and figures 4and 5 on page 148.

Once completed, the thesis will be made available in hard-copy form in the Curtin Library. The material will be provided strictly for educational purposes and on a non-commercial basis.

RECEIVED

PERMISSION REQUEST FORM

ACS COPYRIGHT OFFICE

Date:___17th September 2008____

To :

~To: Copyright Office
Publications Division
American Chemical Society
1155 Sixteenth Street, N.W.
Washington, DC 20036

From:

From: ____Geoffrey Carter _____
___NRI Curtin University of Technology____
___GPO Box U1987_____
___Perth Western Australia 6845_____
____Australia_____

FAX: 202-776-8112

Your Phone No.____+61 8 9266 3781_____
Your Fax No._____+61 8 9266 4699_____ .

I am preparing a paper entitled:

_____ Doctoral thesis control of the precipitation process of value added zirconia

to appear in a **(circle one)** book, magazine, journal, proceedings, other _____
entitled: _____ Doctoral thesis control of the precipitation process of value added zirconia
to be published by: Curtin University of Technology_____

I would appreciate your permission to use the following ACS material in print and other formats
with the understanding that the required ACS copyright credit line will appear with each item and
that this permission is for only the requested work listed above:

From ACS journals or magazines (for ACS magazines, also include issue no.):
ACS Publication Title Issue Date   Vol. No.   Page(s)Material to be used*

Journal of the American Chemical Society 1953 Vol. 75, pp. 3937-3943 Johnson J. S., Kraus K.
A., 'Hydrolytic Polymerisation of Zirconium (IV)', **Figure 2** on page 3940, titled "polymerisation of
Zr(iv) and Hf(iv) as a function of acidity".

From ACS books: include ACS book title, series name and number, year, page(s), book
editor=s name(s), chapter author's name(s), and material to be used, such as Figs. 2 & 3, full text,
etc.*

---

* If you use more than three figures/tables from any article and/or chapter, the author's permission
will also be required.
Questions? Please call Arleen Courtney at (202) 872-4368 or use the FAX number above ____

This space is reserved for
ACS Copyright Office Use

**PERMISSION TO REPRINT IS GRANTED BY
THE AMERICAN CHEMICAL SOCIETY**

ACS CREDIT LINE REQUIRED. Please follow this sample:
Reprinted with permission from (reference citation). Copyright
(year) American Chemical Society.

APPROVED BY: ___*C. Arleen Courtney*___ 11|4|08
ACS Copyright Office

☐ If box is checked, author permission is also required. See
original article for address.

12/3/99

158

12. Bibliography

Ahmed, K., Love J., Ratnaraj R., 'High Performance Cell Development at CFCL', Electrochemical Society Proceedings, 2001.

Anstis, G. R., Chantikul P., Lawn, B.R., Marshall D. B., 'A Critical Evaluation of Indentation Techniques for Measuring Fracture toughness: I, Direct Crack Measurements', Journal of the American Ceramic Society 1981, 64(9), 533-538.

Askeland, D. R., Phule P. P., 'Essentials of Materials Science and Engineering', Thomson ,Toronto Ontario Canada: 2004.

ASTM (1990). ASTM E 384-89 1990, 'Standard Test Method for Microhardness of Materials', ASTM Standards.

ASTM C 112-96 1999 (1999). ASTM C 112-96 1999, 'Standard Test Method for Determining Average Grain Size' ASTM Standards.

ASTM C 1161-94 1996 (1996). ASTM C 1161-94 1996, 'Stanard test method for flexural strength of advanced ceramics at ambient temperature', ASTM Standards.

Badwal, S. P. S., Caicchi F. T., 'Oxygen-Ion Conducting Electrolyte Materials for Solid Oxide Fuell Cells', Ionics 2000, 6, 1-21.

Badwal, S. P. S., Ciacchi F. T., Giampietro K. M., 'Analysis of the conductivity of commercial easy sintering grade 3 mol% Y2O3-ZrO2 materials', Solid State Ionics 2005 176(1-2) 169-178.

Badwal S. P. S., Ciacchi F. T., Milosevic D., 'Scandia-Zirconia Electrolytes for Intermediate Temperature Solid Oxide Fuel Cell Operation', Solid State Ionics 2000, 13(6-7), 91-99.

Badwal S. P. S., Ciacchi F. T., Rajendran S., Drennan, J., 'An Investigation of Conductivity, Microstructure and Stability of Electrolyte Compositions in the system 9 mol% (Sc$_2$O$_3$-Y$_2$O$_3$)-ZrO$_2$(Al$_2$O$_3$)', Solid State Ionics 1998, 109, 167-186.

Badwal S. P. S., Ciacchi F. T., Zelizko V., 'The effect of alumina addition on the conductivity, microstructure and mechanical strength of zirconia-yttria electrolytes', Ionics, 1998, 4, 25-32.

Bannister, M., Garrett W.,' Production of Stabilized Zirconia for use as a Solid-State Electrolyte', Ceramurgia International, 1975 1(3) 127-133.

Beaucage, G., 'Approximations leading to a unified exponential power-law approach to small-angle scattering', Journal of Applied Crystallography, 1995, 28, 717-728.

Beaucage, G., Schaefer D. W., 'Structural Studies of Complex-Systems using Small-Angle Scattering - A Unified Guinier Power-Law Approach', Journal of Non-Crystline Solids, 1994, 172, 797-805.

Beaucage, G., T.A. Ulibarri, E.P. Black, and D.W. Schaefer, Multiple Size Scale Structures in Silica-Siloxane Composites Studied by Small-Angle Scattering, in Hybrid Organic-Inorganic Composites. ACS Symposium Series, 1995, p. 97-111.

Belous, A.G., Kravchyk K.V., Pashkova E.V., Bohnke O., Galven C., 'Influence of the chemical composition on structural properties and electrical conductivity of Y-Ce-ZrO$_2$', Chemistry of Materials, 2007, 19(21), 5179-5184.

Bellon, O., R. Ratnaraj, and D. Rodrigo, '10YSZ based electrolyte materials for electrolyte supported SOFC's', 5th European SOFC Forum, 2002.

Bleier A., Becher P. F., Alexander K. B., Westmoreland C. G., 'Effect of aqueous processing conditions on the microstructure and transformation behavior in AL$_2$O$_3$-ZRO$_2$(CEO$_2$) composites', Journal of the American Ceramics Society, 1992, 75, 2649.

Bokhimi, X., Morales A., Crcia-Ruiz A., Xiao T. D., Chen H., Strutt P. R., 'Transformation of yttrium-doped hydrated zirconium into tetragonal and cubic nanocrystalline zirconia', Journal of Solid State Chemistry, 1999, 142(2), 409-418.

Britton, H., 'Electrometric studies of the precipitation of hydroxides. Part II. The precipitation of the hydroxides of zinc, chromium, beryllium, aluminium, bivalent tin and zirconium by use of the hydrogen electrode, and their alleged amphoteric nature', Journal Chemical Society Transaction., 1925, 127, 2120-2141.

Buckley, C.E., Maitland C., Scott D., Carter G., Connolly J., 'Comparison of Specific Surface Area Determined from Small Angle X-ray Scattering (SAXS) and BET', Journal of the Australasian Ceramic Society, 2004, 40(2), 7-12.

Burtron, H. D., 'Effect of pH on Crystal Phase of ZrO_2 Precipitated from Solution and Calcined at 600ºC', Journal of the American Ceramic Society, 1984, 67(8), C-168-C-168.

Callon, G. J., D. M. Goldie, et al., 'X-ray diffraction analysis of yttria stabilized zirconia powders produced by organic sol-gel method,', Journal of Materials Science Letters, 2000, 19, 1689-1691.

Callister, J., 'Materials Science and Engineering: An Introduction 4th edn.' John Wiley & Sons, Inc., New York: 1997

Carter, G., Hart R. D., Kirby N. M., Milosevic D., Titkov A. N., 'Chemically-Mixed Powders For Solid Oxide Fuel Cells', Journal of the Australasian Ceramic Society, 2003, 39(2),149-153.

Carter, G.A., van Riessen A., Hart R. D., 'Wear of Zirconia Dispersed Alumina at Ambient, 140 ºC and 250 ºC', Journal of the European Ceramic Society, 2006, 26, 3547-3555.

Carter G. A., Ogden M. I., Buckley C. E., Maitland C., Paskevicius M., 'Ammonia-induced precipitation of zirconyl chloride and zirconyl-yttrium chloride solutions

under industrially relevant conditions', Powder Technology, In Press, Corrected Proof doi:10.1016/j.powtec.2008.04.087.

Carter G., Rowles M., Hart R., Ogden M., Buckley C., 'From Zirconyl Chloride to Zirconia Ceramic, A Plant Operation Perspective', Materials Forum, 2008, 32-2008, 82.

Carter G., M. Rowles, Hart R., Ogden M., Buckley C., 'The effect of processing parameters on particle size in ammonia-induced precipitation of zirconyl chloride under industrially relevant conditions', Powder Technology 2008, In Press.

Clearfield, A., 'Structural Aspects of Zirconium Chemistry Review', Pure Applied Chemistry, 1964, 14, 91-108.

Clearfield, A., 'The Mechanism of Hydrolytic Polymerization of Zirconyl Solutions', Journal Materials Research, 1990, 5(1), 161-162.

Ciacchi, F.T., K.M. Crane, and S.P.S. Badwal, 'Evaluation of Commercial Zirconia Powders for Solid Oxide Fuel-Cells', Solid State Ionics, 1994, 73(1-2), 49-61.

Cullity B. D., 'Elements of X-Ray Diffraction Second Edition', Addison-Wesley Publishing Company, Reading Massachusetts, 1978.

Denkewicz R. P., Ten huisen K. S., Adair J. H., 'Hydrothermal crystallization kinetics on m-ZrO_2 and t-ZrO_2' Journal Materials Research 1990, 5, 2698.

Eiji Tani, Masahiro Yoshimura, Shigeyuki Somiya, 'Hydrothermal Preparation of Ultrafme Monoclinic ZrO_2 Powder', Journal of the American Ceramic Society 1981, 64(12), C-181-C-181.

Eiji Tani, Masahiro Yoshimura, Shigeyuki S. Cmiya, 'Formation of Ultrafine Tetragonal ZrO_2 Powder Under Hydrothermal Conditions', Journal of the American Ceramic Society 1983, 66(1), 11-14.

Elinson, S.V., Petrov K. S., 'Analytical Chemistry of Zirconium and Hafnium', Ann Arbor-Humphrey Science Publishers, London: 1974.

Fernandez-Garcia, M., A. Martinez-Arias, J.C. Hanson, and J.A. Rodriguez, 'Nanostructured oxides in chemistry: Characterization and properties', Chemistry Review, 2004, 104(9), 4063-4104.

Foger, K., Badwal S.P.S., 'Materials for Solid-Oxide Fuel Cells', Materals Forum, 1997, 21, 187-224.

Garvie, R.C., 'The Occurrence of Metastable Tetragonal Zirconia as a Crystalite Size Effect', Journal of Physical Chemistry, 1965, 69 (4), 6.

Garvie, R. C., 'Stabilization of the tetragonal structure in Zirconia Microcrystals', The Journal of Physical Chemistry, 1978, 82(2), 218-224.

Green, D. J., Hannink R. H. J., Swain M. V., 'Transformation Toughening of Ceramics', CRC Press, Inc., Florida: 1989.

Guo, G.Y., Chen Y. L., Ying W. L., 'Thermal, spectroscopic and X-ray diffractional analyses of zirconium hydroxides precipitated at low pH values. Materials Chemistry and Physics', 2004, 84(2-3), 308-314.

Guo, G.Y., Chen Y. L., 'A nearly pure monoclinic nanocrystalline Zirconia'. Journal of Solid State Chemistry, 2005. 178(5): p. 1675-1682.

Gupta, N., P. Mallik P., Basu B., 'Y-TZP ceramics with optimized toughness: new results', Journal of Alloys and Compounds 2004 379(1-2), 228-232.

Gupta N., Mallik P., Lewis M. H., Basu B., 'Improvement of toughness of Y-ZrO2: Role of dopant distribution' Euro Ceramics Viii, Pts 1-3. 2004, 264-268: 817-820.

Huang, Y.X., Guo C. J., 'Synthesis of Nanosized Zirconia Particles via Urea Hydrolysis', Powder Technology, 1992, 72(2), 101-104.

Hagfeldt, C., V. Kessler, and I. Persson, 'Structure of the hydrated, hydrolysed and solvated zirconium(IV) and hafnium(IV) ions in water and aprotic oxygen donor solvents. A crystallographic, EXAFS spectroscopic and large angle Xray scattering study', Dalton Transactions, 2004, (14), 2142-2151.

Hannink R.H.J., Kelly P.M., Muddle B.C., 'Transformation toughening in zirconia Containing ceramics', Journal of American Ceramic Society, 2000, vol. 83(3), 461-487.

Hansen, J.P., Hayter J. B., 'A Rescaled MSA Structure Factor for Dilute Charged Colloidal Dispersions', Molecular Physics, 1982, 46(3), 651-656.

Hassan, A. A. E., Menzler N. H., Blass G., Ali M., Buchkremer H. P., Stover D., 'Influence of alumina dopant on the properties of yttria-stabilized zirconia of SOFC applications', Journal of Materials Science, 2002, 37.

Hayter J.B., Penfold J., 'An Analytic Structure Factor for Macroion Solutions', Molecular Physics, 1981, 42(1), 109-118.

Hsieh G. H., Tuan W. H., 'Exaggerated grain growth in yttria-containing zirconia ceramics', journal of Materials Science Letters, 2002, 21, 391-393.

Hu M. Z. C., Harris M. T., Byers C. H., 'Nucleation and growth for synthesis of nanometric zirconia particles by forced hydrolysis', Journal Colloid Interface Science, 1998, 198(1), 87-99.

Huang C., Tang Z., Zhang Z., 'Differences between Zirconium Hydroxide $(Zr(OH)_4.nH_2O)$ and Hydrous Zirconia $(ZrO_2.nH_2O)$', Journal of American Ceramic Society, 2001, 84(7), 1637-1638.

Ilavsky, J., Irena 2 SAS Modelling Macros. Advanced Photon Source, Argonne National Laboratory: 2005,

Ingel R., Lewis D., 'Lattice Parameters and Density of Y_2O_3-Stabilized ZrO_2', Journal of the American Ceramics Society, 1986, 69(4), 325-32.

Jepson, W.B., Rowse J. B., 'The composition of kaolinite-an electron microprobe study', Clays and Clay Minerals, 1975, 23, 310 -317.

Jia L., Lu Z., Miao Jipeng, Liu Zhiguo, Li Guoqing, Su Wenhui, 'Effects of pre-calcined YSZ powders at different temperatures on Ni-YSZ anodes for SOFC', Journal of Alloys and Compounds 2006, 414(1-2), 152-157.

Johnson, J.S., Kraus K. S., 'Hydrolytic Behavior of Metal Ions VI. Ultracentrifugation of Zirconium (IV)and Hafnium (IV) Effect of Acidity on the Degree of Polymerization', Journal of the American Ceramic Society, 1956, 78, 3937-3943.

Jones, S.L., Norman C. J, 'Dehydration of Hydrous Zirconia with Methanol', Journal of the American Ceramic Society, 1998, 71(4), C190-C191.

Kaliszewski, M.S., Heuer A.H., 'Alcohol Interaction with Zirconia Powders', Journal of the American Ceramic Society, 1990, 73(6), 1504-1509.

Kirby, N.M., PhD, Barium zirconate ceramics for melt processing of barium cuprate superconductors, 2003, Curtin University of Technology, Perth,
Western Australia.

Kondoh, J., 'Origin of the hump on the left shoulder of the X-ray diffraction peaks observed in Y_2O_3-fully and partially stabilized ZrO_2', Journal of Alloys and Compounds, 2004, 375, 270-282.

Kondoh J., Shiota H., Kawachi K., Nakatani T., 'Yttria concentration dependence of tensile strength in yttria-stabilized zirconia' Journal of Alloys and Compounds, 2004, 365(1-2), 253-258.

Kovalenko and Bagdasaov, 'The Solubility of Zirconium Hydroxide', Russian Journal of Inorganic Chemistry, 1961, 6(3), 272-275.

Kruzic, J. J., Ritchie R. O., 'Determining the toughness of ceramics from Vickers indentations using the crack-opening displacement: An experimental study', Journal of the American Ceramic Society, 2003, 86(8), 1433-1436.

Larsen E. M. and Gammill M., 'Electrometric Titrations of Zirconium and Hafnium Solutions', American Chemical Society, 1950, Vol. 72, 3615-3619

Lauci, M., 'Powders Agglomeration Grade in the ZrO_2-Y_2O_3 Coprecipitation Process', Key Engineering Materials, 1997, 132-136, 89-92.

Li, M.Q., 'Making spherical zirconia particles from inorganic zirconium aqueous sols', Powder Technology, 2003, 137(1-2), 95-98.

Li, W., Gao L., Guo J. K., 'Synthesis of yttria-stabilized zirconia nanoparticles by heating of alcohol aqueous salt solutions', Nanostructure. Materials, 1998, 10(6), 1043-1049.

Lorimer, G.W., 'Quantitative x-ray microanalysis of thin specimens in the transmission electron microscope; a review', Mineralogical Magazine, 1987, 51, 49-60.

Lopato, L., A. V. Shevchenko, et al., 'Features of Solid Solution Formation with a Fluorite type Structure in the System ZrO_2-HfO_2-Y_2O_3 with Different Sythesis Methods', Powder Metallurgy and Metal Ceramics, 2006, 45(1-2), 1-7.

Mahdjoub, H., Roy P., Filiatre C., Bertrand G., Coddet, C., 'The effect of slurry formation upon the morphology of spray-dried yttria stabilised zirconia particals', Journal of the European Ceramic Society, 2003, 23, 1637-1648.

Maria Isabel Osendi, Jose S. Moya, Carlos J. Serna Javier Soria., 'Metastability of Tetragonal Zirconia Powders', Journal of the American Ceramic Society, 1985, 68(3), 135-139.

Matsui, K., Suzuki, H., Michiharu, O., 'Raman Spectroscopic Studies on the Formation Mechanism of Hydrous-Zirconia Fine Particles', Journal of American Ceramic Society, 1995, 78(1), 146-52.

Matsui K., Michiharu O., 'Formation Mechanism of Hydrous-Zirconia Particles Produced by Hydrolysis of $ZrOCl_2$ Solutions'. Journal of American Ceramic Society, 1997, 80(8), 1949-1956.

Matsui K., Michiharu O., 'Formation Mechanism of Hydrous-Zirconia Particles Produced by Hydrolysis of $ZrOCl_2$ Solutions: II, Powders'. Journal of American Ceramic Society, 2000, 83(6), 1386-1392.

Matsui K., Michiharu O., 'Formation Mechanism of Hydrous-Zirconia Particles Produced by Hydrolysis of $ZrOCl_2$ Solutions: III, Kinetics Study for the Nucleation and Crystal-Growth Processes of Primary particles'. Journal of American Ceramic Society, 2001, 84(10), 2303-2313.

Matsumoto, R. L. K., 'Generation of Powder Compaction Response Diagrams', Journal of the American Ceramic Society, 1986, 69(10), C-246-C-247.

Mawson, A. G., Carter G. A., Hart R. D., Kirby N. M., Nachmann, A. C., 'Mechanical Properties of 8 mole % Yttria-Stabilised Zirconia for Solid Oxide Fuel Cells', Materials Forum, 2006, 30, 148-158.

McEvoy, A. J., 'Materials for High-Temperature Oxygen Reduction in Solid Oxide Fuel cells', Journal of Materials Science, 2001, 36, 1087-1091.

Mistler R. and Twiname E., 'Tape Casting Theory and Practice', American Ceramic Society, Westervill OH: 2000,

Mitsuhashi, T., Ichihara M., Tatsuke U., 'Characterization and Stabilization of Metastable Tetragonal ZrO_2', Journal of the American Ceramic Society, 1974, 57(2), 97-101.

Mitsuhashi T., Fujiki Y., 'Phase Transformation of Monoclinic ZrO_2 Single Crystals', Journal of the American Ceramic Society, 1973, 56(9), 493-493.

Murase Y., Kato E., 'Phase Transformation of Zirconia by Ball-Milling'. Journal of the American Ceramic Society, 1979, 62(9-10), 527-527.

Murase Y., Kato E., 'Role of Water Vapor in Crystallite Growth and Tetragonal-Monoclinic Phase Transformation of ZrO_2'. Journal of the American Ceramic Society, 1983, 66(3), 196-200.

Murase Y., Kato E., Daimon K., 'Stability of ZrO_2Phases in Ultrafine ZrO_2-Al_2O_3 Mixtures'. Journal of the American Ceramic Society, 1986, 69(2), 83-87.

Myerson, A., 'Handbook of Industrial Crystallization Second edition' Butterworth Heinemann, Boston 225 Wildwood Ave Woburn MA 01801-2041: 2002,

O'Connor, B. H. and D. Y. Li., 'Attaining 1% Accuracy in absolute Phase Composition levels by Rietveld Analysis'. Advances In X-ray Analysis, 2000, 43: 305-311.

Oliveira A.P., Torem M. L, 'The influence of precipitation variables on zirconia powder synthesis', Powder Technology, 2001, 119(2-3), 181-193.

Ong, C. L., J. Wang, et al., 'Crystallization in nanosized sol-derived zirconia precursors' Journal of Materials Science Letters, 1996, 15, 1680-1683.

Ong, C. L., J. Wang, et al., 'Effects of Chemical Species on the Crystallization Behavior of a Sol-Derived Zirconia Precursor', Journal of American Ceramic Society, 1998, 81(10), 2624-2628.

Ormerod, R.M., 'Solid oxide fuel cells', Chemical Society Review, 2003, 32(1), 17-28.

Pietsch, W., 'Size Enlargement by Agglomeration'. John Wiley and Son, Baffins Lane Chichester Sussex England: 1991,

Perry, R. and D. Green, Perry's 'Chemical Engineers Handbook seventh Edition'. McGraw-Hill, New York USA, : 1997

Rahaman M.N., 'Ceramic Processing and Sintering Second Edition', Marcel Dekker, New York, 2003.

Rajendran, S., 'Production of Nano-Crystalline Zirconia Powders and Fabrication of High Strength Ultra-Fine-Grained Ceramics', Materals Forum, 1993, 17, 333-350.

Ralph J. M., Schoeler A. C., Krumpelt M., 'Materials for Lower Temperature Solid Oxide Fuel Cells', Journal of Materials Science, 2001, 36, 1161-1172.

Reed, J.S., 'Introduction to the Principles of Ceramic Processing'. 1988, New York: John Wiley and Sons.

Roosen A., Hausner H., 'Techniques for Agglomeration Control During Wet-Chemical Powder Synthesis'. Advanced Ceramic Materials, 1988, 3(2), 131-37.

Ram Srinivasan, Burtron H., et al., 'Crystallization and Phase Transformation Process in Zirconia: An in situ High-Temperature X-ray Diffraction Study'. Journal of the American Ceramic Society, 1992, 75(5), 1217-1222.

Ram Srinivasan, Larry Rice, Burtron H. Davis, 'Critical Particle Size and Phase Transformation in Zirconia: Transmission Electron Microscopy and X-ray Diffraction Studies'. Journal of the American Ceramic Society, 1990, 73(11), 3528-3530.

Ram Srinivasan,   R. J. De Angelis, et al. 'Factors influencing the stability of the tetragonal form of zirconia'. Journal Materials Research, 1986, 1(4), 483-488.

SagelRansijn C.D., Winnubst A.J.A., Kerkwijk B., Burggraaf A.J., and Verweij H., 'Grain growth in ultrafine-grained Y-TZP ceramics'. Journal of the European Ceramic Society, 1997, 17(6), 831-841.

SagelRansijn C.D., Winnubst A.J.A., Kerkwijk B., Burggraaf A.J., Verweij H., 'The Influence of Crystallization and Washing Medium on Characteristcs of nanocrystalline Y-TZP'. Jounal of the European Ceramic Society, 1996, (16),759-766.

Shukla S., Seal S., 'Mechanisms of room temperature metastable tetragonal phase stabilisation in zirconia'. International Materials Reviews, 2005, 50(1), 45-64.

Singh, R.P., Banerjee N. R., 'Electrometric Studies on the precipitation of hydrous oxides of some Quadravalent Cations. Part 1. Precipitation of Zirconium Hydroxide from solutions of zirconium salts'. Journal of Indian Chemistry Society, 1961, 38(11), 865-870.

Southon P.D., Bartlett J. R., Woolfrey J. L., Ben-Nissan B., 'Formation and characterization of an aqueous zirconium hydroxide colloid'. Chemistry Materials, 2002, 14(10), 4313-4319.

Solovkin, A.S., Tsvetkova S. V., 'The Chemistry of Aqueous Solutions of Zirconium salts (Does The Zirconyl Ion Exist?)'. Russian Chemistry Revue, 1962, 31(11), 655-669.

Standard O. C., Sorrell C. C., 'Densification of Zirconia - Conventional Methods', Key Engineering Materials, 1998, 153-154, 251-300.

Stevens R., Introduction to Zirconia, Vol. No 13, Magnesium Elektron, Swinton Manchester, 1986.

Tadokoro S. K., Muccillo E. N. S., 'Synthesis and characterization of nanosized powders of yttria-doped zirconia', Journal of Alloys and Compounds, 2002, 344(1-2), 186-189.

Toth, L.M., Lin J. S., Felker L. K., 'Small-Angle X-ray Scattering from Zirconium(IV) Hydrous Tetramers'. Journal of Physics Chemistry, 1991, 95(8), 3106-3108.

Turrillas X., Barnes P., Dent A. J., Jones S. L., Norman C. J., 'Hydroxide Precursor TO Zirconia - Extended X-Ray-Absorption Fine-Structure Study'. Journal of Materials Chemistry, 1993, 3, 583.

Upadhyaya, Ghosh A., Dey G. K., Prasad R., Suri A. K., 'Microwave sintering of zirconia ceramics'. Journal of Materials Science, 2001, 36(19), 4707-4710.

Wang S.Y., Li, X., Zhai Y.C., Wang K. M., 'Preparation of homodispersed nano zirconia'. Powder Technology, 2006, 168(2), 53-58.

Young R. A., 'The Rietveld Method'. International Union Of Crystallography Oxford University Press, West st Oxford, 1993.

Zaitsev, L.M., Bochkarev G. S., 'Peculiarities in the behaviour of zirconyl in Solutions'. Russian Journal Inorganic Chemistry, 1962, 7(4), 411-414.

Zhu, W. Z., 'Effect of cubic phase on the kinetics of the isothermal tetragonal to monoclinic transformation in ZrO_2(3 mol% Y2O3) ceramics'. Ceramics International, 1998, 24(1), 35-43.